AD710 604

PB196003

Final Report

A PRACTICAL, MULTIPURPOSE URBAN DIFFUSION MODEL FOR CARBON MONOXIDE

By: F. L. LUDWIG
ALBERT E. MOON
WARREN B. JOHNSON
ROBERT L. MANCUSO

Prepared for:

COORDINATING RESEARCH COUNCIL, INC.
30 ROCKEFELLER PLAZA
NEW YORK, NEW YORK 10020

CONTRACT CAPA-3-68

NATIONAL AIR POLLUTION CONTROL ADMINISTRATION
411 WEST CHAPEL HILL STREET
DURHAM, NORTH CAROLINA 27701

CONTRACT CPA 22-69-64

STANFORD RESEARCH INSTITUTE
Menlo Park, California 94025 · U.S.A.

Reproduced by
NATIONAL TECHNICAL INFORMATION SERVICE
Springfield, Va. 22151

184

STANDARD TITLE PAGE FOR TECHNICAL REPORTS

1. Report No. APTD-0604

2. Govt. Accession No.

3. Recipient's Catalog No.

4. Title and Subtitle
A Practical, Multipurpose Urban Diffusion Model for Carbon Monoxide

5. Report Date September 1970

6. Performing Organization Code

7. Author(s)
F. L. Ludwig et al.

8. Performing Organization Rept. No.

9. Performing Organization Name and Address
Stanford Research Institute
Menlo Park, California 94025

10. Project/Task/Work Unit No.

11. Contract/Grant No. CPA 22-69-64

12. Sponsoring Agency Name and Address
National Air Pollution Control Administration Technical Center
411 Chapel Hill Street
Durham, North Carolina 27701

13. Type of Report & Period Covered

14. Sponsoring Agency Code

15. Supplementary Notes

16. Abstracts

~~This report describes~~ the development and current status are described of a receptor-oriented diffusion model that can be applied to urban areas to give the following outputs: (1) carbon monoxide (CO) concentration isopleths for a given set of meteorological conditions and times of day, (2) sequences of hourly CO concentrations at specific locations for given sequences of meteorological conditions, and (3) climatological summaries of CO concentration for specific locations if an historical record of meteorological data is available. The model can be used to obtain the frequency distributions of concentrations averaged over various time intervals for specific hours of the day or days of the week. Model inputs are traffic volumes on major streets and highways in the urban area, atmospheric stability, mixing depth, and wind speed and direction. Traffic volumes can be obtained from either past measurements or forecast values. Methods are described for obtaining atmospheric stability and mixing depth from conventional (i.e., airport) hourly meteorological measurements and twice daily radiosonde data. Meteorological parameters are assumed uniform throughout the urban area. When the airport winds are calm the model (over)

17. Key Words and Document Analysis. (a). Descriptors

Air pollution
Urban areas
Atmospheric diffusion
Mathematical models
Carbon monoxide
Maps
Periodic variations
Seasonal variations
Vehicular traffic
Stability
Wind (meteorology)
Urban planning

17b. Identifiers/Open-Ended Terms

Isopleths
Mixing Depth

17c. COSATI Field/Group 13/02, 04/01, 12/01

18. Distribution Statement
Unlimited

19. Security Class (This Report) UNCLASSIFIED

20. Security Class. (This Page) UNCLASSIFIED

21. No. of Pages 204

22. Price

ORM NBS-687(1-70)

This report was furnished to the Air Pollution Control Office by the Stanford Research Institute in fulfillment of Contract No. CPA 22-69-64.

16. Abstracts (Cont'd)

uses a small finite value of wind speed and the last observed wind direction. The concentrations calculated with the model are compared with observations of CO concentration from Continuous Air Monitoring Program (CAMP) stations. Although the agreement is not good--the model generally calculates concentrations lower than those observed--improvement is obtained by empirical corrections. Possible reasons are given for the disagreement between calculations and observations, and a field measurement program is described that the authors feel will help to define the sources of the discrepancies and provide the information necessary for their correction.

STANFORD RESEARCH INSTITUTE
Menlo Park, California 94025 · U.S.A.

Final Report

September 1970

A PRACTICAL, MULTIPURPOSE URBAN DIFFUSION MODEL FOR CARBON MONOXIDE

By: F. L. LUDWIG
ALBERT E. MOON
WARREN B. JOHNSON
ROBERT L. MANCUSO

Prepared for:

COORDINATING RESEARCH COUNCIL, INC.
30 ROCKEFELLER PLAZA
NEW YORK, NEW YORK 10020

CONTRACT CAPA-3-68

NATIONAL AIR POLLUTION CONTROL ADMINISTRATION
411 WEST CHAPEL HILL STREET
DURHAM, NORTH CAROLINA 27701

CONTRACT CPA 22-69-64

SRI Project 7874

Approved:

R. T. H. COLLIS, *Director*
Aerophysics Laboratory

RAY L. LEADABRAND, *Executive Director*
Electronics and Radio Sciences Division

Copy No. 329

ABSTRACT

This report describes the development and current status of a receptor-oriented diffusion model that can be applied to urban areas to give the following outputs: (1) carbon monoxide (CO) concentration isopleths for a given set of meteorological conditions and times of day, (2) sequences of hourly CO concentrations at specific locations for given sequences of meteorological conditions, and (3) climatological summaries of CO concentration for specific locations if an historical record of meteorological data is available. The model can be used to obtain the frequency distributions of concentrations averaged over various time intervals for specific hours of the day or days of the week.

Model inputs are traffic volumes on major streets and highways in the urban area, atmospheric stability, mixing depth, and wind speed and direction. Traffic volumes can be obtained from either past measurements or forecast values. Methods are described for obtaining atmospheric stability and mixing depth from conventional (i.e., airport) hourly meteorological measurements and twice daily radiosonde data. Meteorological parameters are assumed uniform throughout the urban area. When the airport winds are calm the model uses a small finite value of wind speed and the last observed wind direction.

The concentrations calculated with the model are compared with observations of CO concentration from Continuous Air Monitoring Program (CAMP) stations. Although the agreement is not good--the model generally calculates concentrations lower than those observed--improvement is obtained by empirical corrections. Possible reasons are given for the disagreement between calculations and observations, and a field measurement program is described that the authors feel will help to define the sources of the discrepancies and provide the information necessary for their correction.

SUMMARY

If city planners and highway planners are to include air pollution effects among the factors to be considered in the urban and highway design processes, then some method must be made available that will allow them to estimate the magnitude and nature of the effects that will arise from implementation of various plans. This report describes the results of the first year's efforts to develop a method for determining the air pollution consequences of various city and highway planning alternatives. The approach taken has been that of the numerical model, i.e., a scheme for calculating air pollution concentrations from information about air pollution sources and meteorological conditions.

The long-term objectives of the program are to develop a model that will accurately calculate the concentrations of any pollutant at virtually any point in any city, if meteorological conditions and pollution sources are known. The objectives include being able to calculate the statistical distributions of concentrations at a point, as well as single values appropriate to some specific set of conditions.

During this first year we limited ourselves to developing a calculational scheme for carbon monoxide concentrations, largely because this pollutant is relatively nonreactive, permitting us to focus our efforts on the meteorological side of the problem. After this is in hand, work to extend the model to chemically active pollutants will be in order. The model as presently developed incorporates diffusion submodels based upon both Gaussian and uniform (to the top of the mixing layer) vertical concentration profiles. It can calculate concentrations of carbon

monoxide at any point in a city using readily available meteorological and traffic data. Techniques have been developed to estimate, from observed quantities, those model inputs that are not directly observed. The model can provide statistical summaries and estimates for individual situations. The model has been applied to five different cities (St. Louis, Washington, Chicago, Cincinnati, and Denver) in several different ways to demonstrate its versatility. This report contains examples of the following different types of calculations:

(1) Maps of concentration isopleths for the five cities, based on calculated concentrations at 625 points (25 × 25 grid). Inputs were specific observed meteorological conditions from 1964 or 1965 weather records and historical, diurnally corrected 1965 average traffic data.

(2) Week-long sequences of calculated hourly concentrations at single points in each of the five cities. Inputs were historical average traffic data and hourly meteorological observations.

(3) Maps of concentration isopleths for St. Louis based on forecasts of 1980 traffic, two hypothesized levels of exhaust emission control, and specific meteorological conditions corresponding to those used for a 1964 case.

(4) Ten different concentration frequency distributions for a location in St. Louis, based on a five-year (1960-64) meteorological record and historical average traffic data. The frequency distributions presented include those of

- Concentrations during all hours
- Concentrations during weekday, Saturday, or Sunday hours
- Concentrations at the following hours: 0800, 1200, 1800, or 2400 local time (includes daylight savings time corrections)
- 8-hour and 12-hour averages of concentration.

(5) The same ten frequency distributions based on St. Louis traffic forecasts and the same five-year meteorological record.

(6) The median and 90-percentile values of hourly concentrations at nine St. Louis locations, based on the same data as Item (4).

(7) The median and 90-percentile values of hourly concentrations at nine St. Louis locations, based on the same data as Item (5).

When the concentrations calculated by the model are compared with those measured at Continuous Air Monitoring Program (CAMP) stations, the agreement is found to be generally poor, with observations usually higher than calculations. There are many possible sources for the discrepancies, but each falls into one or more of three categories:

(1) Inadequate input data for the model

(2) Inappropriate assumptions used in the modeling

(3) Unrepresentative or inaccurate CAMP observations.

The consequences of several possible sources of error in the first category have been studied in an investigation of the model's sensitivity to its various inputs. The inputs include source strength (determined from traffic data), wind speed and direction (measured at the local airport), atmospheric stability (determined from conventional airport meteorological observations), and mixing depth (determined from airport radiosonde temperature measurements). The calculated concentrations are directly proportional to source strengths, but, in general, sources nearest the receptor are the most important in determining the calculated concentration.

Calculated concentrations are inversely proportional to wind speed. Stability changes can cause large changes in calculated concentration, particularly when the mixing layer is deep. If the air is relatively unstable so that mixing proceeds rapidly and if the mixing layer is relatively shallow, then calculated concentrations are almost proportional to the mixing depth used. As the stability and mixing depth increase, the sensitivity of the model to changes in the mixing depth becomes less and less.

The possible sources of error that can be included in the category of inappropriate assumptions include those that would arise from taking airport meteorological observations to be valid throughout the city, from the assumption of Gaussian dispersion, and from our handling of the calm-wind case. The report concludes that local values of input meteorological parameters would provide an improvement over the present assumption of uniform meteorology. The Gaussian dispersion assumption is also discussed, and it is concluded that the dispersion rates used may not be seriously in error, but further study is needed. As presently constituted, the model takes a measured (airport) calm to correspond to an urban wind of small finite speed (1 m/s) from the most recently measured (airport) direction. Better methods of treating this difficult case are being sought.

The only CO data available for checking our model in the five cities to which it was applied are the CAMP station data. The model evaluation thus depends upon the representativeness and accuracy of these data. Some of the CAMP stations are located near parking lots or large buildings, where aerodynamic effects are likely to be a significant factor. All measure CO concentrations at single points rather than over areas comparable to the spatial resolution of the model. These factors could contribute importantly to differences between observed and calculated concentrations. Other possible sources of error include water vapor interference and the relatively poor precision (1 ppm) of the observations.

Attempts have been made to correct some of the model's discrepancies using a least squares statistical method in conjunction with St. Louis CAMP Station observations. These attempts focused on errors that might arise because of differences between winds observed at the airport and those in the city, and on errors that might come from poor estimates of the fractions of the total daily traffic that occur during individual hours. After the statistical adjustments have been made, the model can reproduce the high concentration parts of the observed frequency distribution of independent data with good accuracy. Its performance on individual hourly values is slightly better than "predictions" based upon a long-term mean value of concentration. The model also performs about as well as "persistence," i.e., assuming that concentration has the value observed 24 hours earlier.

The report concludes with a discussion of our plans for a program of field measurements that should help to define the most serious sources of discrepancies between observed and calculated concentrations. This measurement program should also provide much of the information necessary to correct the discrepancies.

Meteorological and CO measurements are planned for several locations and at several heights above street level in and around downtown intersections in San Jose and St. Louis. These should help define the characteristics of aerodynamic flow effects around buildings and of differences in meteorology between the airport and the downtown area. When combined with the detailed traffic data available from downtown San Jose, these data should also provide a test of the accuracy of the relationship used to determine CO emissions from traffic data. Study of the detailed traffic data should provide information on the probable representativeness of historical traffic data, which are based on very limited counting periods. We also plan field measurements of CO concentrations at various points in the vicinity of the St. Louis CAMP Station. These should serve as a check on the accuracy and representativeness of the available CAMP data.

CONTENTS

ABSTRACT. iii

SUMMARY v

LIST OF ILLUSTRATIONS xv

LIST OF TABLES. xix

I INTRODUCTION 1

- A. Scope and Objectives. 1
- B. Fundamental Concepts. 3

II ELEMENTS OF THE BASIC MODEL. 5

- A. Spatial Partitioning of Emissions 5
- B. The Gaussian Model. 7
- C. The Box Model 9
- D. Transition from Gaussian to Box Models. 9
- E. Required Inputs for the Basic Model 10
- F. Simplifying Assumptions 11

III DETERMINATION OF THE INPUTS. 15

- A. Emission Inventory Design 15
  - 1. General. 15
  - 2. Calculation of Primary Network Emissions Using Historical Data. 22
  - 3. Calculation of Secondary Traffic Emissions Using Historical Data. 24
  - 4. Calculation of Emissions Using Forecast Traffic Data 25
- B. Meteorological Inputs 28
  - 1. Gaussian Standard Deviation Function 28
  - 2. Stability Category 30

3. Mixing Depth 32
4. Wind Speed and Direction 33

IV ORGANIZATION AND APPLICATIONS OF THE SYNOPTIC AND CLIMATOLOGICAL MODELS. 37

A. Introduction. 37

B. The Synoptic Model. 38

1. Description. 38
2. Applications 40

C. The Climatological Model. 58

1. Background 58
2. Description. 59
3. Applications 62

V TESTING AND IMPROVING THE MODEL. 77

A. Sensitivity Tests 77

1. Source Strength. 78
2. Wind Speed 80
3. Wind Direction 80
4. Location of the Receptor 81
5. Stability and Mixing Depth 83

B. Use of Observations to Improve the Model. 88

1. Introduction 88
2. Attempted Improvements 89
3. Example. 93

VI DISCUSSION AND FUTURE PLANS. 99

Appendix A--PRINCIPAL SOURCES OF CO IN URBAN AREAS. 107

Appendix B--THE URBAN TRANSPORTATION PLANNING PROCESS 113

Appendix C--METHODS FOR DETERMINING STABILITY CATEGORY. . . . 121

Appendix D--METHODS FOR DETERMINING MIXING DEPTH. 129

Appendix E--INCREASING THE SPATIAL RESOLUTION FOR EMISSIONS IN THE FIRST SEGMENT. 143

Appendix F--TREATMENT OF EXTRAURBAN SOURCES AND STREET EFFECTS. 147

Appendix G--PROGRAM FOR PREPROCESSING OF THE DATA FOR THE CLIMATOLOGICAL MODEL. 155

Appendix H--THE EQUIVALENCE OF CERTAIN COMBINATIONS OF STABILITY AND MIXING DEPTH 161

Appendix I--CONTINUOUS AIR MONITORING PROGRAM STATIONS. . . . 167

ACKNOWLEDGMENTS 177

REFERENCES. 179

BLANK PAGE

ILLUSTRATIONS

Figure 1 Diagram of Segments Used for Spatial Partitioning of Emissions. 6

Figure 2 Computer-Generated Display of Traffic Links in a 24-by-24-Mile Central Portion of the Primary Network for Washington, D.C.. . 16

Figure 3 Hourly Distribution of Trips in Washington, D.C. 18

Figure 4 Hourly Distribution of Traffic for Two Facility Types in St. Louis. 18

Figure 5 Simplified Schematic Diagram of Traffic Link Assignment Subroutine Used for the Five Segments Closest to the Receptor 20

Figure 6 Illustration of the Grid-Point Transformation Technique Used for Computing the CO Emissions within the Four Most Distant Segments 21

Figure 7 σ_z Functions Used in the Model 31

Figure 8 Simplified Flow Chart for Synoptic Model Calculations 39

Figure 9 Simplified Flow Chart for Concentration Calculations 41

Figure 10 Calculated Washington, D.C., Concentration Patterns 43

Figure 11 Calculated St. Louis Concentration Patterns 0700-0800, 15 October 1964 44

Figure 12 Calculated Concentration Patterns Based on Forecast of 1990 St. Louis Traffic 45

Figure 13 Calculated St. Louis Concentration Patterns for Two Grid Sizes 47

Figure 14 Calculated Carbon Monoxide Concentrations (PPM) for Chicago. 48

Figure 15 Calculated Carbon Monoxide Concentrations (PPM) for Cincinnati 49

Figure 16 Calculated Carbon Monoxide Concentrations (PPM) for Denver 50

Figure 17 Observed and Calculated CO Concentrations at the St. Louis CAMP Station, 18-24 January 1965 51

Figure 18 Observed and Calculated CO Concentrations at the St. Louis CAMP Station, 19-25 October 1964 52

Figure 19 Observed and Calculated CO Concentrations at the Washington, D.C., CAMP Station, 19-25 October 1964 54

Figure 20 Observed and Calculated CO Concentrations at the Cincinnati CAMP Station, 14-20 December 1964. 55

Figure 21 Observed and Calculated CO Concentrations at the Chicago CAMP Station, 20-26 July 1964. 56

Figure 22 Observed and Calculated CO Concentrations at the Denver CAMP Station, 19-25 April 1965 57

Figure 23 Simplified Flow Chart of Climatological Model. 63

Figure 24 Simplified Flow Chart for a Program to Determine Ten Different Frequency Distributions. 65

Figure 25 Calculated St. Louis CAMP Station CO Concentration Frequency Distribution for 1965 Traffic Conditions; Weekday, Saturday, and Sunday Hours 67

Figure 26 Calculated St. Louis CAMP Station CO Concentration Frequency Distribution for 1965 Traffic Conditions; 0800, 1200, and 1800 Hours 68

Figure 27 Calculated St. Louis CAMP Station CO Concentration Frequency Distribution for 1965 Traffic Conditions; 1-Hour, 8-Hour, and 24-Hour Averages 69

Figure 28 Spatial Variations of Calculated St. Louis Median and 90 Percentile Concentrations for 1965 Traffic Data. 70

Figure 29 Calculated St. Louis CAMP Station CO Concentration Frequency Distribution for 1990 Traffic Conditions; Weekday, Saturday, and Sunday Hours 71

Figure 30 Calculated St. Louis CAMP Station CO Concentration Frequency Distribution for 1990 Traffic Conditions; 0800, 1200, and 1800 Hours 72

Figure 31 Calculated St. Louis CAMP Station CO Concentration Frequency Distribution for 1990 Traffic Conditions; 1-Hour, 8-Hour, and 24-Hour Averages 73

Figure 32 Spatial Variations of Calculated St. Louis Median and 90 Percentile Concentrations for 1990 Traffic Conditions. 74

Figure 33 Effect of Wind Direction on Concentrations Computed for the Washington, D.C., CAMP Station. 82

Figure 34 Effect of Moving Receptor Point. 84

Figure 35 Normalized Concentration as a Function of Stability and Mixing Depth. 86

Figure 36 Diurnal Emission Patterns for St. Louis. . . . 94

Figure 37 Observed and Calculated Frequency Distributions for Five Months of Independent Data 98

Figure D-1 Schematic Representation of the Diurnal Temperature/Time Interpolation of Mixing Depth. 140

Figure G-1 Simplified Flow Chart of Program for Converting Holzworth's Mixing Depths to Hourly Values 158

Figure G-2 Simplified Flow Chart of the Data Processing Program Used with the Climatological Model 159

Figure I-1 St. Louis CAMP Station 171

Figure I-2 Cincinnati CAMP Station. 172

Figure I-3 Chicago CAMP Station 173

Figure I-4 Washington CAMP Station. 174

Figure I-5 Denver CAMP Station. 175

TABLES

Table I	Average Speeds for Washington, D.C., Highway Facilities	24
Table II	Percentage Increase in Calculated CO Concentration Resulting from the Doubling of Emission Rates in Different Segments. . . .	79
Table III	Results of Model Calibration	96
Table A-I	Percent CO Contribution by Source Category . .	110
Table C-I	Stability Categories	124
Table H-I	Mixing Depth Classes	164
Table H-II	Values of $(\chi/Q)_{i,j,m}$ for Unit Wind Speed . . .	166

BLANK PAGE

I INTRODUCTION

A. Scope and Objectives

There is a need for an objective, practical method of simulating the current and future impact of motor vehicles on air pollution in urban communities. Such a technique could be used to assess current concentration patterns of primary vehicular pollutants in cities, and to predict the effects of exhaust emission controls and expressway routings on future concentration patterns. This report describes our progress in developing a simulation model designed to meet these objectives. Further refinements of this model are indicated and will be made in the course of our continuing study. In this sense, the model is not yet a completely finished product, and any present applications should be carried out with caution.

In developing the model, we have been aided considerably by previous urban diffusion modeling studies, which have been reviewed and summarized by Wanta (1968),* Stern (1969), Moses (1969), and Neiburger (1968). An investigation of carbon monoxide diffusion in Washington, D.C., by Ott et al. (1967) and Clarke's (1964) model could be considered prototypes for the model described here.

For simplicity, the modeling effort has been restricted to carbon monoxide (CO), since (1) the gas is relatively inert in the atmosphere

---

*References are listed at the end of the report.

with no known significant natural sources or sinks in urban areas,*
(2) motor vehicles are known to be the most important source of the CO in urban air, and (3) CO is an important pollutant in terms of health effects.

Our goal has been to develop a versatile, practical model to predict street-level CO concentrations at any point in a city. Calculations of the following types can be made using the model:

(1) Hourly concentrations as a function of time, for verification use and possible operational applications, and

(2) The frequency distribution of concentrations for selected averaging times, including statistical prediction of the frequency of occurrence of specified high concentrations for planning purposes.

To improve the accuracy of the model, we have developed calculation schemes to assess the concentration contributions resulting from diffusion on various scales, including the treatment of:

(1) Extraurban transport and diffusion, mainly from upwind cities, and

(2) General intraurban diffusion from arterial and feeder streets.

Too little is yet known about the effects of nearby buildings and streets to permit these influences to be included in the model, but studies currently underway should substantially add to our knowledge in this area.

---

*Although evidence is mounting that such sources and sinks may be found in the biosphere (Swinnerton et al., 1969; Went, 1966; Robinson and Robbins, 1967). Concentrations arising from such sources could be included as part of the background concentrations entering an urban area.

In developing the model we have attempted to:

1. Bring together into a single model the best features of previous efforts and supplement these with original contributions where necessary.
2. Maintain simplicity unless additional complexity is required to achieve greater accuracy, and is clearly justified in terms of the accuracy of the available input data and the resulting increased computing costs.

B. Fundamental Concepts

Our plan has been to develop the model around individual pieces, or "modules." These modules were to be organized in different ways to accomplish different objectives. In computer programming terms, this means that several subroutines were used in the program. This approach has been useful, although it has been applied differently than originally anticipated. The same general organization is used in all the applications, but modules are changed to reach the different objectives. This characteristic has allowed us to change different aspects of the model, and to experiment with a minimum of disruption of the overall system.

The organization of this report reflects the modular nature of the diffusion model it describes. We have chosen to describe the basic model and then the various forms that the subunits of that model have taken. Much of the detailed description of the subunits is confined to the appendices of this report. Results obtained with the model are also presented. The research has revealed some shortcomings of the model, of the available input information, and of the data available to verify the results. These deficiencies are also discussed.

II ELEMENTS OF THE BASIC MODEL

A. Spatial Partitioning of Emissions

Our diffusion model is a modified form of the receptor-oriented model developed by Clarke (1964). The concentration at the receptor is considered to be due only to emissions located within logarithmically spaced segments, such as shown in Figure 1. This arrangement of segments allows more precise selection of effective emissions near the receptor. The closest segment extends from the receptor to 125 m, roughly comparable to the size of a city block, and the farthest segment extends to 32 km, approximately the diameter of a large city.

The 22.5° sector width is convenient and fits reasonably well the angular plume widths, between $\pm 2\ \sigma$ points, predicted by Gifford's (1961) model for slightly unstable conditions. The sector width is expanded to 45° within the closest 1 km to allow for the large initial lateral dispersion observed during the St. Louis tracer studies (Pooler, 1966; McElroy, 1969).

Because nearly all urban carbon monoxide emissions are from internal combustion vehicles (see Appendix A), the model assumes emissions to be at ground level. Furthermore, the emissions within each segment are assumed to be uniformly distributed. Thus the total emission from all the highway links and parts of links that lie within a segment is averaged over the area of that segment. The emissions from the smaller and residential streets are also included. The methods for determining emissions are described in a later section of this report. Here, it is sufficient to note that each upwind segment is assigned an average emission rate taken to apply throughout the segment and with the units gm $m^{-2}\ s^{-1}$.

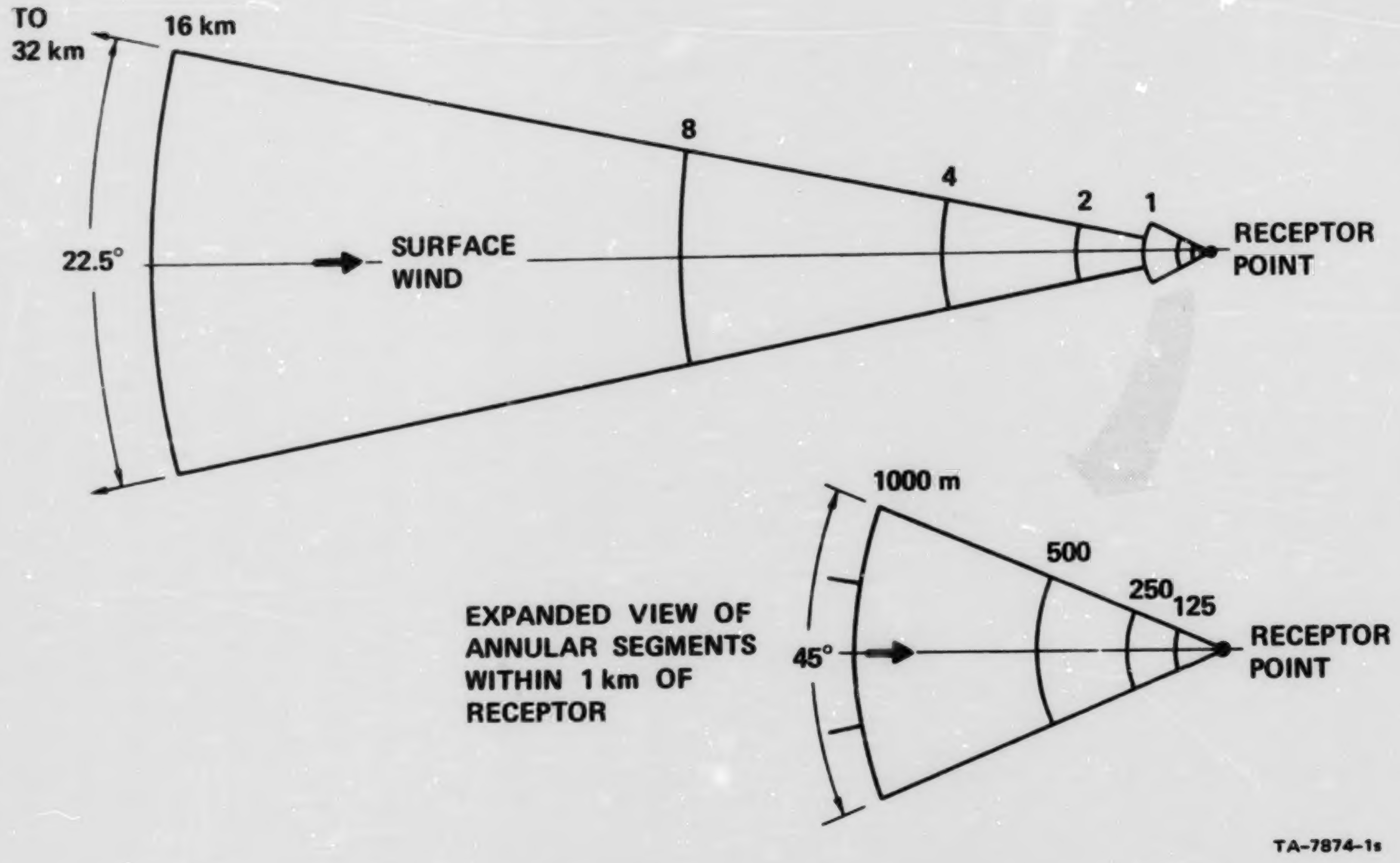

FIGURE 1 DIAGRAM OF SEGMENTS USED FOR SPATIAL PARTITIONING OF EMISSIONS

The small size of the segments near the receptor provides good spatial resolution for the close sources, where such resolution is important. For farther areas the detailed location of individual sources is not very important because diffusion processes during transport intermingle the individual emissions before they reach the receptor. The sacrifice of resolution at greater distances simplifies the calculations, but does not substantially affect the results.

B. The Gaussian Model

Gifford (1961) has developed a generalized diffusion model to describe the plume from a continuous ground-level point source, assuming perfect reflection at the ground. In its simplest form, the ground-level concentration from a ground-level source is given by

$$C = \frac{Q}{\pi \sigma_y \sigma_z u} \exp\left(-y^2/2\sigma_y^2\right) \quad , \qquad \text{(II-1)}$$

where

C = ground-level concentration (g/m^3)

Q = source strength (g/s)

u = average wind speed (m/s)

y = lateral (crosswind) distance from the plume axis (m)

σ_y, σ_z = lateral and vertical standard deviations of plume concentration (m); these parameters are functions of distance between the source and the receptor and of atmospheric stability.

When Eq. (II-1) is integrated over y, we obtain the following basic form for ground-level concentrations from a ground-level line source:

$$C = Q_L\left(\frac{2}{\pi}\right)^{1/2}\left(u\sigma_z\right)^{-1} \quad . \tag{II-2}$$

In this formulation Q_L has the units g m^{-1} s^{-1}.

Estimates of σ_z as a function of atmospheric stability and pollutant travel distance or time have been proposed by Gifford (1961) and Smith and Singer (1966), and urban observations of this type have been reported by Pooler (1966) and McElroy (1969). We have used Gifford's[*] values, but the model is flexible and can use any set of functions that can be reasonably approximated, over the intervals between segment boundaries, with expressions of the form

$$\sigma_z = a_{ij}\, r^{b_{ij}} \quad , \tag{II-3}$$

where r is the travel distance, the subscript i refers to annular segments upwind of the receptor point (see Figure 1), and j refers to different stability classes. The determination of stability class is discussed later in the report. The σ_z functions are generally well approximated by this set of power functions.

Substituting Eq. (II-3) into the line-source equation and integrating with respect to r from $r = r_i$ to r_{i+1} gives the contribution to the calculated concentration from the i^{th} segment area source for stability class j:

---

[*] Gifford's work is a modification of that by F. Pasquill (1961). The Gifford-Pasquill curves are based upon data from open country, and probably underestimate the diffusion in urban areas. We are examining possible improvements in this area.

$$\left(\frac{C}{Q_A}\right)_{ij} = \frac{0.8}{u\, a_{ij}} \left(1 - b_{ij}\right)^{-1} \left(r_{i+1}^{1-b_{ij}} - r_i^{1-b_{ij}}\right) \qquad b_{ij} \neq 1$$

$$= \frac{0.8}{u\, a_{ij}} \ln \left(\frac{r_{i+1}}{r_i}\right) \qquad b_{ij} = 1 \quad \text{(II-4)}$$

where r_i and r_{i+1} are, respectively, the distance to the downwind and upwind boundaries of the i^{th} segment. In this expression Q_A is the average emission rate from the i^{th} segment and has the units g m^{-2} s^{-1}. This basic Gaussian model applies when there is no effective limitation to vertical mixing or when the cloud has not spread sufficiently to be affected by such a limitation.

C. The Box Model

When the layer into which the pollutants are being dispersed is restricted, then they will tend to become uniformly distributed in the vertical after sufficient travel has taken place. Under these conditions, the "box" model is used. According to the box model, the concentration arising from a uniform area source in the i^{th} annular segment is defined by (see Miller and Holzworth, 1967):

$$\left(\frac{C}{Q_A}\right)_i = \frac{r_{i+1} - r_i}{uh} \quad , \qquad \text{(II-5)}$$

where h is the depth of the layer into which the pollutants are mixed.

D. Transition from Gaussian to Box Models

We have chosen to change from the Gaussian model to the box model at that point where the two (in their respective line source formulations) give equal concentration values. The equivalent of Eq. (II-5) for a line source is:

$$C = Q_L/uh \quad . \tag{II-6}$$

Setting the right-hand sides of Eqs. (II-2) and (II-6) equal to each other, and solving for r gives:

$$r_T = \left(0.8h/a_{ij}\right)^{1/b_{ij}} \quad . \tag{II-7}$$

In Eq. (II-7), r_T is that value of r for which the box and Gaussian models give equivalent results. At this distance, we change from Eq. (II-4) to Eq. (II-5) in calculating concentrations. The part of an annular segment downwind of r_T is treated according to the Gaussian model, and the part that is upwind, according to the box model. If the transition occurs in segment i, then r_T is substituted for r_{i-1} in the Gaussian equation and for r_i in the box equation.

E. Required Inputs for the Basic Model

Equations (II-4) and (II-5) are the basis of the model. In order to use these equations to calculate the concentration at a receptor, the values of certain input variables are required. These inputs are:

(1) The wind direction

(2) The average transport wind speed

(3) The average emission strength within each of the upwind segments

(4) The depth of the mixing layer

(5) The variation of σ_z with travel distance.

The last item requires that we select some empirically or theoretically determined function that describes the dependence of σ_z on distance for the meteorological conditions for which we are calculating the concentration. As will be discussed later, these functions may be conveniently approximated in the form given by Eq. (II-3).

None of the necessary inputs are routinely measured, except wind speed and direction. To satisfy the requirement that the model be generally applicable in a variety of cities, we have had to develop methods of deriving the model inputs from readily available information. Section III of this report describes the ways in which the inputs can be determined from conventional traffic data and from routine meteorological measurements.

F. Simplifying Assumptions

Before proceeding to the next section, it should be noted that two broad simplifying assumptions have been made with regard to the meteorological data. First, the meteorological inputs have been taken to be uniform throughout the urban area, and second, they have been assumed to remain constant during the travel of the pollutants between source and receptor. For example, it may take two hours for pollutants to travel to the receptor from the farthest segment, but we assume that the meteorological parameters such as stability and mixing depth have remained constant at the value they have when those pollutants arrive at the receptor. The assumption of horizontal uniformity of the meteorological factors is made, in large part, because it represents the best available estimate of the situation. Winds are seldom measured at more than a very few locations in an urban area, so we must generally make do with a single measured wind. There appears to be no reason, in principle, why the emission segments upwind of the receptor could not be laid out along a wind trajectory, if the trajectories were known and the added complexity were warranted by improved results.

Variations of mixing depth and stability almost certainly occur through a city, but at present there are seldom, if ever, sufficiently detailed data to determine such variations. As a matter of fact, the measurements required to determine a mixing depth are usually made at some distance outside the urban area. A similar situation exists with the information required for stability estimates. We must therefore assume the estimates of mixing depth and stability are typical of the area, although we do make some adjustments to account for the gross effects of urbanization.

The assumption that diffusing pollutants have been subjected, throughout their trajectory, to the conditions prevailing at the time of their arrival at the receptor is justified when the quality of the input data is considered. We have already conceded our inability to determine the spatial changes. In general, we would expect the temporal changes to be comparable with the spatial, so treating one without treating the other could constitute an unwarranted complexity. Though the winds are measured hourly, as are the data from which stability is determined, mixing depths must be interpolated between values estimated at half-day intervals. Again the principle of consistency suggests that added complexity to account for changes in conditions during the travel period of the pollutants is unwarranted.

One other factor that concerns the assumption of temporal constancy of inputs is the relative importance of emissions at different distances to the observed concentrations at a point. Calculations with the model indicate that contributions of emissions to the concentration at a point decrease with increasing distance, other things being equal. Thus, the nearby sources, with correspondingly short travel times, are the major factors in determining the concentration. The short travel times from these sources minimize the likelihood of substantial change in the meteorological parameters. This factor alone is probably sufficient to justify the simplification of taking meteorological factors to be constant during the time that pollutants travel from their source to the receptor.

BLANK PAGE

III DETERMINATION OF THE INPUTS

A. Emission Inventory Design

1. General

The emission inventory for the model consists entirely of the emissions from vehicular sources, since these sources are responsible for almost all urban CO emissions (see Appendix A). The inventory of vehicular emissions has two components: (1) primary network link emissions from vehicles traveling on the network of major arterial streets and freeways, and (2) secondary background emissions from vehicles traveling over the less densely traveled local and feeder streets.

The primary network links for which the emissions are computed are the sections of major arterial streets and freeways between intersections with other major arterials and freeways. The average length of the links on the primary network is approximately one mile, although the links may be much shorter in densely traveled downtown areas, and more widely spaced in outlying areas. Figure 2 illustrates the network used for the Washington, D.C., area. Computer-generated displays of the links, like that in Figure 2, are very useful for detecting errors in coding.

Traffic volumes on links vary hour-by-hour over a day and are different for weekend days than for weekdays. Further, there are smaller seasonal variations. Highway engineers and planners average these variations into a quantity that they call average daily traffic (ADT).

Preceding page blank

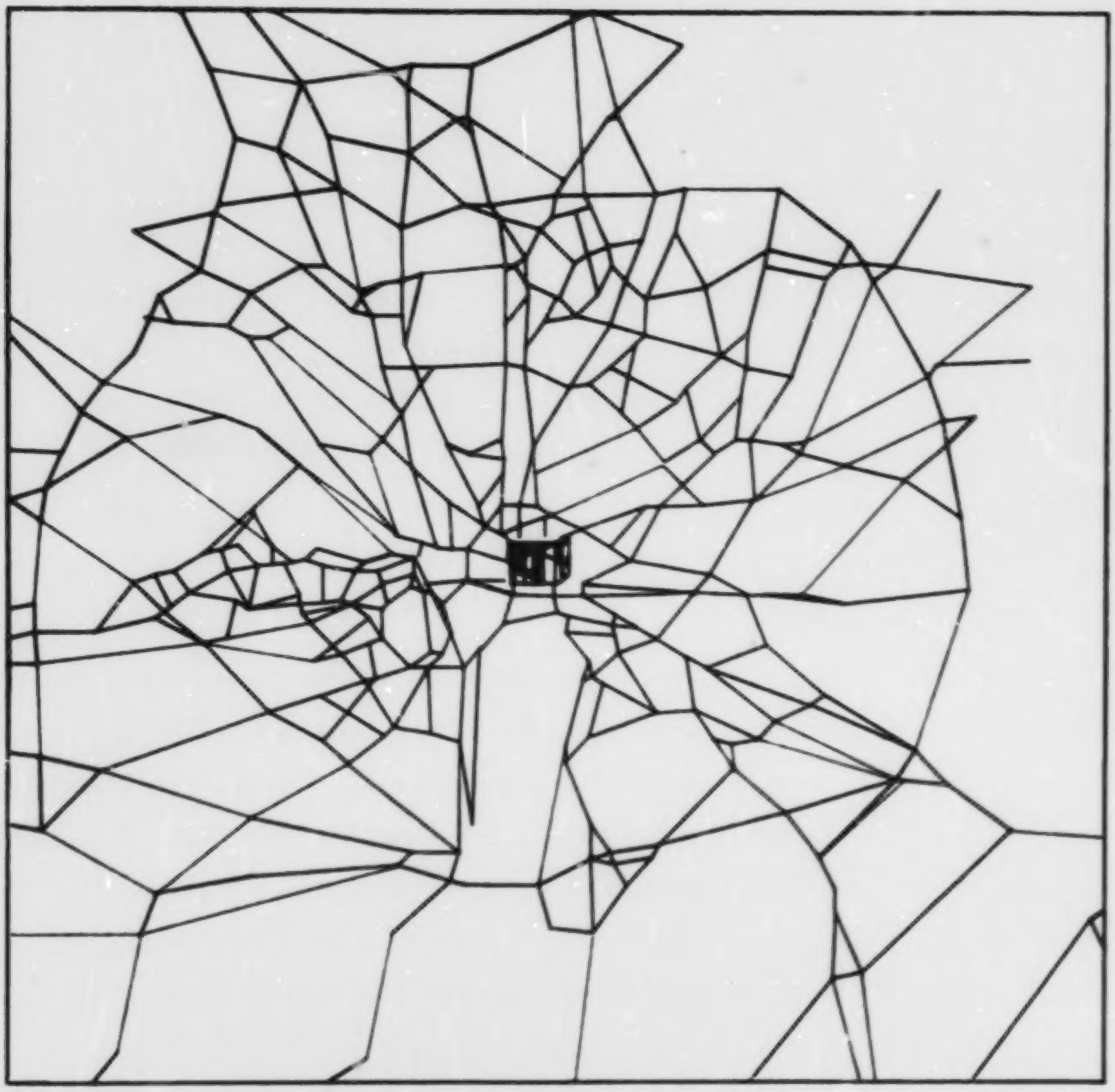

TA-7874-18s

FIGURE 2 COMPUTER-GENERATED DISPLAY OF TRAFFIC LINKS IN A 24-BY-24-MILE CENTRAL PORTION OF THE PRIMARY NETWORK FOR WASHINGTON, D.C.

For use in the synoptic model, the emissions must be expressed as hourly averages, so the average daily traffic is expressed as a function of time. The amount taken to occur within any given hour is based on the hourly distribution of trips compiled by the traffic study agencies of many areas. A typical weekday diurnal pattern of trips is shown in Figure 3. There are, however, limitations to the accuracy of the assumption that the traffic on each link is distributed like the hourly trip pattern. We know that trips taken during the morning and evening peak hours are longer than those taken during other times of the day, and that the pattern of use of different kinds of streets in different parts of the city is different, as shown by the comparison in Figure 4 of hourly volume on a freeway and a downtown arterial in the St. Louis area. It is preferable to use the data on hourly distribution of trips, rather than hourly traffic volume, because it is easier to use and more widely available. In Section V of this report, an hourly traffic pattern has been determined on the basis of statistical comparisons of calculated concentrations and those measured at the Continuous Air Monitoring Program (CAMP) Station in St. Louis. That diurnal pattern clearly reflects the traffic in the central city area around the CAMP Station.

Urban transportation studies generally do not explicitly survey or forecast weekend travel. This is because peak traffic loads on most of the facilities in the area occur on weekdays during the morning and evening commute hours. Urban highway networks are therefore designed to handle these peak loads. Because of this preoccupation with peak weekday traffic, little weekend travel data is available. It is known, however, that peak loads occur on certain rural or suburban roads used for travel to recreational areas during weekends, and that the traffic patterns on Sunday vary significantly over time and space from weekday patterns.

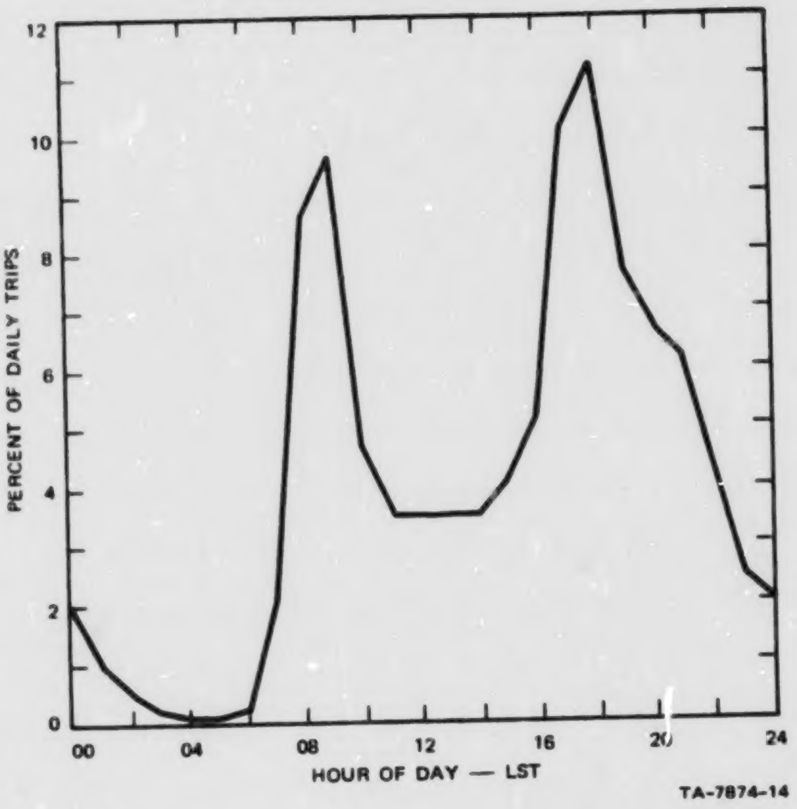

FIGURE 3 HOURLY DISTRIBUTION OF TRIPS IN WASHINGTON, D.C.

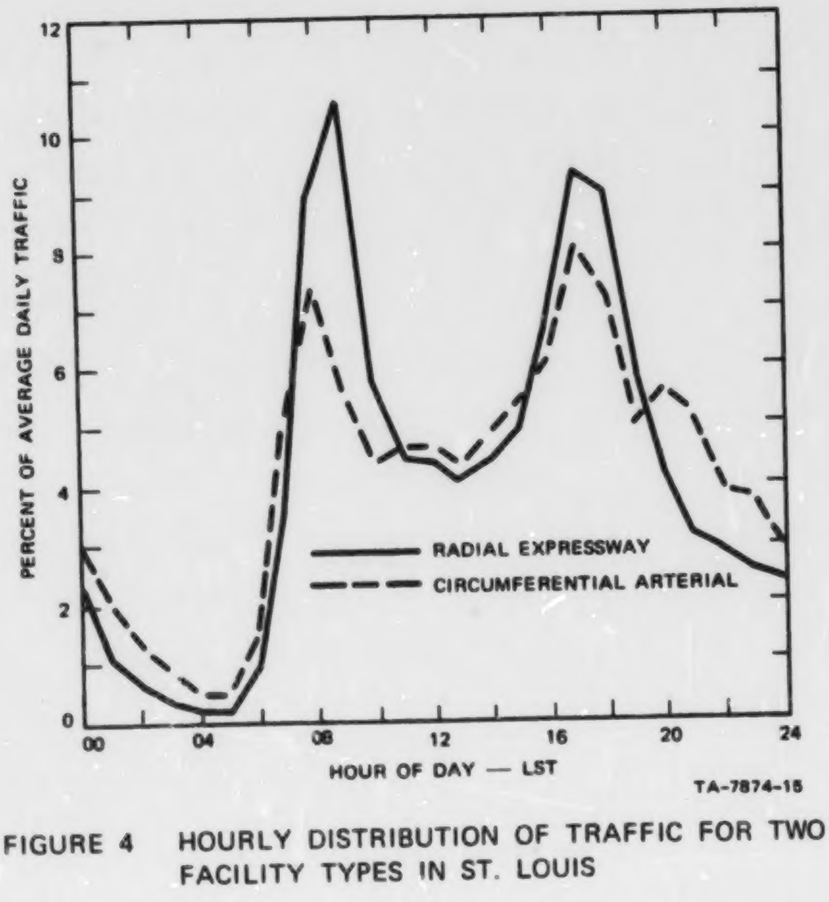

FIGURE 4 HOURLY DISTRIBUTION OF TRAFFIC FOR TWO FACILITY TYPES IN ST. LOUIS

Data that show weekend travel patterns are based upon a very limited sample--from five permanent locations in Nashville, Tennessee (Institute of Traffic Engineers, 1965). These data show that total Saturday traffic is about the same as the average daily traffic (ADT), and that total Sunday traffic is about 70 percent of ADT. Hourly traffic flows are also available from these counting stations. From these data, diurnal traffic patterns for Saturday and Sunday have been prepared and used in the diffusion model operation.

In order to calculate the contribution of the emissions from traffic links within the five closest segments, the links are first identified with the segments through which they pass. Then the length of the link that lies within a given segment is determined. The computational scheme developed for making these determinations is illustrated in Figure 5. For these calculations, the segment boundaries are taken as straightline fits to the curved boundaries illustrated in Figure 1. The coordinate system is transformed to one that originates at the receptor and is oriented in the upwind direction.

The emissions within the four segments farthest from the receptor are calculated by a different technique than that used for the closer segments. The outermost segments are larger than those nearby, and it was felt that the spatial resolution achieved by the link assignment technique was not necessary when the emissions were to be averaged over the entire large area of each outer segment. The scheme that was developed requires less computation time than the link assignment method.

Before other computations begin, the city is divided into a grid of one-mile (1.6 km) squares. The traffic link data are used to determine the average daily CO emission in each of these squares. This is accomplished by dividing each link into small increments, less than 0.08 km long. The average daily emission from each of these small pieces

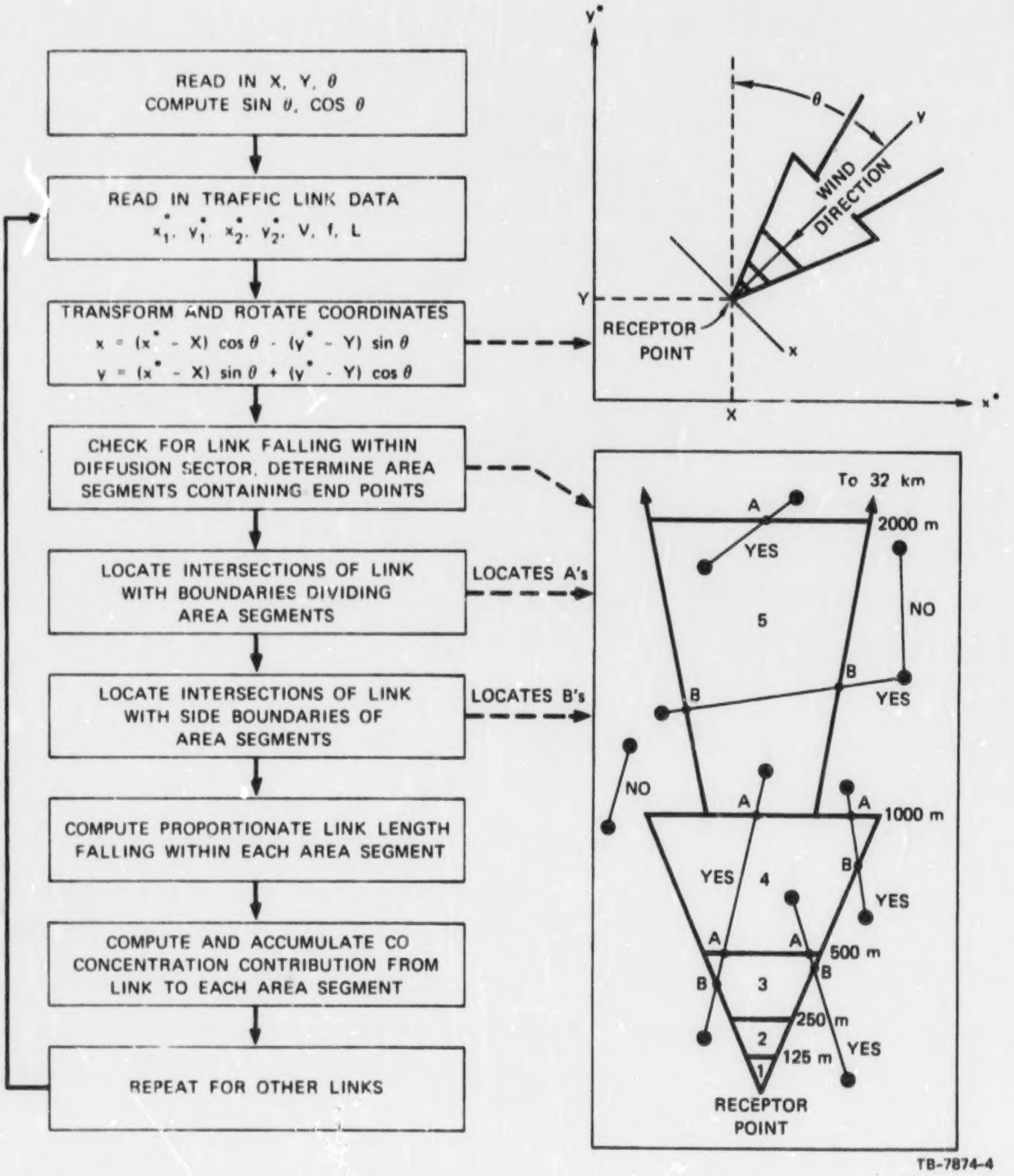
READ IN X, Y, θ
COMPUTE SIN θ, COS θ
READ IN TRAFFIC LINK DATA
x*1, y*1, x*2, y*2, V, f, L
TRANSFORM AND ROTATE COORDINATES
x = (x* − X) cos θ − (y* − Y) sin θ
y = (x* − X) sin θ + (y* − Y) cos θ
CHECK FOR LINK FALLING WITHIN DIFFUSION SECTOR, DETERMINE AREA SEGMENTS CONTAINING END POINTS
LOCATE INTERSECTIONS OF LINK WITH BOUNDARIES DIVIDING AREA SEGMENTS
LOCATES A's
LOCATE INTERSECTIONS OF LINK WITH SIDE BOUNDARIES OF AREA SEGMENTS
LOCATES B's
COMPUTE PROPORTIONATE LINK LENGTH FALLING WITHIN EACH AREA SEGMENT
COMPUTE AND ACCUMULATE CO CONCENTRATION CONTRIBUTION FROM LINK TO EACH AREA SEGMENT
REPEAT FOR OTHER LINKS
y*
θ
y
WIND DIRECTION
Y
RECEPTOR POINT
x
X
x*
To 32 km
2000 m
A
YES
NO
5
B
YES
B
NO
A
A
1000 m
YES
4
B
YES
A
A
500 m
B
B
3
250 m
2
125 m
1
YES
RECEPTOR POINT
TB-7874-4

FIGURE 5 SIMPLIFIED SCHEMATIC DIAGRAM OF TRAFFIC LINK ASSIGNMENT SUBROUTINE USED FOR THE FIVE SEGMENTS CLOSEST TO THE RECEPTOR

is determined by assuming emissions are spread uniformly along the link. Then, the emissions from all the small pieces of link within a square are added together to give total daily emissions for that square. This total is paired in the computer memory with the coordinates of the point at the center of the square. These calculations are done only once for the city.

A trapezoidal grid system is used in the four outer emission segments. As the location of the receptor changes or the wind direction changes, these trapezoidal grids are superimposed on different parts of the fixed city emission grid described in the preceding paragraph. Figure 6 shows a superposition of a movable trapezoidal grid (marked by the circles) on the fixed city grid (marked by the crosses). The average emissions at each point on the trapezoidal grid are determined by interpolation between the values at the points on the fixed grid. The average of the emission values determined for the points on the trapezoidal grid defines the emission rate for the segment.

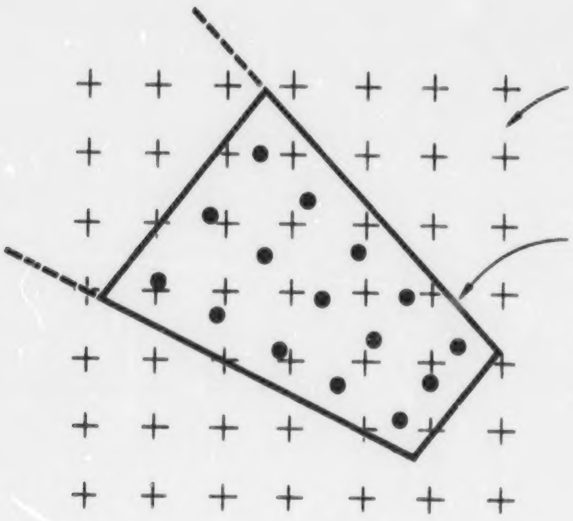

Small section of fixed emission grid (crosses). The CO emission per unit area is initially computed at these grid points from traffic link data.

Eighth segment of diffusion sector and movable trapezoidal grid (circles). Emission values for segment grid are interpolated from the values of the fixed emission grid (crosses).

TA-7874-77

FIGURE 6 ILLUSTRATION OF THE GRID-POINT TRANSFORMATION TECHNIQUE USED FOR COMPUTING THE CO EMISSIONS WITHIN THE FOUR MOST DISTANT SEGMENTS

A technique similar to that just described was used to determine the emissions due to traffic on the secondary streets. The average secondary emissions were determined for squares two miles (3.6 km) on a side (see Section III-A-3). The secondary emissions were then determined from the value on the fixed two-mile grid for each of the nine movable segments, using basically the same superimposed-grid technique just described. However, for the small segments near the receptor, the trapezoidal grid was replaced by a single point at the segment center. Once the emissions due to the secondary traffic were determined, they were added to those already determined, either directly (for the first five segments) or indirectly (for the outermost segments), from the primary traffic link data.

Traffic data sources and the data handling varied with the use of the model. Data obtained from measurements of past traffic were used as inputs to produce comparisons with the CAMP Station data. Traffic forecasts were used to calculate pollution concentrations for future years. The traffic data were obtained and treated as described below.

2. Calculation of Primary Network Emissions Using Historical Data

Historical data for the network description, the node coordinates, and link distances are obtained from highway and street maps. The network is described by assigning numbers to the intersections, or nodes, of the network and by identifying the pairs of nodes that are connected by links. The coordinates of the nodes establish the locations of the traffic links in the network. Link distances are measured along the links, rather than as the shortest distance between the nodes, although, as noted in the preceding section, the assignment of the emissions assumes that the link is a straight line between the nodes.

Historical link-volume data are obtained from traffic departments in the cities, towns, and counties in the region being studied. These agencies sample traffic volumes by means of portable counting units and a few fixed installations. Their observations may be almost continuous, or as infrequent as once every two or three years. Because traffic varies according to seasonal, weekly, and daily cycles, an observation of volume for one day must be adjusted for the weekly and seasonal fluctuations. The resultant corrected value is recorded as the average daily traffic (ADT) for that location.

The emission rate, e (g/vehicle-mile), is determined from the equation

$$e = c\ S^{\beta} \qquad \text{(III-1)}$$

where S is the average speed over the link, in mi/hr, and c and β are constants. For vehicles in use before exhaust control systems, $c = 1121$ and $\beta = -0.849$, as determined by Rose et al. (1964) from observations on a number of vehicles in several locations.

Link speeds for use in the emission rate calculation are determined from averages for peak and off-peak travel hours on various kinds of route facilities. Speed data were obtained from the traffic survey. For example, speeds used in the Washington, D.C., area were based upon the study by Wilbur Smith and Assoc. (1958) and are shown in Table I.

For other locations, the peak traffic hour speeds were taken as equal to 80 percent of the off-peak speeds. Peak-hour speeds were generally assigned to the four heaviest traffic hours of the day.

Table I

AVERAGE SPEEDS FOR WASHINGTON, D.C., HIGHWAY FACILITIES

Facility Type	Average Speeds (mi hr) Peak Traffic Hours (0700-0900, 1600-1800)	Off-Peak Traffic Hours (0000-0700, 0900-1500, 1800-0000)
Suburban Freeway	42	48
Downtown Freeway	33	39
Suburban Arterial	30	36
Downtown Arterial	24	30
Local or Feeder Street	10	12

Accuracy of the historical data is limited by the frequency with which it is recorded and by the accuracy of the factors used to correct it to average daily traffic. However, since locations with heaviest traffic are generally monitored most often, the most confidence may be placed in data of highest volumes.

3. Calculation of Secondary Traffic Emissions Using Historical Data

The number of vehicle-miles traveled on streets not represented by the primary network is computed from an estimate of the total vehicle-miles traveled in the area and the total vehicle-miles on the links of the primary network. The local street mileage is taken to be the difference between the two. It is distributed over the study area by estimating the relative density of local streets as opposed to parks, open spaces, or streets already coded, for each four-square-mile area in a two-mile-by-two-mile grid covering the area. The emissions from the local street travel in a given square are assumed to emanate uniformly from that square. Although the emission per mile per vehicle is high on these local streets because of low speeds, the overall contribution is small because of the small number of vehicles on these local streets.

4. Calculation of Emissions Using Forecast Traffic Data

Most urban areas in the United States have completed or are conducting an area-wide transportation study to determine traffic demands and transportation facility needs for future years, e.g., 1980 or 1990. Such studies are required for participation in federal highway programs. An important result of these studies is a design of a future traffic network for the area and a forecast of the traffic volumes on the links of this network. The procedure for conducting these studies has been highly developed and partially standardized (see Appendix B). The emission inventory components of the model are designed so that the network description (including link length and facility types), link volume, and link speed data of the widely used traffic-planning computer programs, in magnetic tape form, can serve as input for the diffusion model. In most cases, the only manual step required will be the measurement and coding of node coordinates for the network.

Traffic forecasts include travel on both primary and secondary networks. The primary network links are usually represented in the analysis just as they appear on the street map. However, local or feeder streets are represented in the traffic forecast analysis as connectors between the assumed center of population of a traffic zone, where all traffic in that zone is assumed to originate, and points on the primary network. The vehicle-miles on connector links therefore approximate those expected on local streets, but the traffic is concentrated on a few links, rather than spread over a broad area. This is compensated for in the model by averaging the emissions from these links over a background grid. The connector links never explicitly appear in the spatial positioning process where individual links are analyzed.

Accuracy of the forecast traffic data is difficult to establish. One study that sought to appraise the accuracy of earlier forecasts was unsuccessful in finding a case where the planning recommendations had been followed sufficiently closely to make the actual situation equivalent to the conditions for which the forecast was made (Highway Research Board, 1968). Checks made to establish the adequacy of calibration of the forecasting models are usually considered successful if the forecast for present conditions gives link volumes in wide corridors within 10 to 20 percent of counted volumes. Variations between the volumes on individual streets within the corridor may be much wider since the models do not distinguish between parallel routes as readily as do drivers.

Historical emission rates were computed from a formula derived from emission data taken from actual highway driving. Comparable data for the 1966-70 model vehicles are not available. It was therefore necessary to develop a baseline of performance for the 1968-70 autos in order to apply the proportional controls for future model years. The controls used in the 1968-70 era improved emission performance for acceleration, deceleration, and idle conditions more than for steady cruise conditions. Since the acceleration, deceleration, and idle conditions are more prevalent at the lower average speeds, the greatest reduction in emissions due to new control devices is realized for the lower average speeds.

To determine the approximate nature of the improvement, data on an engine with and without emission controls (Beckman et al., 1967) have been used together with data on driving conditions encountered on various types of roads. These driving data were collected by SRI for an earlier project. A computer program was developed to determine the carbon monoxide emissions per mile versus average speed for route segments sampled in the road-test data.

One hundred thirty-nine emission values were calculated from emission data presented by Beckman et al. (1967) and from actual observations of speeds, speed changes, and stops for a variety of road types and traffic congestion conditions. Regression analysis was used to examine the relation between emissions and average speed, both with and without controls. The following power function proved to be the best fit for 1969 model year automobiles:

$$e = 245\ S^{-0.48} \quad , \qquad \text{(III-2)}$$

where e is the carbon monoxide emission in grams per mile, and S is the average speed on the network link in miles per hour.

Increasingly stringent regulations on exhaust emissions will require further reductions in CO emissions from automobiles. The best estimates of future levels of controls are that allowable emission values on the test cycle will be reduced from the equivalent of 34 grams per mile (1.5 percent by volume) in 1969, measured on the federal test cycle, to 4.5 grams per mile on the test cycle for 1980 and later model year automobiles. These values were derived from estimates provided by Mr. Seward of the Ford Motor Company and from work done at NAPCA (Rose and Krostek, 1969). Although it has been shown that emissions at lower speeds were reduced more than at higher speeds for the 1969 controls, the best estimates of future emission control performance is that emissions will be reduced by the same amount under all engine performance conditions. Therefore, a proportional reduction of the emission model coefficient, equal to the ratio of the allowable emission values in 1969 and 1980, has been applied to the 1969 emission model to make it applicable to post-1980 automobiles. The resulting emission model for 1980 and later model year automobiles is:

$$e = 34\ S^{-0.48} \quad , \qquad \text{(III-3)}$$

where e and S are as defined before.

B. Meteorological Inputs

1. Gaussian Standard Deviation Function

The Gaussian model requires that we know how the standard deviation, σ_z, of the vertical distribution of the concentration from a line source changes as the pollutants travel downwind. There are several authorities for these functions (see Slade, 1968). In one approach different functions are given for different atmospheric stabilities. In the other approach, a single function is specified, containing parameters whose values may depend on the stability or turbulent mixing conditions.

There are several criteria for the selection of one set of functions over another. First, the functions should describe diffusive behavior as accurately as possible. For our model, they must be capable of being accurately approximated by power functions over the intervals defined by the boundaries of the model's emission segments. Finally, and very importantly, the proper function or parametric values for a given atmospheric stability must be easily determinable from routine meteorological observations. With regard to the last item, it is preferable that the functions be determinable from observations made at short intervals, rather than from those made only once or twice a day. The observations should also be made within the environs of the city being studied. Thus functions dependent upon hourly surface meteorological observations are preferable to those based on the twice-daily upper air observations.

Several authors have given estimates of σ_z as a function of atmospheric stability and the distance that a cloud or plume has traveled (e.g., Hilsmeier and Gifford, 1962; Smith, 1968; Pooler, 1961). On the basis of the criteria presented earlier, we have selected a set of curves developed by Gifford (1961) from Pasquill's (1961) work. In this presentation, atmospheric turbulent conditions are divided into six categories, and a curve of σ_z versus distance traveled is given for each of the six. Methods for selecting the proper stability category have been developed; these are discussed in the next section.

After selecting the Pasquill-Gifford curves, they were approximated by power functions as required by the model. The behavior of the cloud has not been defined by Pasquill or Gifford for distances less than 100 m. Pooler (1966) and McElroy (1969) have found that there is an initial rapid mechanical mixing of pollutants released from ground level sources in urban areas. To approximate this effect the pollutants were assumed to mix immediately upon release to the point where σ_z was equal to its value at 125 m according to the Pasquill-Gifford curves. It then remains constant at that value throughout the first segment. Using this assumption, the Pasquill-Gifford curves were extended to very short travel distances.

For those conditions where there is rapid mixing, σ_z quickly becomes very large. The Pasquill-Gifford curves do not extend to values of σ_z greater than 3 km. Because the box model will generally be in effect for such large values of σ_z, and because the ground level concentrations accompanying these large σ_z's will, in any event, be very small, it was felt that the curves could be arbitrarily extrapolated beyond σ_z values of 3 km without serious consequence to the calculated results.

Figure 7 shows the σ_z curves used for the calculations with the model. For the first segment ($i = 1$, $r < 125$ m), σ_z is a constant for each stability type, j. Beyond that the Pasquill-Gifford curves have been approximated by the power law representations--shown as straight line segments on the log-log plot.

Although the model currently is based on the Pasquill-Gifford specification of σ_z as a function of travel distance, it would be a simple matter to change to another specification should that be desired. All that is required is a new set of constants, the a_{ij}'s and b_{ij}'s in Eq. (II-3), to describe the new functions. As long as the new functions are described by exponential expressions, the rest of the basic model remains the same.

2. Stability Category

Once we have a set of σ_z functions, we must be able to select the proper one for the calculations. Methods were sought for determining atmospheric stability from conventional meteorological measurements. To be useful, any method chosen had to define stability in a way that was consistent with the definitions used originally to determine the σ_z functions. Other sets of σ_z functions might require different approaches than those given in this section.

Two methods of stability determination have been used with this model. One was developed from Pasquill's criteria by Turner (1964) for use with another model and was simply cast in computer-compatible form for these studies. Turner's technique was used for the examples

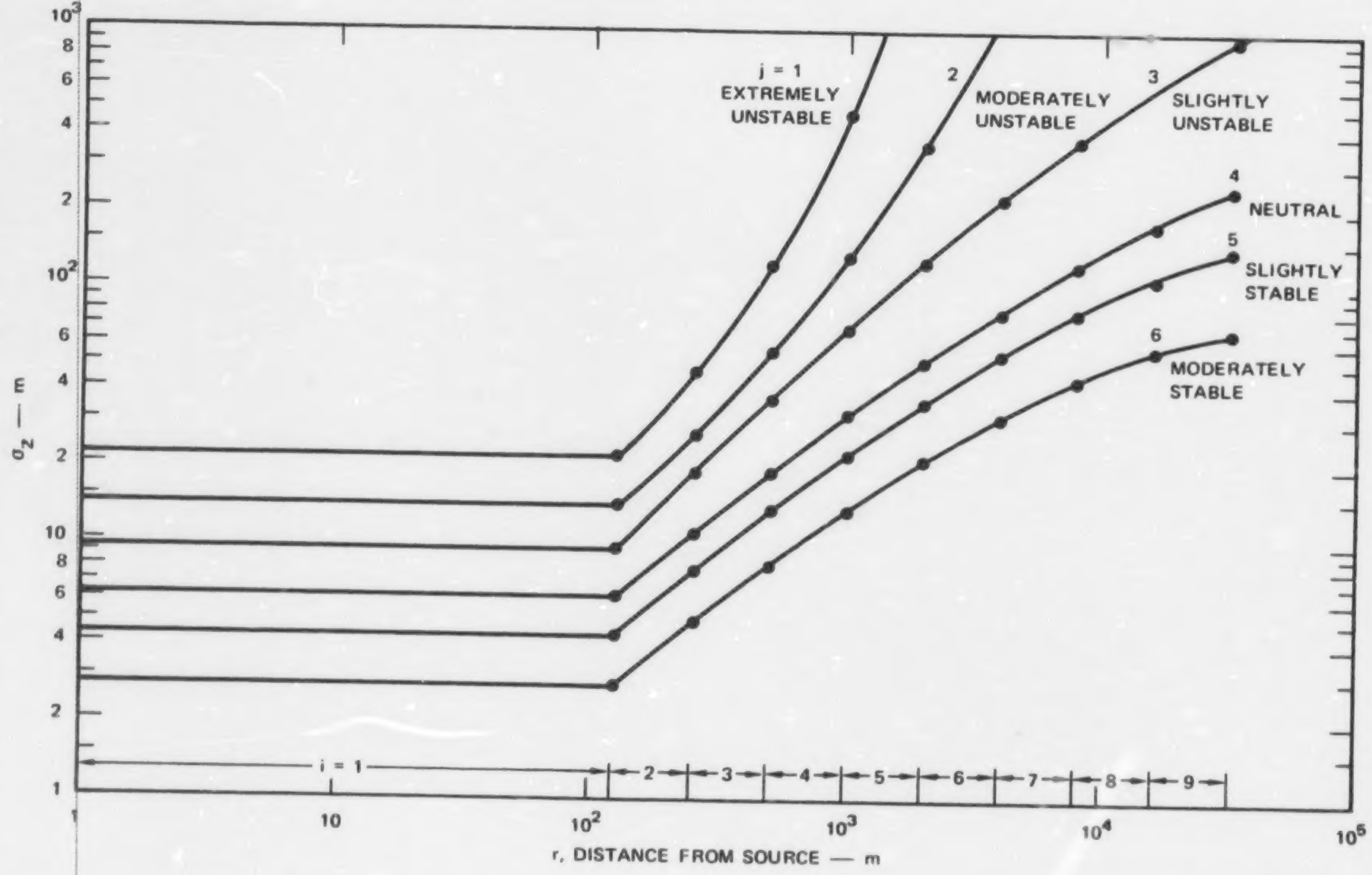

TA-7874-46

FIGURE 7 σ_z FUNCTIONS USED IN THE MODEL of synoptic calculations given in later sections. Because this method was rather complicated, we returned to the original definitions of stability used by Pasquill to classify his data and developed a somewhat simpler approach directly from these. This technique was used for the climatological examples presented in later sections. The two methods generally, but not always, give the same stability category for a given set of data. The methods are described in more detail in Appendix C.

3. Mixing Depth

To apply the box model it is necessary to know the depth to which the pollutants will be mixed. Considerable effort was expended to find a method of estimating mixing depth that required only surface meteorological observations. Our attempts started with the assumption that the daytime mixing depth should be closely related to the amount of heat added to the lower layers of the atmosphere and to the resulting change in temperature during the period of heating. When mixing depths were determined by these methods and compared with mixing depths determined from temperature soundings, it was found that the two sets of values were virtually uncorrelated. For this reason we were forced to use upper air data, either directly or indirectly, to determine mixing depth. We had hoped to avoid the use of these extra data for reasons of simplification. At this time, that does not seem feasible.

Two methods have been devised for calculating mixing depth. They are described in detail in Appendix D. The method used for the synoptic calculations presented in later sections of this report uses the morning temperature sounding taken by the nearest U.S. Weather Bureau station. This sounding, when combined with the afternoon maximum temperature, allows us to calculate an afternoon mixing depth. Early morning mixing depths make use of a simple model of the mixing layer over urban areas proposed by Summers (1966) and an empirical relationship among city size and urban and rural nighttime temperatures developed by Ludwig (1970). A single value of mixing depth is assumed to apply throughout the urban area, although mixing depth variations have been observed by Clarke (1969) and Bornstein (1969), and modeled in limited fashion by Summers (1966) and Leahey (1969).

The other method, which has been used with the climatological model, is basically the same, but makes use of preprocessed mixing depth data obtained from Mr. George Holzworth of the National Air Pollution Control Administration. Use of Mr. Holzworth's tabulations simplifies the data processing.

Neither method discussed above provides values of mixing depth for all hours of the day, so interpolation must be used. Again, two methods were employed. For the climatological model, mixing depth was interpolated on the basis of time between its early morning and its afternoon values. The synoptic model interpolated hourly mixing depths on the basis of observed hourly temperatures for daylight hours and on the basis of time for the premidnight evening hours. Both interpolation schemes assumed that mixing depth remained constant during the hours between midnight and dawn. The reasons for this are discussed in Appendix D. In general, all the methods gave consistent, though not identical, results.

4. Wind Speed and Direction

The wind velocity is the only input parameter that is available as a routine measurement. However, these observations are mostly taken at airports, where the surface roughness and atmospheric stability are generally quite different than within the built-up part of the city. It is known that these different conditions cause variations in wind speed and direction between the outskirts (where the airports are located) and the center of the city. Available measurements of these wind variations, however, are fairly meager.

In one study, Graham (1968) found an urban/rural average wind speed ratio for Ft. Wayne of 0.67 at 15-m height and 0.64 at 60 m. These observations also show the wind direction over the city to be backed by 10° to 15° from that at the outskirts. In Nashville, Schnelle et al. (1969) found the roof-level wind speed (U_r) to be related to the airport wind speed (U_a) as

$$\overline{U}_r = 0.33\ \overline{U}_a + 1.0\ \mathrm{m/s} \quad , \qquad \text{(III-4)}$$

where the overbars refer to daily averages. These results are mostly for daytime conditions. At night the wind speed at low levels over the city is likely to be higher than that at the airport, due to the greater mechanical and thermal mixing and the presence of convective local circulations over the city.

In view of the uncertainties in our knowledge of the modification of the airflow by the city, we have used the airport surface wind velocity measurements directly as the transport wind input for the model. Particularly for daytime use, this may not be a bad approximation. Although the airport surface wind is generally higher (in daytime) than the urban "surface" wind, the appropriate input for the model is a mean wind in the layer between from 50 to 100 m above the surface. Since the wind speed increases with height, a higher wind speed than that at the urban "surface" is appropriate, and the higher airport wind may help compensate for this.

At any rate, we have used airport winds directly[*] in the model trials, with the idea of correcting the winds for urban effects later by using a statistical technique to adjust the wind input for the best agreement between observed and calculated CO concentrations. The results of this "calibration" procedure are given in Section V-B.

A further point of some importance is that the present model cannot handle the case of calm winds (which are fairly common at airports) without some adjustments. The nocturnal urban circulation for the stagnation case has been reasonably well documented (e.g., Pooler, 1963; Hilst and Bowne, 1966; Clarke, 1969) and takes the form of a convective cell driven by the urban heat island. On this basis, and taking into account the fact that most anemometers will not respond to very light winds, we assume in the model a minimum speed of 1.0 m/s[†] for an airport wind reported as calm. We assume further that the wind direction is the same as the most recently measured direction. Other approaches to this problem are possible, but they require the development of special models, which was beyond the scope of this first-year's work.

---

[*] In terms of direction, to the nearest 10° or sixteenth point of the compass, as appropriate for the different model configurations.

[†] In some of the early calculations, a minimum speed of 2.0 m/s was used.

IV ORGANIZATION AND APPLICATIONS OF THE SYNOPTIC AND CLIMATOLOGICAL MODELS

A. Introduction

The synoptic model takes the data for a single hour, calculates and displays concentrations for one or more points within the city for that hour, and then proceeds to the next hour. This is repeated on an hour-by-hour basis for some limited time period of interest. The temporal changes of concentration for a specific location can be compared with the measured values during the same period. The climatological model provides the statistics of CO concentration for different locations and various averaging periods.

It was originally planned that the two models would employ significantly different approaches. The synoptic model was to calculate concentrations, in sequence, using hour-by-hour meteorological observations, whereas the climatological model was to use meteorological statistics to determine the frequency of occurrence of different CO concentrations.

As the work has proceeded, the constraints imposed on the climatological model, particularly by the requirements for the statistics of the concentrations averaged over periods longer than an hour, have caused the climatological model to become very much like the synoptic model. The two models are discussed in the following sections: first the synoptic, then the climatological model. This order is important because the climatological model eventually developed through simplification of the synoptic model. In its final version, it appears that the climatological model could very serviceably replace the synoptic model with little sacrifice in accuracy.

Preceding page blank

B. The Synoptic Model

1. Description

The organization of the synoptic model is shown in Figure 8. In this flow chart it is assumed that the traffic data for the city are already stored and that the inputs consist of the meteorological parameters and the city population and latitude. These items are necessary for the application of the subroutines for computing stability category and the mixing depth. The calculations start by determining the afternoon and early morning mixing depths from the appropriate sounding. Then the meteorological parameters for the starting hour are read and the stability class determined. Mixing depths are interpolated by the appropriate method, concentrations are calculated, and then the next hour's data are read.

The calculations referred to in the box with the double outline in Figure 8 are performed using the basic models. The appropriate form of the model, Gaussian or box, must be applied in each of the upwind segments. Thus, the Gaussian formula, Eq. (II-4), is used for all segments up to the distance, r_T, that marks the transition to the box model. The box model, Eq. (II-5), is used for those segments beyond r_T. If r_T occurs in segment N, then the model is summarized by the following equation

$$C = \frac{1}{u}\left\{\sum_{i=1}^{N-1}\bar{Q}_i\left[\frac{0.8\left(r_{i+1}^{1-b_{ij}} - r_i^{1-b_{ij}}\right)}{a_{ij}\left(1 - b_{ij}\right)}\right] + \bar{Q}_N\left[\frac{0.8\left(r_T^{1-b_{ij}} - r_N^{1-b_{ij}}\right)}{a_{ij}\left(1 - b_{ij}\right)} + \frac{r_{N+1} - r_T}{h}\right] + \sum_{i=N+1}^{9}\bar{Q}_i\left[\frac{r_{i+1} - r_i}{h}\right]\right\} . \qquad \text{(IV-1)}$$

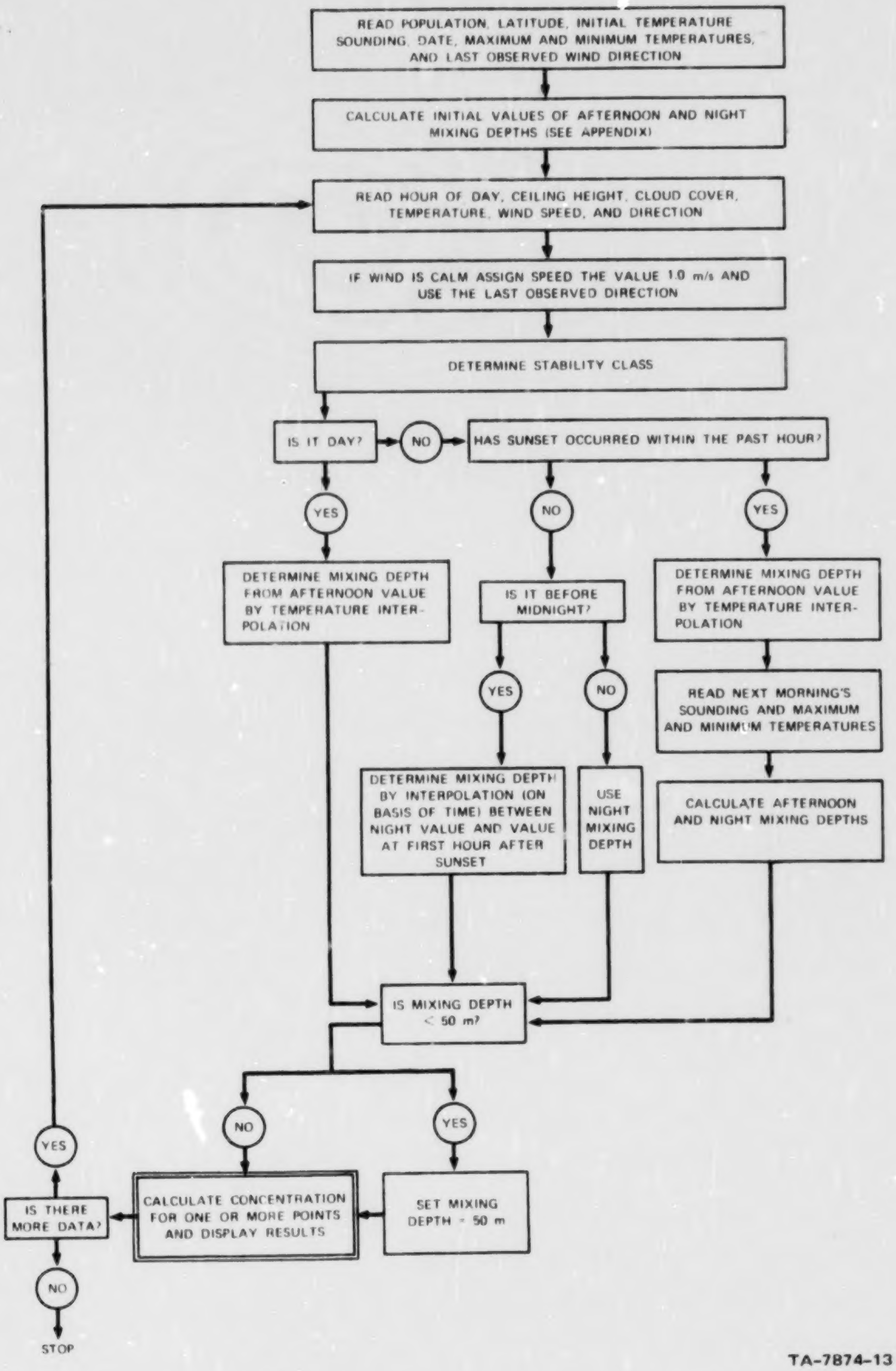
READ POPULATION, LATITUDE, INITIAL TEMPERATURE SOUNDING, DATE, MAXIMUM AND MINIMUM TEMPERATURES, AND LAST OBSERVED WIND DIRECTION
CALCULATE INITIAL VALUES OF AFTERNOON AND NIGHT MIXING DEPTHS (SEE APPENDIX)
READ HOUR OF DAY, CEILING HEIGHT, CLOUD COVER, TEMPERATURE, WIND SPEED, AND DIRECTION
IF WIND IS CALM ASSIGN SPEED THE VALUE 1.0 m/s AND USE THE LAST OBSERVED DIRECTION
DETERMINE STABILITY CLASS
IS IT DAY?
NO
HAS SUNSET OCCURRED WITHIN THE PAST HOUR?
YES
NO
YES
DETERMINE MIXING DEPTH FROM AFTERNOON VALUE BY TEMPERATURE INTERPOLATION
IS IT BEFORE MIDNIGHT?
DETERMINE MIXING DEPTH FROM AFTERNOON VALUE BY TEMPERATURE INTERPOLATION
YES
NO
READ NEXT MORNING'S SOUNDING AND MAXIMUM AND MINIMUM TEMPERATURES
DETERMINE MIXING DEPTH BY INTERPOLATION (ON BASIS OF TIME) BETWEEN NIGHT VALUE AND VALUE AT FIRST HOUR AFTER SUNSET
USE NIGHT MIXING DEPTH
CALCULATE AFTERNOON AND NIGHT MIXING DEPTHS
IS MIXING DEPTH < 50 m?
NO
YES
YES
IS THERE MORE DATA?
CALCULATE CONCENTRATION FOR ONE OR MORE POINTS AND DISPLAY RESULTS
SET MIXING DEPTH = 50 m
NO
STOP

TA-7874-13 R

FIGURE 8 SIMPLIFIED FLOW CHART FOR SYNOPTIC MODEL CALCULATIONS. Using radiosonde data, Turner's stability index and temperature interpolation.

This equation can be expressed in simplified fashion as

$$C = \frac{1}{u} \sum_{i=1}^{9} \bar{Q}_i \left[\frac{\chi}{Q}\right]_{ij} \quad . \tag{IV-2}$$

In the simplified version the terms $[\chi/Q]_{ij}$ refer to the appropriate square-bracketed terms in Eq. (IV-1).

The application of the equation to the calculation of concentration is shown in the simplified flow chart of Figure 9. This flow chart is a description of the calculations required in the box with the double outline in Figure 8.

2. Applications

The synoptic model, as described above, has been used in two different types of application. In one type, concentration is calculated for a single hour at 625 points in a square grid covering all or a selected area of a city. These 625 values are then used for an isopleth analysis. The other application presents the calculated CO concentrations at hourly intervals for a week.

We have taken advantage of computer techniques for objective contour analysis and graphical display. In this work we have used special subroutines called "CONTOOR" and "GRAPH 4"* with the CDC 6400 computer and the CDC 280 cathode-ray tube (CRT) peripheral display system. The CONTOOR subroutine furnishes objective isolines describing the CO concentration distribution over an urban area, on the basis of the grid point values calculated by the diffusion model. These automatic graphical techniques expedite trial and evaluation procedures.

---

*These subroutines were developed, respectively, by S. Briggs and B. Sifford of Stanford Research Institute.

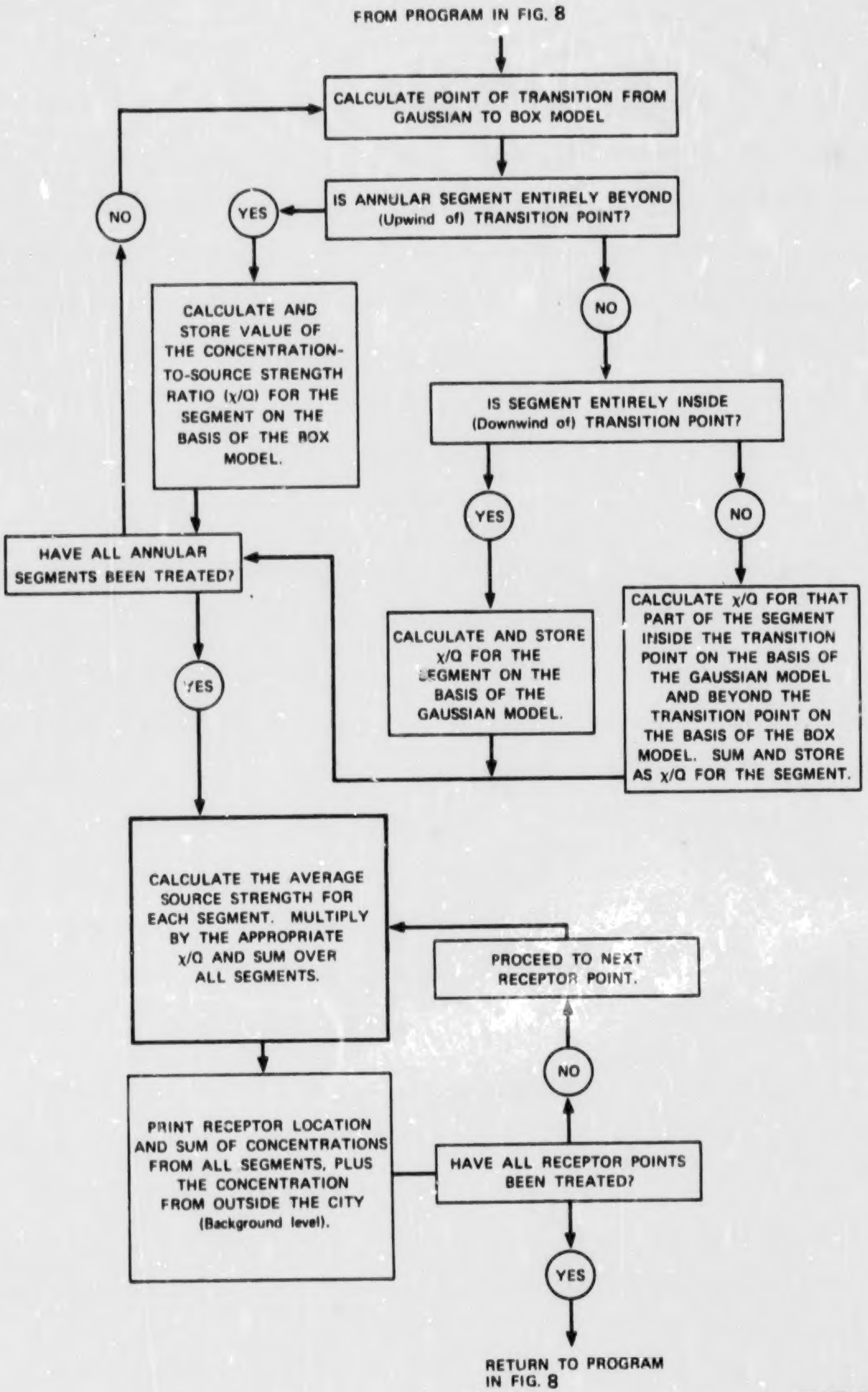
FROM PROGRAM IN FIG. 8
CALCULATE POINT OF TRANSITION FROM GAUSSIAN TO BOX MODEL
IS ANNULAR SEGMENT ENTIRELY BEYOND (Upwind of) TRANSITION POINT?
YES
NO
CALCULATE AND STORE VALUE OF THE CONCENTRATION-TO-SOURCE STRENGTH RATIO (χ/Q) FOR THE SEGMENT ON THE BASIS OF THE BOX MODEL.
NO
IS SEGMENT ENTIRELY INSIDE (Downwind of) TRANSITION POINT?
YES
NO
HAVE ALL ANNULAR SEGMENTS BEEN TREATED?
YES
CALCULATE AND STORE χ/Q FOR THE SEGMENT ON THE BASIS OF THE GAUSSIAN MODEL.
CALCULATE χ/Q FOR THAT PART OF THE SEGMENT INSIDE THE TRANSITION POINT ON THE BASIS OF THE GAUSSIAN MODEL AND BEYOND THE TRANSITION POINT ON THE BASIS OF THE BOX MODEL. SUM AND STORE AS χ/Q FOR THE SEGMENT.
CALCULATE THE AVERAGE SOURCE STRENGTH FOR EACH SEGMENT. MULTIPLY BY THE APPROPRIATE χ/Q AND SUM OVER ALL SEGMENTS.
PROCEED TO NEXT RECEPTOR POINT.
NO
PRINT RECEPTOR LOCATION AND SUM OF CONCENTRATIONS FROM ALL SEGMENTS, PLUS THE CONCENTRATION FROM OUTSIDE THE CITY (Background level).
HAVE ALL RECEPTOR POINTS BEEN TREATED?
YES
RETURN TO PROGRAM IN FIG. 8
TB-7874-2 R

FIGURE 9 SIMPLIFIED FLOW CHART FOR CONCENTRATION CALCULATIONS. Corresponds approximately to the box with the double outline in Figure 8.

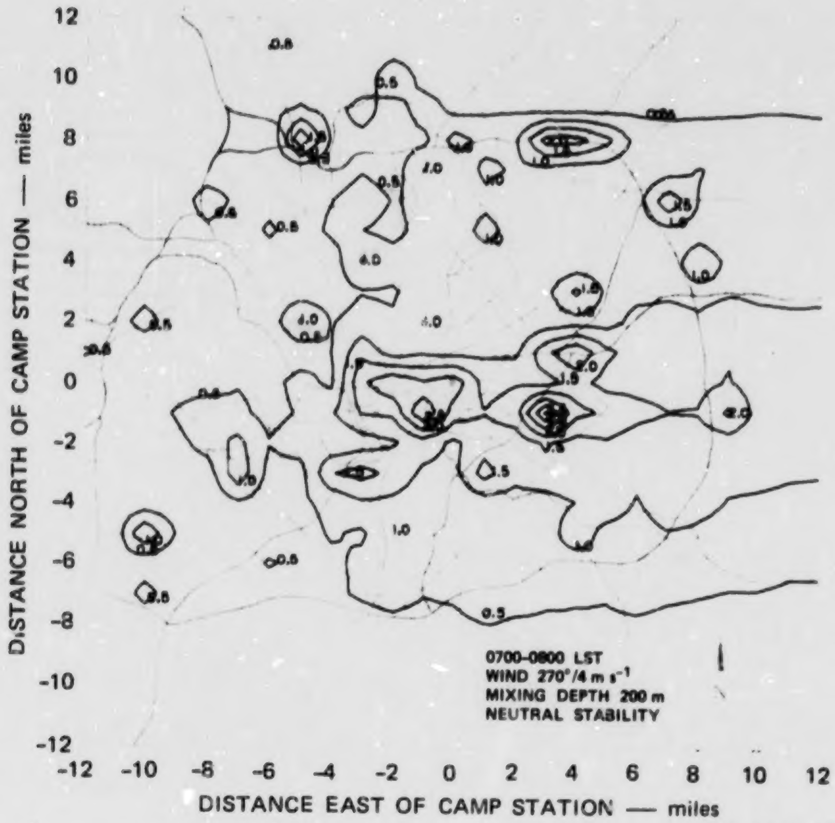

TB-7874-9s

(a) MACHINE ANALYSIS

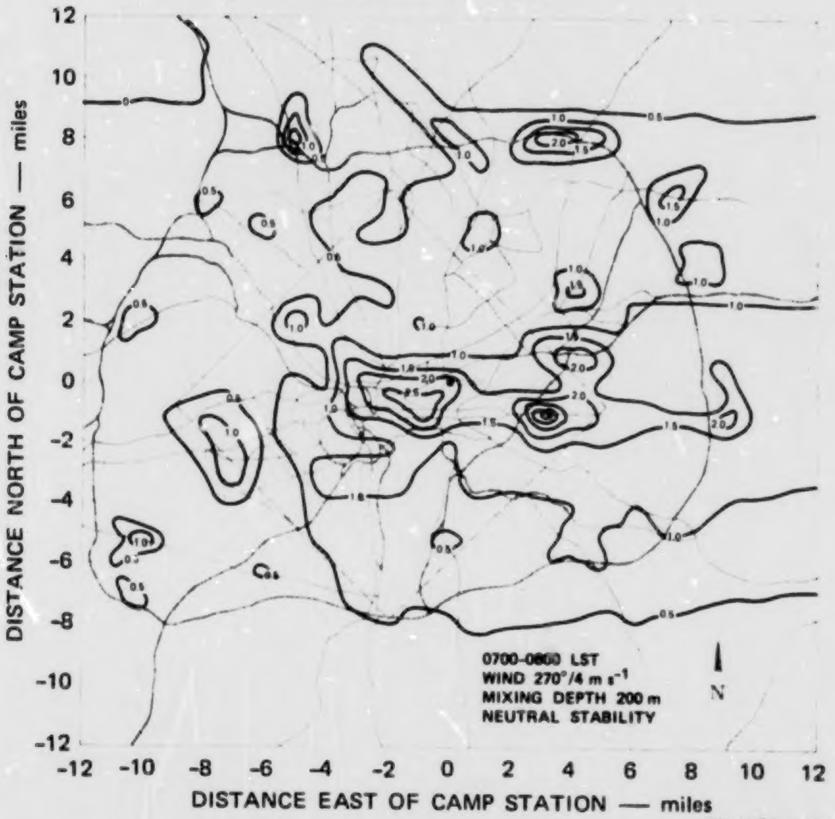

TB-7874-8s

(b) SUBJECTIVE ANALYSIS

FIGURE 10 CALCULATED WASHINGTON, D.C., CONCENTRATION PATTERNS

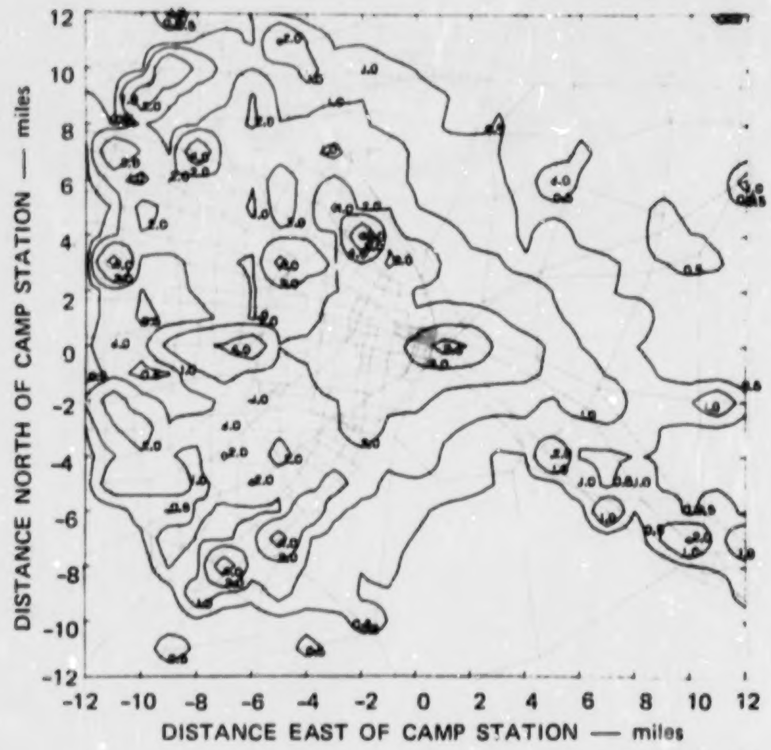

TA-7874-25s

(a) BASED ON HISTORICAL TRAFFIC DATA

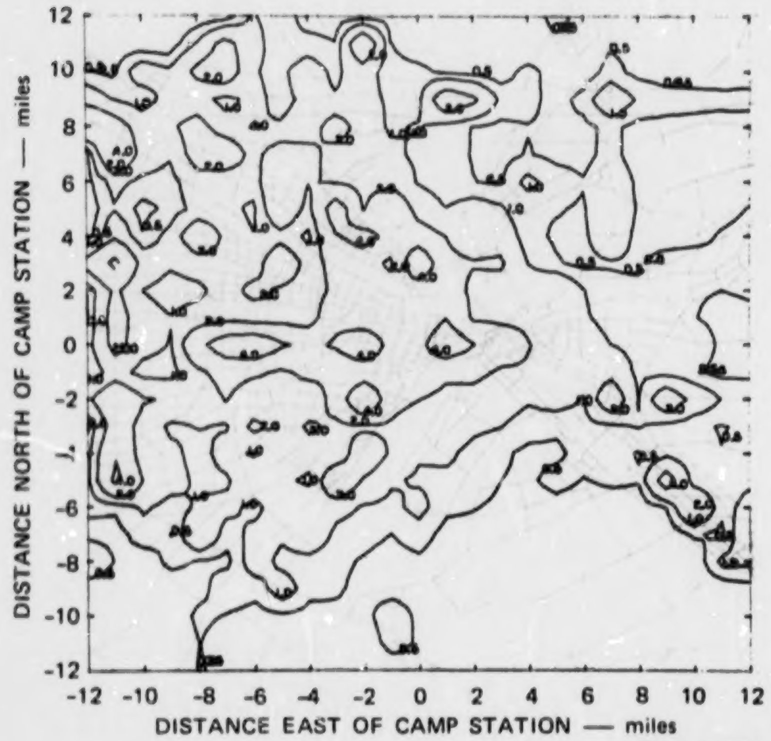

TA-7874-60

(b) BASED ON SIMULATED FORECAST TRAFFIC DATA

FIGURE 11 CALCULATED ST. LOUIS CONCENTRATION PATTERNS 0700-0800, 15 OCTOBER 1964

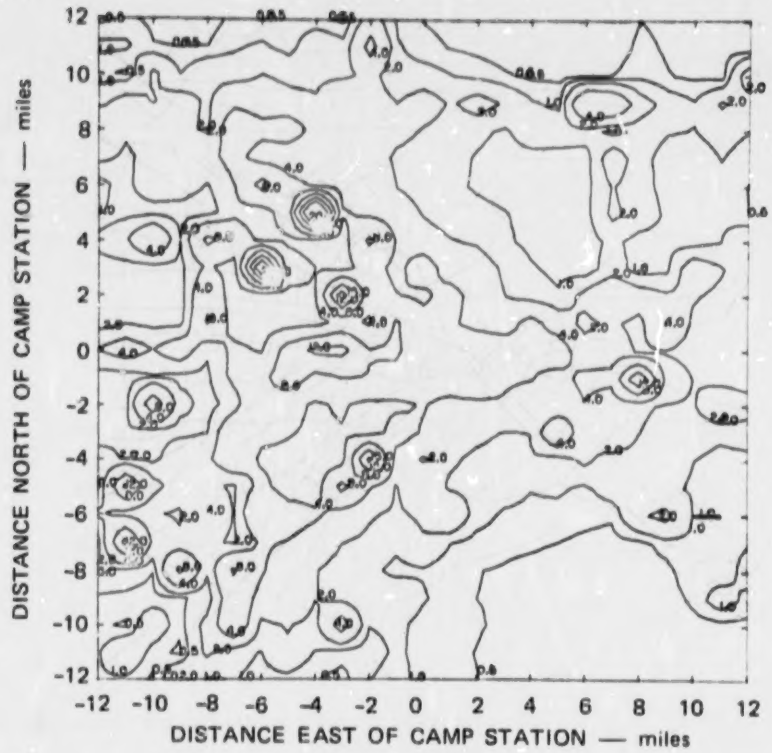

(a) WITHOUT EXHAUST EMISSION CONTROLS

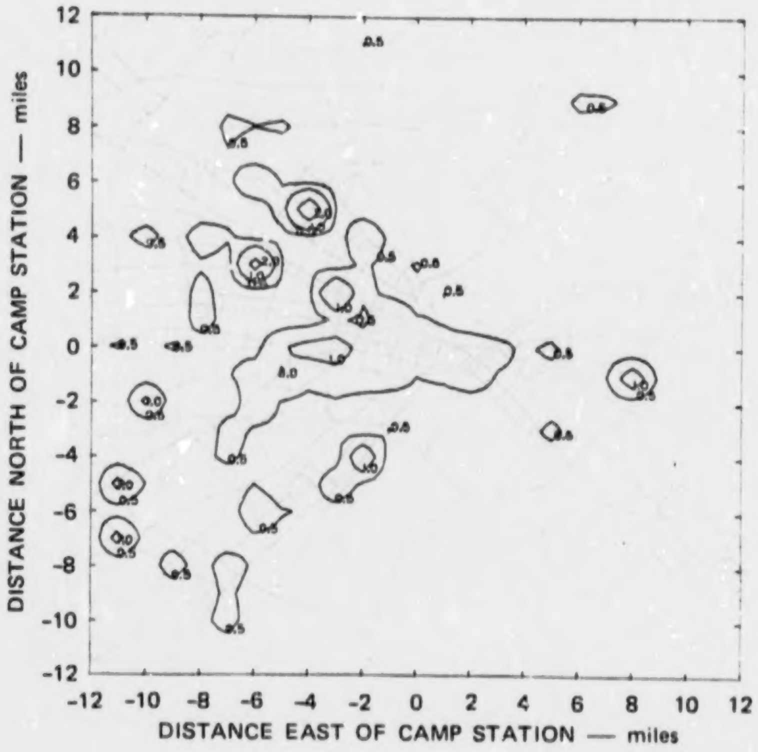

TA-7874-61

(b) WITH EXHAUST EMISSION CONTROLS

FIGURE 12 CALCULATED CONCENTRATION PATTERNS BASED ON FORECAST OF 1990 ST. LOUIS TRAFFIC. Meteorological conditions same as in Figure 11.

this pattern with that in Figure 11(a) shows a very large increase in forecast concentrations. Figure 12(b) shows the results for the case where the hypothetical emission control (as described in Section III) has been applied. The significant reduction in CO concentrations is readily apparent.

By choosing different grid point spacing, the spatial resolution of the model can be changed. Figure 13 illustrates this. The two halves of the figure show analyses of CO concentrations in St. Louis for the same hour. In Figure 13(a) the grid point spacing is 1 mile; in 13(b), 0.1 mile. Both are centered on the CAMP Station. The figure shows that the model is capable of providing concentration patterns in considerable detail. It is limited in its spatial resolution, however, by the size of the emission segments, particularly those nearest the receptor.

The model has been used to obtain concentration patterns in five different cities. Examples have already been shown for Washington and St. Louis. Figures 14, 15, and 16 show results obtained for Chicago, Cincinnati, and Denver. These figures are all based on 1965 historical traffic data. They show, as do the other figures, the expected high concentrations downwind of congested downtown areas and major arterials.

Results of trials using the synoptic model to calculate hourly concentrations continuously for a week are presented in Figures 17 and 18. To provide a true test of the model's capabilities, weeks were selected during which a variety of concentration magnitudes were observed, as shown by the dashed curves in the figures. These figures and those that follow do not necessarily show examples of the best agreement between calculations and observations, but are representative of the kinds of results achieved. In an attempt to treat the effects of nearby sources more accurately, the closest diffusion area segment was divided

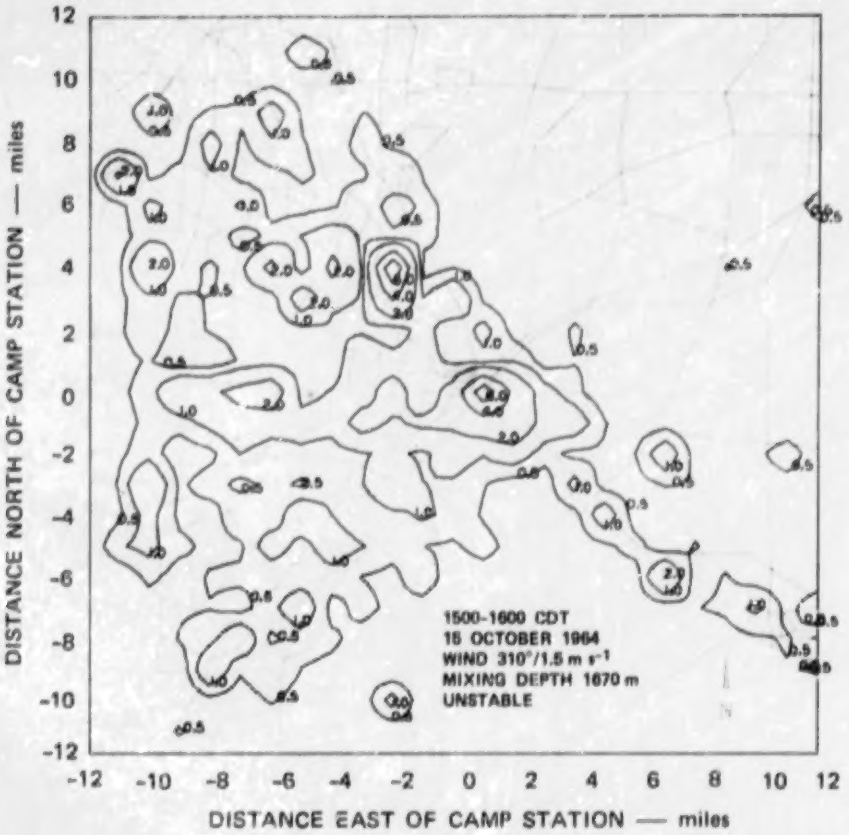

TA-7874-26a

(a) 1-MILE (1.6 km) GRID SPACING

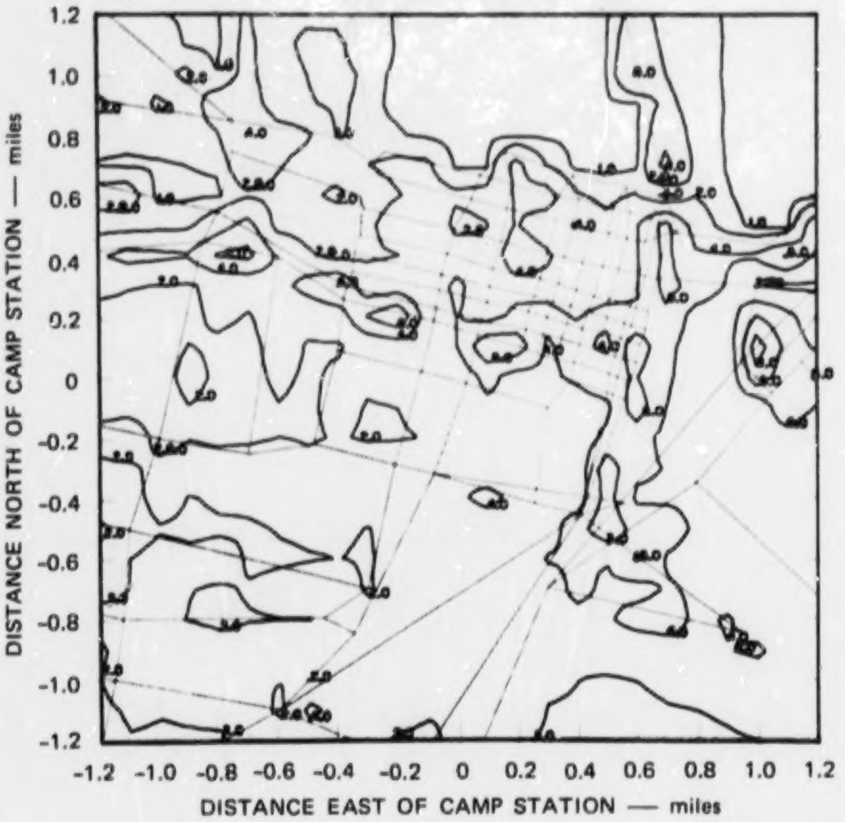

TA-7874-24a

(b) 0.1-MILE (0.16 km) GRID SPACING

FIGURE 13 CALCULATED ST. LOUIS CONCENTRATION PATTERNS FOR TWO GRID SIZES

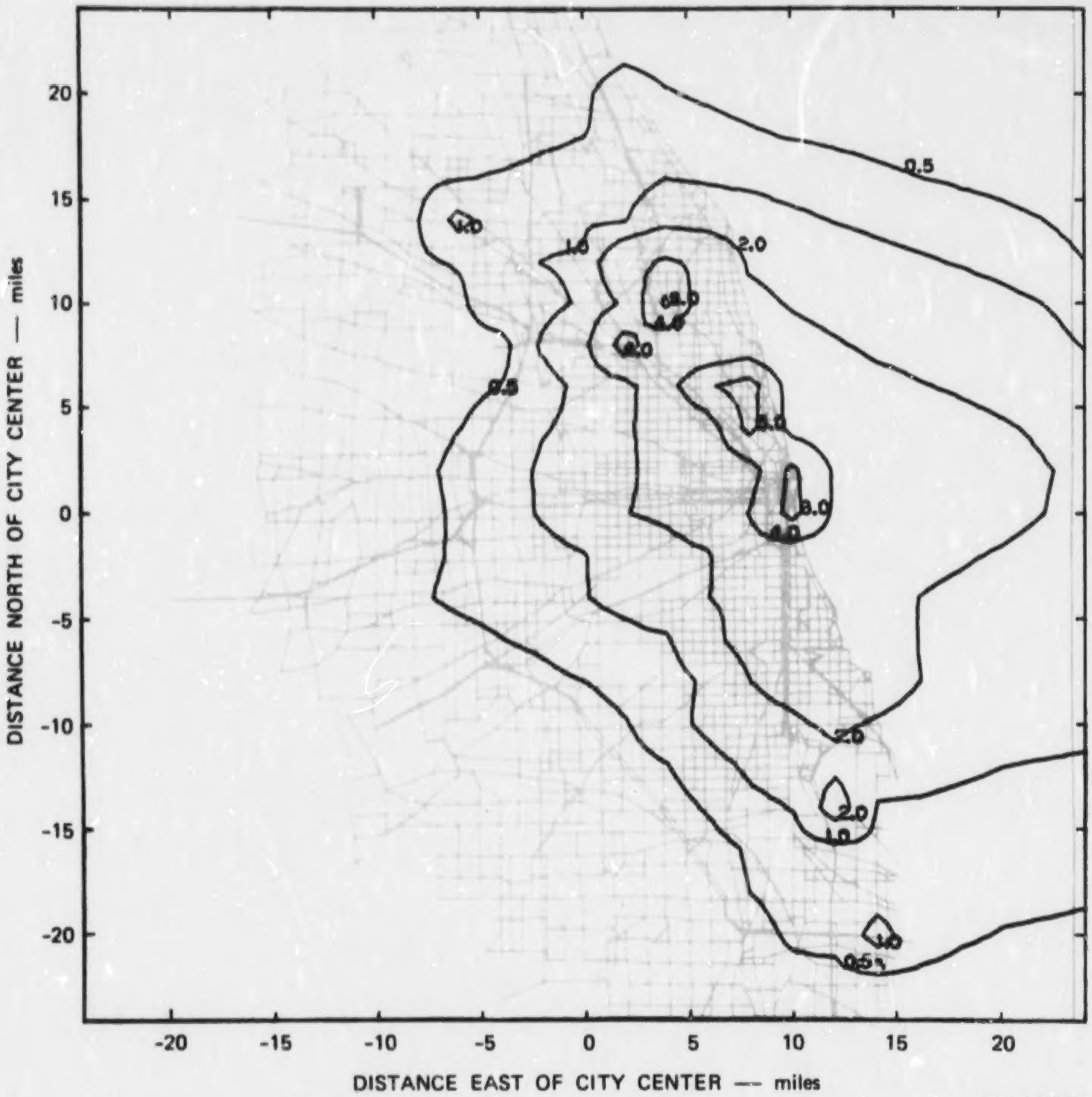

TA-7874-62

FIGURE 14 CALCULATED CARBON MONOXIDE CONCENTRATIONS (PPM) FOR CHICAGO. (0700-0800 LST, wind 270°/4 ms^{-1}, mixing depth 200 m, neutral stability)

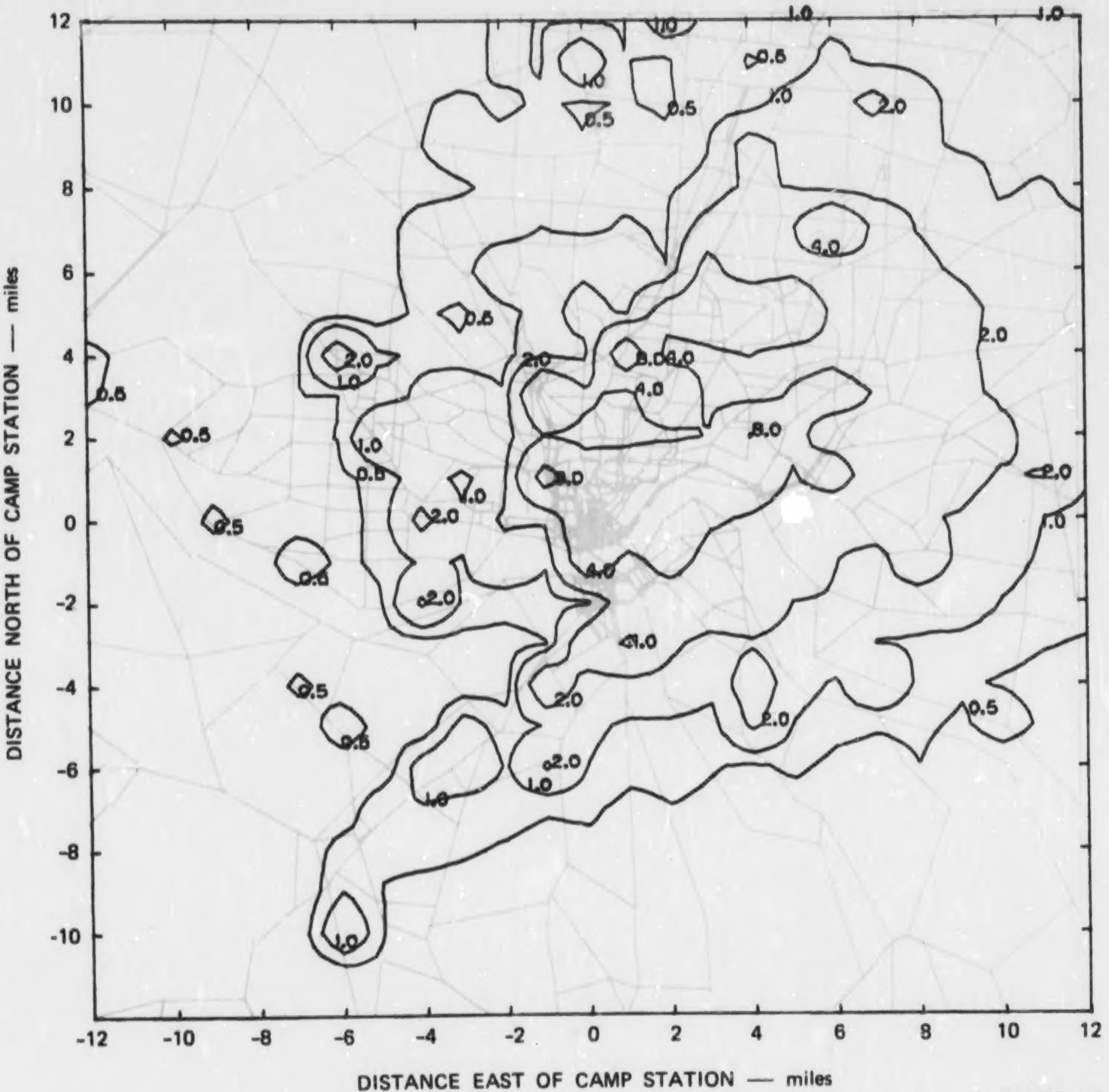

TA-7874-73

FIGURE 15 CALCULATED CARBON MONOXIDE CONCENTRATIONS (PPM) FOR CINCINNATI. (0700-0800 LST, wind 270°/2 ms^{-1}, mixing depth 200 m, slightly stable)

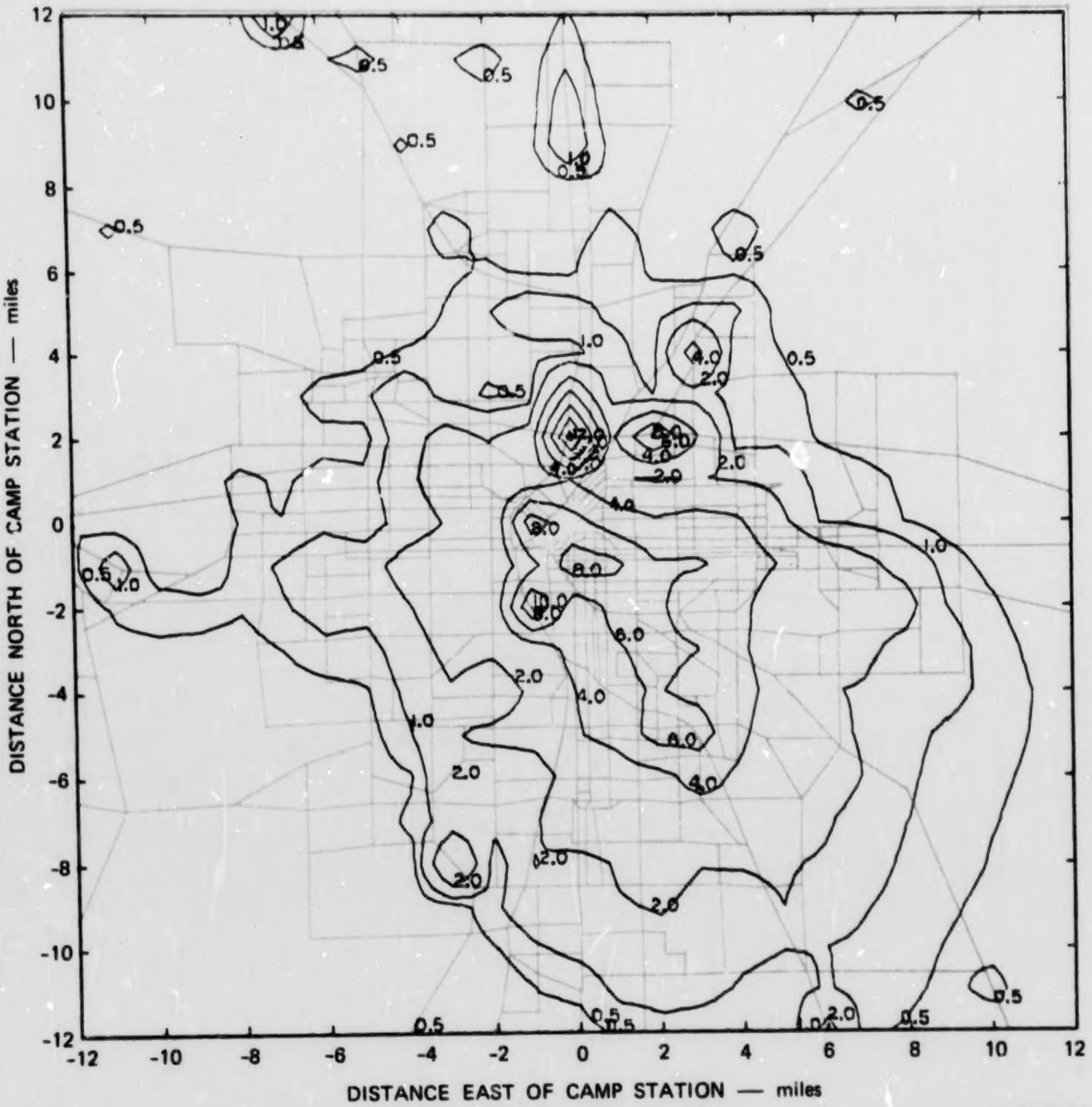

12
10
8
6
4
2
0
-2
-4
-6
-8
-10
-12
-12
-10
-8
-6
-4
-2
0
2
4
6
8
10
12
DISTANCE NORTH OF CAMP STATION — miles
DISTANCE EAST OF CAMP STATION — miles
0.5
1.0
2.0
4.0
6.0
8.0
12.0

TA-7874-63

FIGURE 16 CALCULATED CARBON MONOXIDE CONCENTRATIONS (PPM) FOR DENVER. (0700-0800 LST, wind 315°/2 ms^{-1}, mixing depth 400 m, slightly stable)

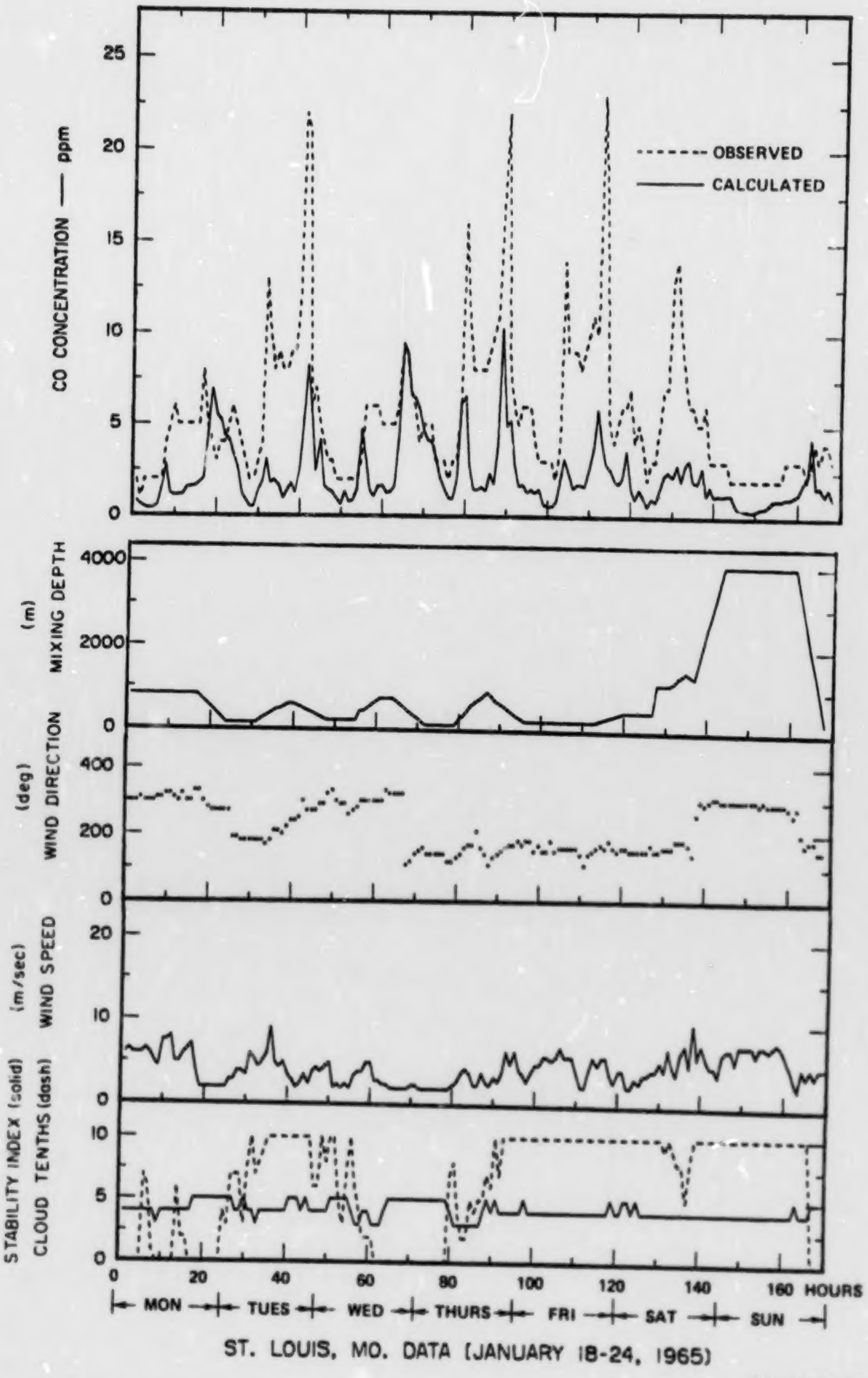

ST. LOUIS, MO. DATA (JANUARY 18-24, 1965)

TA-7874-47

FIGURE 17 OBSERVED AND CALCULATED CO CONCENTRATIONS AT THE ST. LOUIS CAMP STATION, 18–24 JANUARY 1965. The meteorological inputs to the model are also shown.

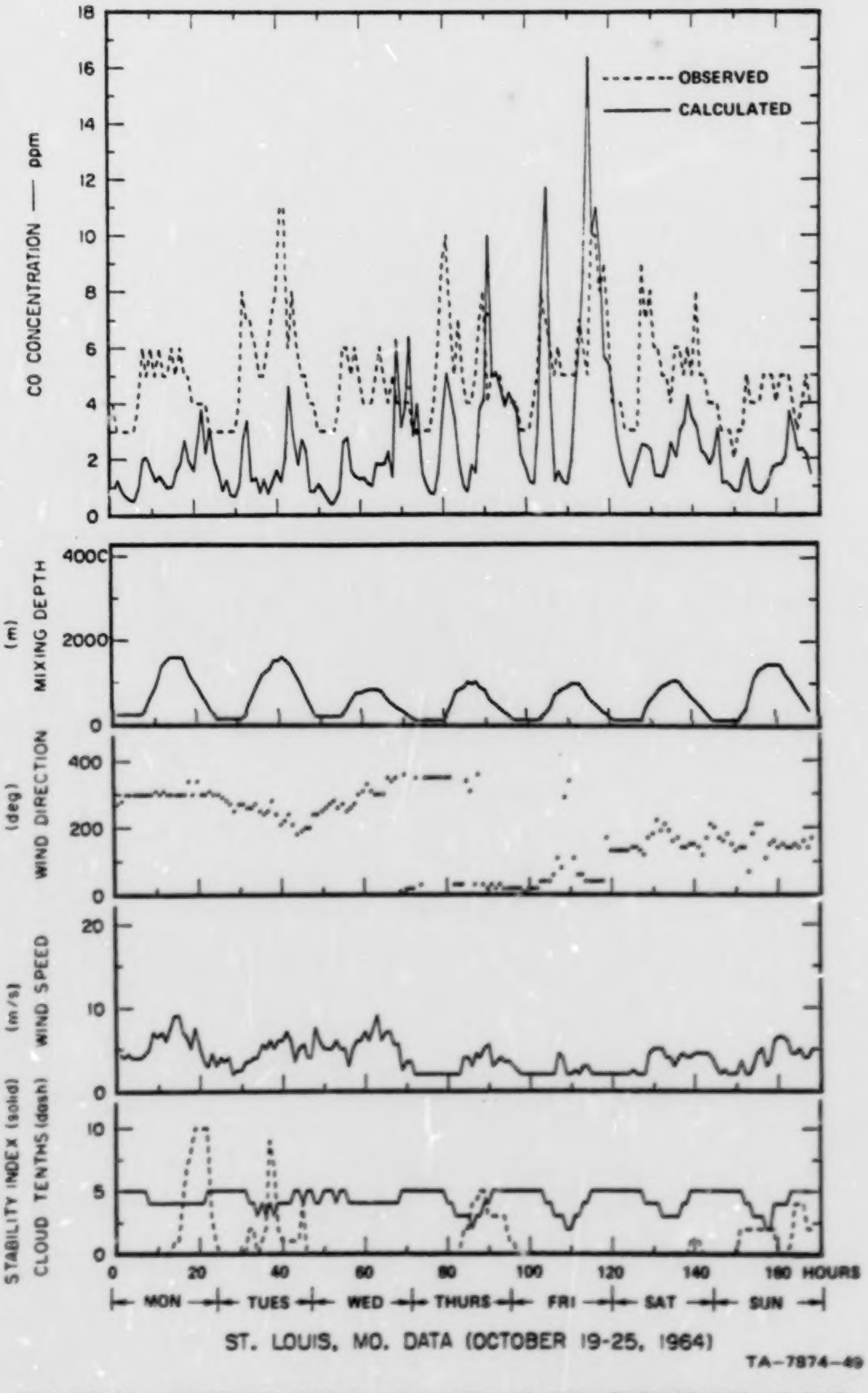

FIGURE 18 OBSERVED AND CALCULATED CO CONCENTRATIONS AT THE ST. LOUIS CAMP STATION, 19–25 OCTOBER 1964. The meteorological inputs to the model are also shown.

into two sections for these calculations (see Appendix E). One segment extends from the receptor to 62.5 m in range, and the other extends from 62.5 out to 125 m. The calculations also include estimates of the extraurban background, i.e., contributions from emissions outside the city, made with the model described in Appendix F. Figures 17 and 18 also show the values of the meteorological inputs to the model, either as observed or as calculated.

The CO observations during the January period (Figure 17) were anomalously high, and the model generally gives underestimates for this week.* A variety of weather conditions prevailed; cold fronts passed St. Louis on the evenings of 17, 19, and 23 January. The poorest performance of the model occurs on 19, 21, and 22 January, when the wind was generally southerly. This suggests that the high observed concentrations may be caused by the nearby sources on the adjacent streets, since the St. Louis CAMP Station is located on the northwest corner of an intersection.

Weather conditions during the October period (Figure 18) were not so variable, and more typical CO concentrations were observed. In contrast to the January period, the predicted concentrations are often too high. The worst agreement occurs when the airport winds are reported as very light or calm. For these calculations, the model used a minimum wind speed of 2 m/s and, as noted earlier, the last observed wind direction. It is probable that much of the prediction error is due to this uncertainty in winds.

---

*The possibility of water vapor interference as a source of some of the discrepancy between observed and calculated concentrations is discussed in Section VI of this report.

Many additional calculations of the type illustrated in Figures 17 and 18 for St. Louis have been carried out for Washington, D.C.; Cincinnati, Ohio; Chicago, Illinois; and Denver, Colorado. Some examples of these are given in Figures 19 through 22. Prevailing meteorological conditions are also shown in Figures 20 through 22. It can be seen that a wide variety of meteorological situations are represented. In general, the agreement between calculations and observations leaves much to be desired. The measurement program to be conducted during the coming year should help us to identify the sources of the discrepancies and to make corrections.

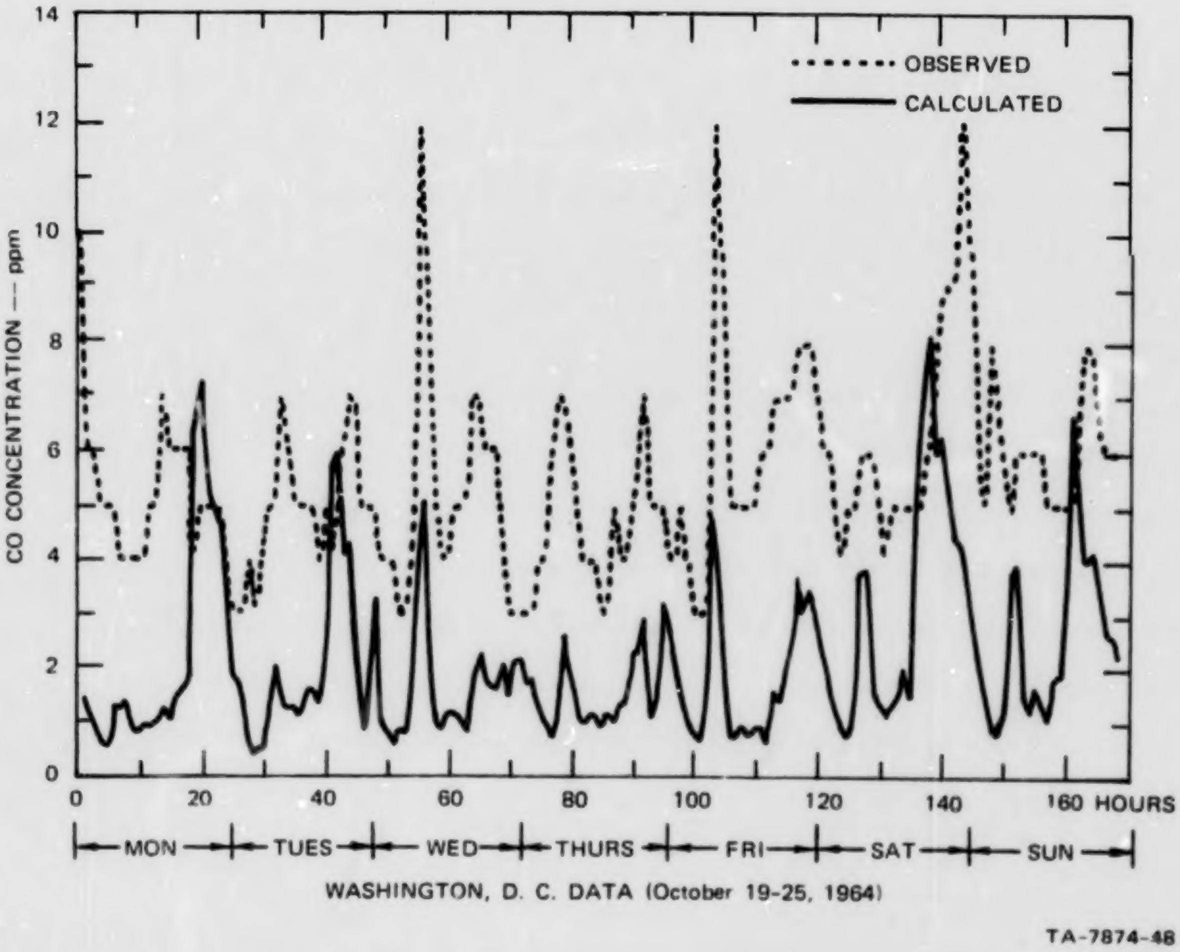

FIGURE 19 OBSERVED AND CALCULATED CO CONCENTRATIONS AT THE WASHINGTON, D.C., CAMP STATION, 19-25 OCTOBER 1964

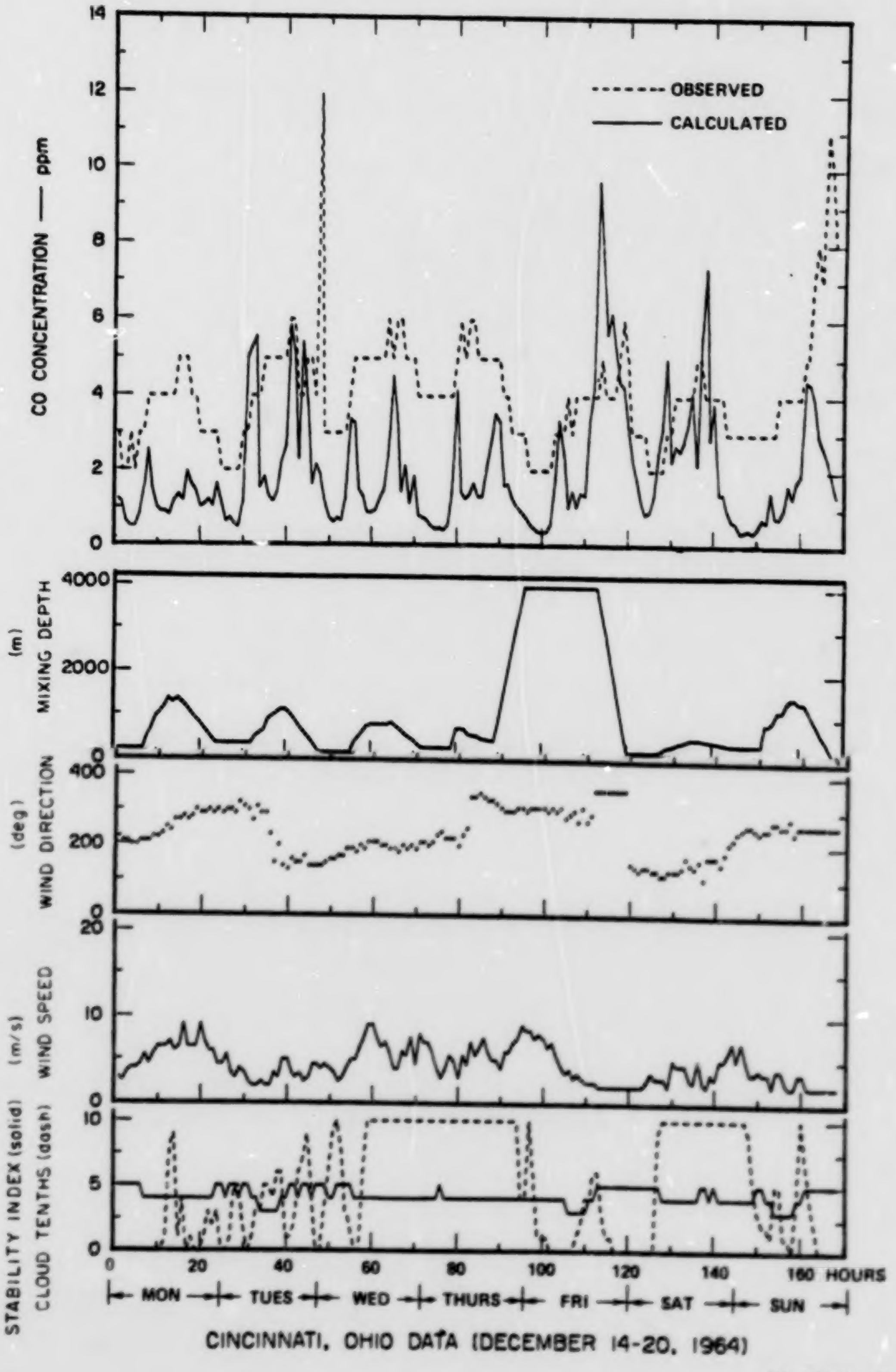

TA-7874-50

FIGURE 20 OBSERVED AND CALCULATED CO CONCENTRATIONS AT THE CINCINNATI CAMP STATION, 14-20 DECEMBER 1964. The meteorological inputs to the model calculations are also shown.

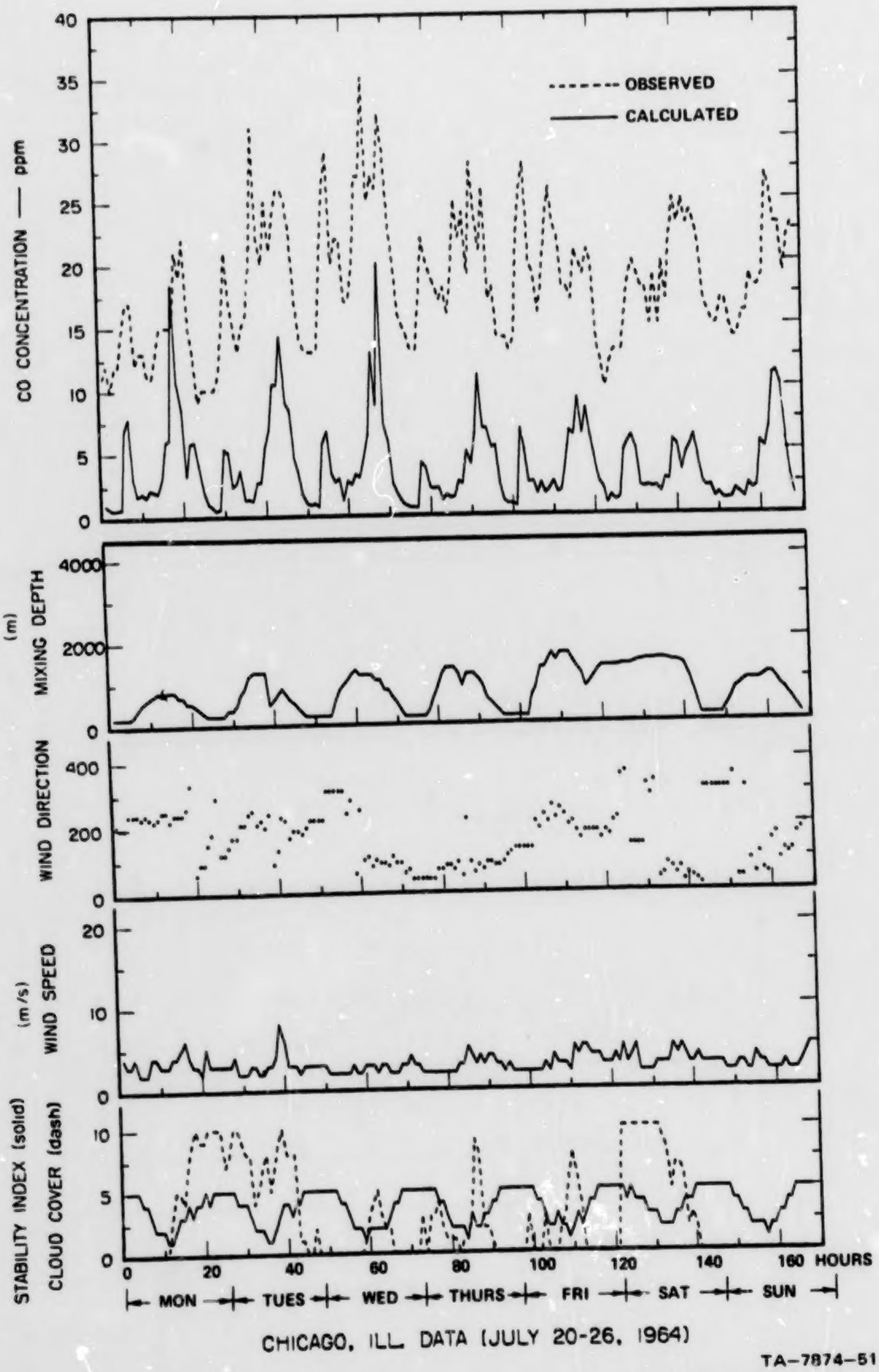

FIGURE 21 OBSERVED AND CALCULATED CO CONCENTRATIONS AT THE CHICAGO CAMP STATION, 20-26 JULY 1964. The meteorological inputs to the model calculations are also shown.

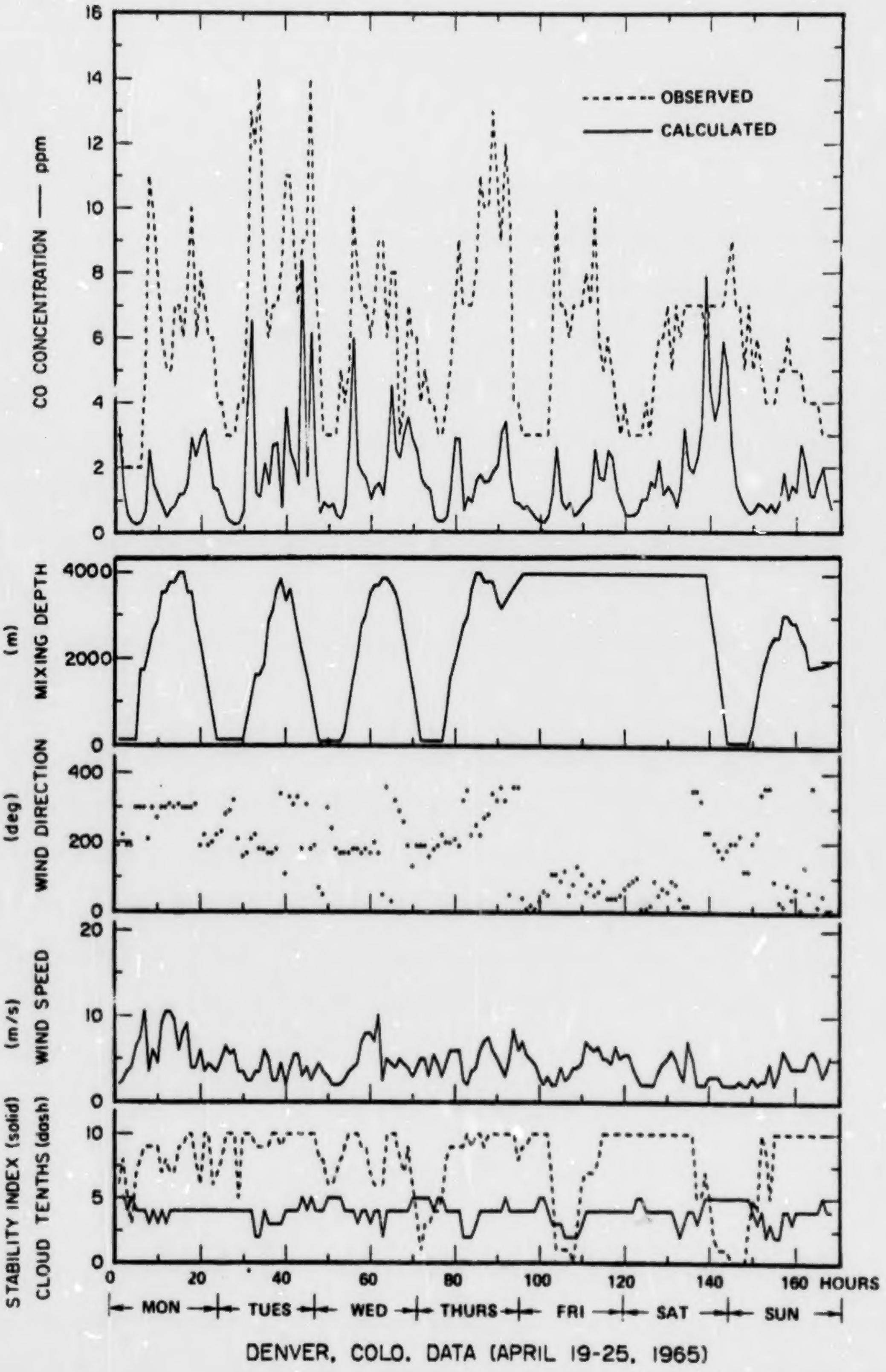

TA–7874–52

FIGURE 22 OBSERVED AND CALCULATED CO CONCENTRATIONS AT THE DENVER CAMP STATION, 19-25 APRIL 1965. The meteorological inputs to the model calculations are also shown.

C. The Climatological Model

1. Background

There are two different approaches to calculating climatological summaries of the concentration of carbon monoxide at a site. The most commonly used approach starts with a joint frequency distribution of all the meteorological variables that affect the concentration. For our model there are five variables: wind speed and direction, time of day, mixing depth, and stability. There would be 24 categories of time, and 16 of wind direction. Six categories each for wind speed and mixing depth, and five categories for stability would probably provide sufficient resolution for climatological purposes. With these numbers of categories, the joint frequency distribution would have 69,120 entries.

As will be shown in a later section, some combinations of stability and mixing depth are essentially equivalent to others. By combining equivalent categories it should be possible to reduce the number of categories by about a third to a half. This reduction would make the indexing of the variables slightly more difficult but would reduce the number of entries in our joint frequency table to about 4×10^4. If only eight wind-direction categories were used, this number could be halved to about 2×10^4.

The method that has been described above gives the frequency distribution of hourly values of CO concentration. To obtain the frequency distribution of the 8-hour or 24-hour average values requires some statistical model, such as Larsen's (1969). Since there is some uncertainty about the validity of Larsen's model (e.g., McGuire and Noll, 1970) we felt that it might be better to approach the problem more directly. If the individual calculated hourly values of concentration are available, in sequence, it is possible to use "running mean" type operators to get the distribution of concentrations averaged over periods greater than an hour.

We have already shown that a very large number of categories have to be considered for the conventional approach using the joint frequencies of the input parameters. In fact, the number of categories could be very nearly as large as the number of hours in a five- to ten-year period. Thus, it seemed reasonable to consider the possibility of calculating hourly values in sequence. This approach, which is described below, was found to be practical and was adopted.

2. Description

a. Simplifications

To calculate a long series of concentrations economically requires some simplification of the model. It is possible to represent the source strengths of the segments as the product of a time-dependent factor and a time-independent factor. Thus

$$Q_{i,d,t} = P_t \bar{Q}_{i,d} \quad , \qquad \text{(IV-3)}$$

where

$Q_{i,d,t}$ = the source strength of the i^{th} segment, in the d^{th} direction, for the t^{th} hour. (gm m^{-2} s^{-1})

$\bar{Q}_{i,d}$ = the average daily source strength, based on total traffic and average speeds on the different roads within the segment. (gm m^{-2} s^{-1})

P_t = a factor that gives the source strength for the t^{th} hour, based on daily distribution of traffic, and changes in average speed during peak hours. P_t is assumed to be independent of the location in the city. In some of the previously presented synoptic applications, P_t has assumed different values for different road types.

To further limit the number of conditions to be considered, mixing depths have been classified into seven categories (<100 m, 100-200 m, 200-400 m, ..., >3200 m). With these simplifications, the model can be written as follows:

$$C = \frac{P_t}{u} \sum_{i=1}^{9} \left(\frac{\chi}{Q}\right)_{i,j,m} \bar{Q}_{i,d} \qquad \text{(IV-4)}$$

where

C = CO concentration at the receptor

u = wind speed

$(\chi/Q)_{i,j,m}$ = ratio of the CO concentration received from the i^{th} segment to the emissions in that segment (for unit wind speed). The values of these ratios depend on stability class, j, and mixing depth class, m.

The values of $(\chi/Q)_{i,j,m}$ are calculated using a mixing depth equal to the geometric mean of the geometrically spaced bounds of the mixing depth class intervals. Equation (IV-4) is essentially identical to Eq. (IV-2) given earlier as the operating synoptic model equation.

The summation term in Eq. (IV-4) can be defined as follows

$$X_{j,m,d} \equiv \sum_{i=1}^{9} \left(\frac{\chi}{Q}\right)_{i,j,m} \bar{Q}_{i,d} \quad . \qquad \text{(IV-5)}$$

Then, for a given receptor site, all possible values of $X_{j,m,d}$ can be calculated and stored in a 5 × 7 × 16 (stability type × mixing depth category × direction) array. These values need only be calculated once for each receptor. These numbers, when combined with the 24-item list of P_t values, provide the information necessary to calculate concentration at a given receptor. The storage space required is less than 600 numbers. The operating equation for the climatological model is

$$C = X_{j,m,d}\left(\frac{P_t}{u}\right) \quad . \qquad \text{(IV-6)}$$

b. *Preprocessing of the Meteorological Data*

Equation (IV-6) can be applied most easily when we have converted the usual meteorological observations to a sequence of records of time (t), stability (j), mixing depth category (m), direction on a 16-point compass (d), and wind speed (u). This preprocessing of the data is described in Appendix G. Five years (1960-1964) of St. Louis meteorological data have been condensed and recorded on magnetic tape. These five years of data constitute a reasonably stable climatological description of that city, although anomalies of this duration do occasionally occur. Five years of data are used partly because Holzworth's tabulations of mixing depth cover only a five-year period, and partly because longer periods of record would increase the calculation time disproportionately to the small increase in climatological accuracy. Although it is quite possible in principle to use radiosonde data from the National Weather Records Center to extend the period of record, their data are not universally available on magnetic tape for all U.S. stations, and the processing of large quantities of punched cards presents practical difficulties.

3. Applications

The preprocessed data are used as the climatology of the city. The effects of changes in the transportation network or of emission controls are then assessed by determining a set of values of $\bar{Q}_{i,d}$, which are used to calculate $X_{j,m,d}$. The five-year meteorological data sequence is used with Eq. (IV-6) to determine a sequence of CO concentrations. A simplified flow chart showing this process is given in Figure 23.

In Appendix H it is shown that there are different combinations of stability and mixing depth that give the same value of $(X/Q)_{i,j,m}$ for all the upwind segments. Because this is the case, we were able to reduce the stored number of values of $(\chi/Q)_{i,j,m}$. This results in a corresponding reduction in the required number of values $X_{j,m,d}$, from 560 to 400 per site. The simplified model makes it feasible to calculate a sequence of CO concentrations for each of a number of points in the city. Once this is done, these sequences can be treated as though they were sequences of real observations. Thus, it is possible, without resorting to a statistical model, to calculate any of the statistical parameters that can be determined from sequences of real hourly observations. This includes the frequency distribution of 8-hour averages, 24-hour averages, or the frequency distribution of any special subset of the data.

As noted above, the output of the climatological model can be treated in any way that observed data can be treated. This means that the potential number of outputs is virtually unlimited. For purposes of illustration, a computer program has been written to determine ten

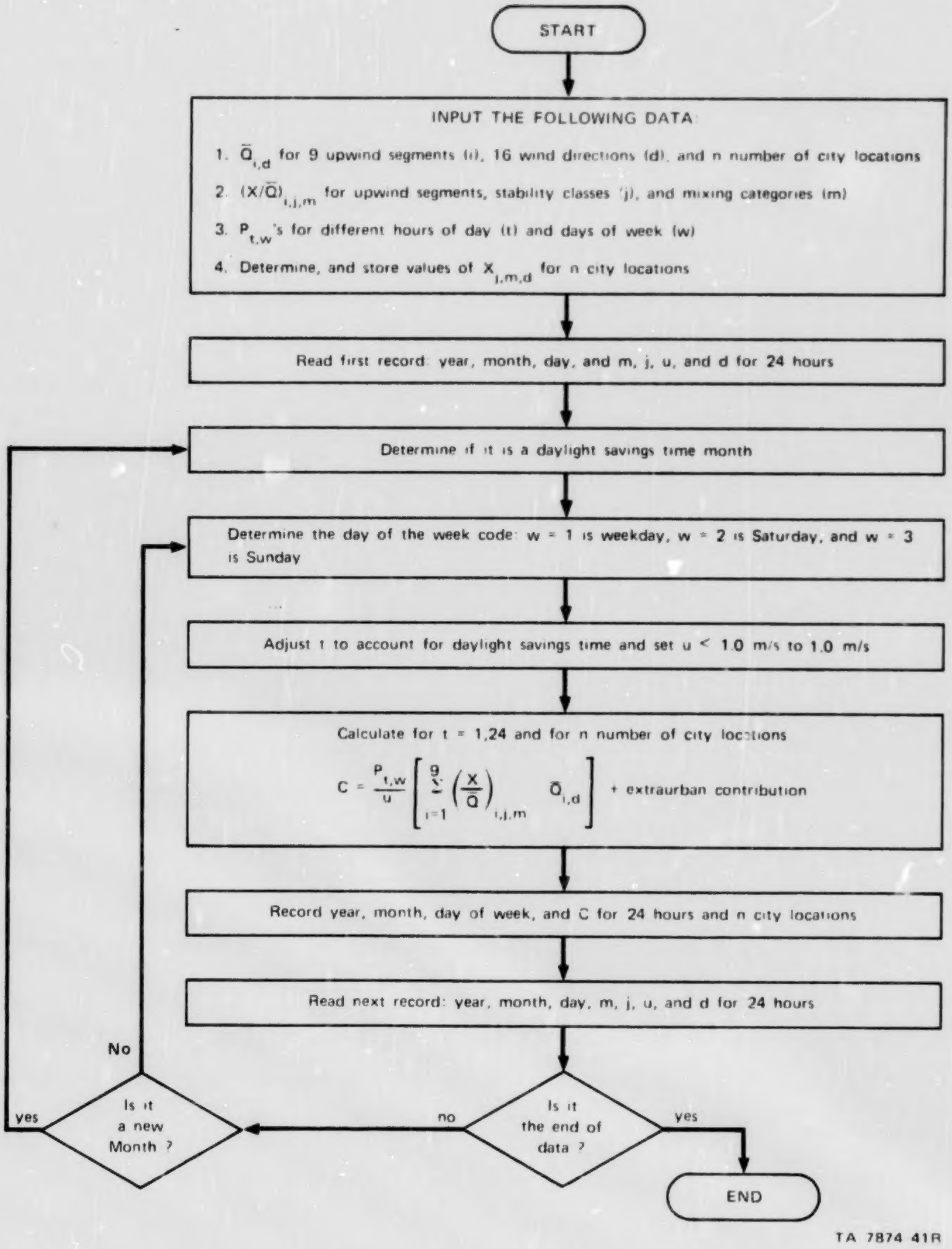
START
INPUT THE FOLLOWING DATA:
1. $\bar{Q}_{i,d}$ for 9 upwind segments (i), 16 wind directions (d), and n number of city locations
2. $(X/\bar{Q})_{i,j,m}$ for upwind segments, stability classes (j), and mixing categories (m)
3. $P_{t,w}$'s for different hours of day (t) and days of week (w)
4. Determine, and store values of $X_{j,m,d}$ for n city locations
Read first record: year, month, day, and m, j, u, and d for 24 hours
Determine if it is a daylight savings time month
Determine the day of the week code: w = 1 is weekday, w = 2 is Saturday, and w = 3 is Sunday
Adjust t to account for daylight savings time and set u < 1.0 m/s to 1.0 m/s
Calculate for t = 1,24 and for n number of city locations
$C = \frac{P_{t,w}}{u}\left[\sum_{i=1}^{9}\left(\frac{X}{\bar{Q}}\right)_{i,j,m}\bar{Q}_{i,d}\right]$ + extraurban contribution
Record year, month, day of week, and C for 24 hours and n city locations
Read next record: year, month, day, m, j, u, and d for 24 hours
Is it the end of data ?
yes
no
END
Is it a new Month ?
yes
No
TA 7874 41R

FIGURE 23 SIMPLIFIED FLOW CHART OF CLIMATOLOGICAL MODEL

different frequency distributions based on the output from the climatological model:

(1) All hours, a frequency distribution based on the total five-year set of hourly calculated concentrations

(2) All weekday hours

(3) All Saturday hours

(4) All Sunday hours

(5) All 0800 hours

(6) All 1200 hours

(7) All 1800 hours

(8) All 2400 hours

(9) 8-hour means; frequency distribution of the averages of the values calculated for all 8-hour periods in the five-year sequence

(10) 24-hour means; same as (9), except for 24-hour averages.

A simplified flow chart for the program used to calculate the above frequency distributions is shown in Figure 24. This program also computes cumulative distributions, and determines median (50 percentile) and 90-percentile values by log-linear interpolation between the points calculated on the cumulative distributions.

We used the climatological model to calculate a five-year sequence of CO concentrations at nine locations, including the CAMP Station in St. Louis. For these calculations, a constant 0.25 ppm background concentration was added, based on the observations of

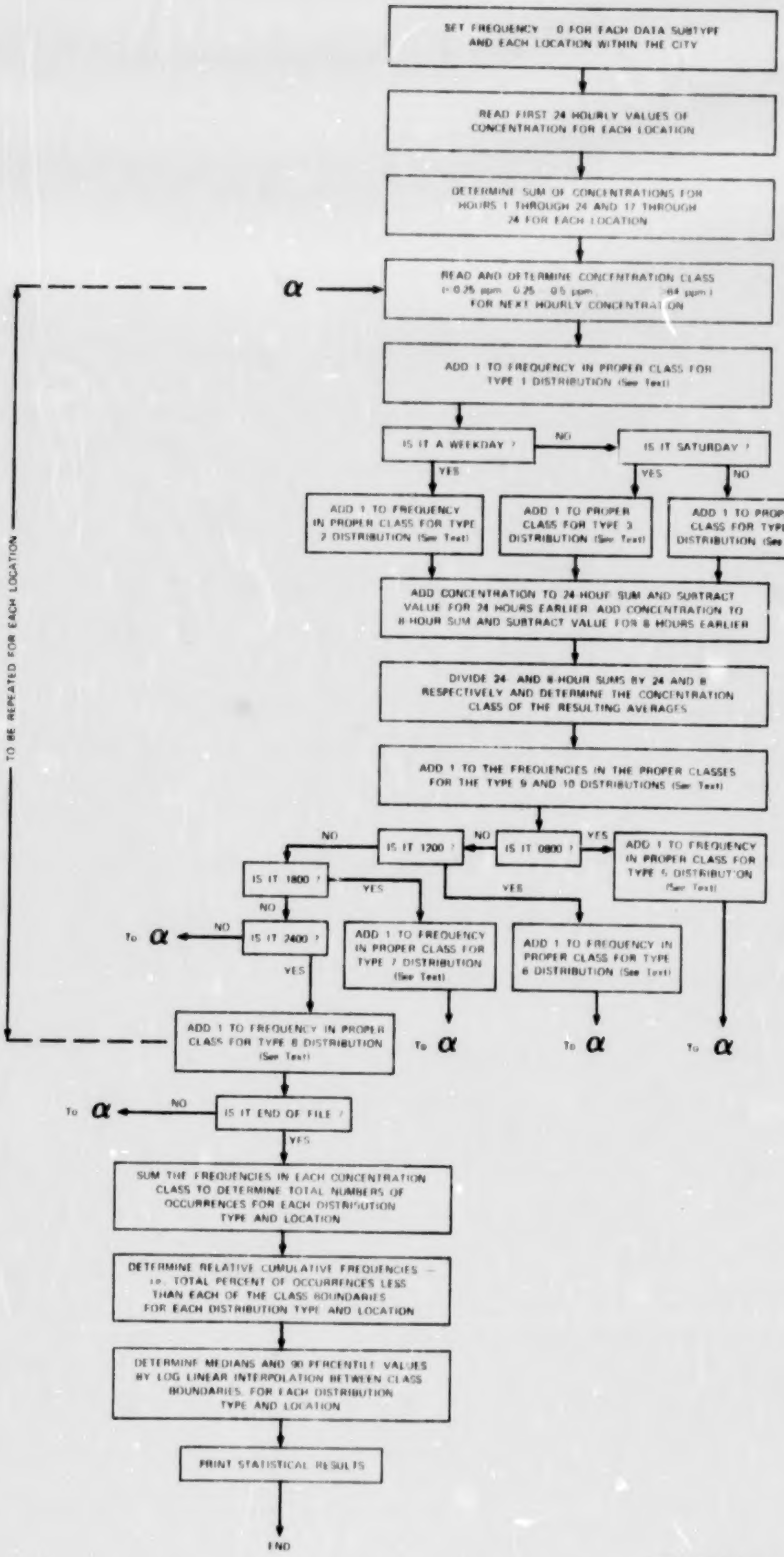
SET FREQUENCY 0 FOR EACH DATA SUBTYPE AND EACH LOCATION WITHIN THE CITY
READ FIRST 24 HOURLY VALUES OF CONCENTRATION FOR EACH LOCATION
DETERMINE SUM OF CONCENTRATIONS FOR HOURS 1 THROUGH 24 AND 17 THROUGH 24 FOR EACH LOCATION
α
READ AND DETERMINE CONCENTRATION CLASS (< 0.25 ppm 0.25 – 0.5 ppm, >64 ppm) FOR NEXT HOURLY CONCENTRATION
ADD 1 TO FREQUENCY IN PROPER CLASS FOR TYPE 1 DISTRIBUTION (See Text)
IS IT A WEEKDAY ?
NO
IS IT SATURDAY ?
YES
YES
NO
ADD 1 TO FREQUENCY IN PROPER CLASS FOR TYPE 2 DISTRIBUTION (See Text)
ADD 1 TO PROPER CLASS FOR TYPE 3 DISTRIBUTION (See Text)
ADD 1 TO PROPER CLASS FOR TYPE 4 DISTRIBUTION (See Text)
ADD CONCENTRATION TO 24-HOUR SUM AND SUBTRACT VALUE FOR 24 HOURS EARLIER. ADD CONCENTRATION TO 8-HOUR SUM AND SUBTRACT VALUE FOR 8 HOURS EARLIER
DIVIDE 24- AND 8-HOUR SUMS BY 24 AND 8 RESPECTIVELY AND DETERMINE THE CONCENTRATION CLASS OF THE RESULTING AVERAGES
ADD 1 TO THE FREQUENCIES IN THE PROPER CLASSES FOR THE TYPE 9 AND 10 DISTRIBUTIONS (See Text)
TO BE REPEATED FOR EACH LOCATION
NO
IS IT 1200 ?
NO
IS IT 0800 ?
YES
ADD 1 TO FREQUENCY IN PROPER CLASS FOR TYPE 5 DISTRIBUTION (See Text)
IS IT 1800 ?
YES
YES
NO
To α
NO
IS IT 2400 ?
ADD 1 TO FREQUENCY IN PROPER CLASS FOR TYPE 7 DISTRIBUTION (See Text)
ADD 1 TO FREQUENCY IN PROPER CLASS FOR TYPE 6 DISTRIBUTION (See Text)
YES
ADD 1 TO FREQUENCY IN PROPER CLASS FOR TYPE 8 DISTRIBUTION (See Text)
To α
To α
To α
To α
NO
IS IT END OF FILE ?
YES
SUM THE FREQUENCIES IN EACH CONCENTRATION CLASS TO DETERMINE TOTAL NUMBERS OF OCCURRENCES FOR EACH DISTRIBUTION TYPE AND LOCATION
DETERMINE RELATIVE CUMULATIVE FREQUENCIES — i.e., TOTAL PERCENT OF OCCURRENCES LESS THAN EACH OF THE CLASS BOUNDARIES FOR EACH DISTRIBUTION TYPE AND LOCATION
DETERMINE MEDIANS AND 90 PERCENTILE VALUES BY LOG LINEAR INTERPOLATION BETWEEN CLASS BOUNDARIES, FOR EACH DISTRIBUTION TYPE AND LOCATION
PRINT STATISTICAL RESULTS
END

TA-7874-64

FIGURE 24 SIMPLIFIED FLOW CHART FOR A PROGRAM TO DETERMINE TEN DIFFERENT FREQUENCY DISTRIBUTIONS

Robinson and Robbins (1967). The calculations used traffic emissions appropriate to 1965. We then applied the program diagrammed in Figure 24 to these results and obtained frequency distributions of the types enumerated above for each of the nine sites.

Figure 25 shows the calculated St. Louis CAMP Station frequency distributions for weekday, Saturday, and Sunday hours. The figure shows the expected decrease in the frequency of the higher concentrations on the weekend, and the corresponding increase in the lower concentrations. Figure 26 shows the frequency distributions of concentrations at 0800, 1200, and 1800 Local Standard Time. The greater frequencies of high concentrations at 1800 are quite evident. The 0800 also shows a considerably greater number of occurrences of concentrations above 2 ppm than does the 1200 distribution. Figure 27 shows the frequency distributions of concentrations averaged over three different time intervals, 1-hour, 8-hours, and 24-hours. Qualitatively, the results are just as expected. The mode remains the same, between 1 and 2 ppm, but the spread of the distributions decreases appreciably with increased averaging time.

The output of the program can also be used to determine spatial variations of certain statistical parameters. For example, Figure 28 shows the variation of the median and 90-percentile values for nine sites along a north-south line passing through the St. Louis CAMP Station. As expected, the highest values are calculated for the downtown area, where the CAMP Station is located.

The calculations described in the preceding paragraphs were repeated using the emissions based on the 1990 traffic forecast for St. Louis. The results are displayed in Figures 29 through 32. As was evident in Figure 12, the hypothesized emission controls result in a decrease in CO concentration from 1965 to 1990, although the amount of traffic increases. Some of the same qualitative features are seen in

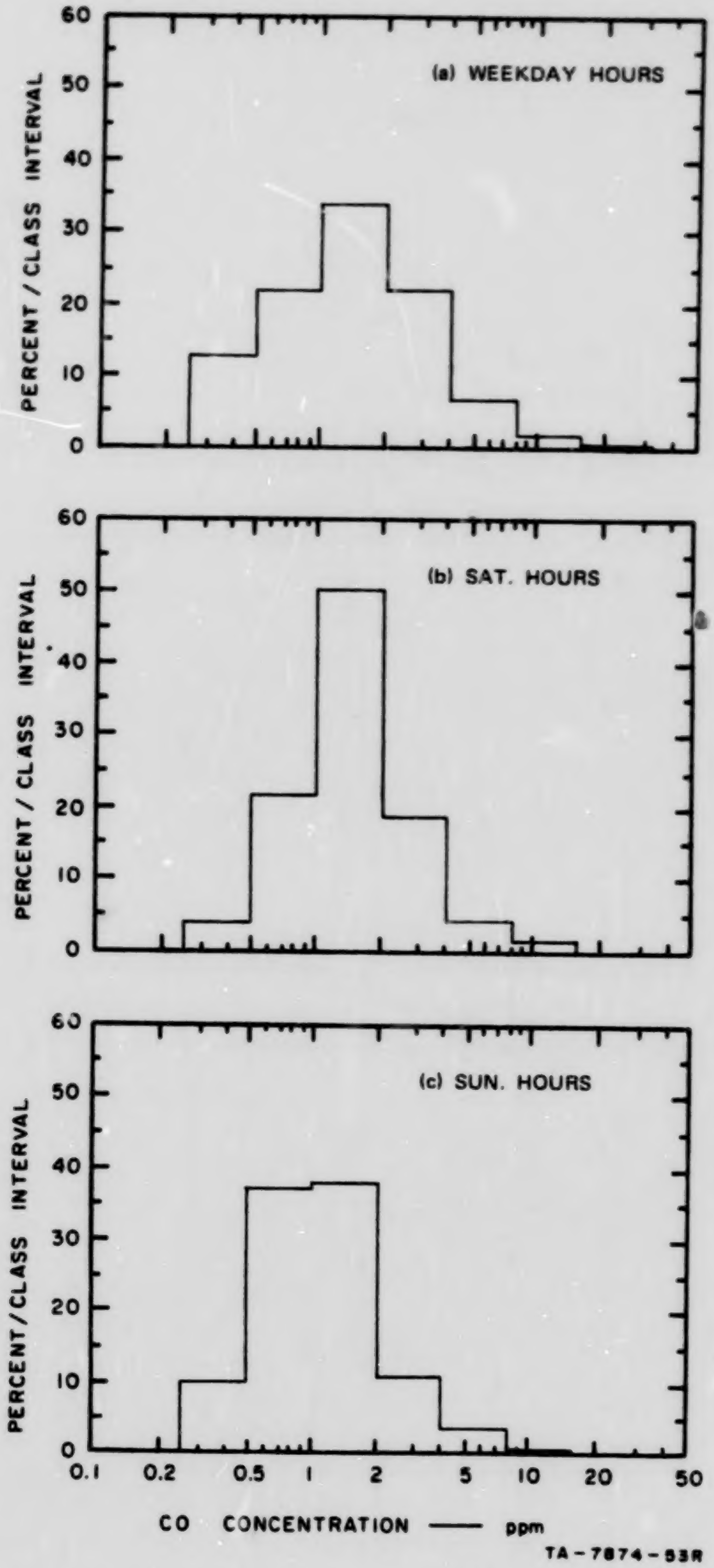

FIGURE 25 CALCULATED ST. LOUIS CAMP STATION CO CONCENTRATION FREQUENCY DISTRIBUTION FOR 1965 TRAFFIC CONDITIONS; WEEKDAY, SATURDAY, AND SUNDAY HOURS

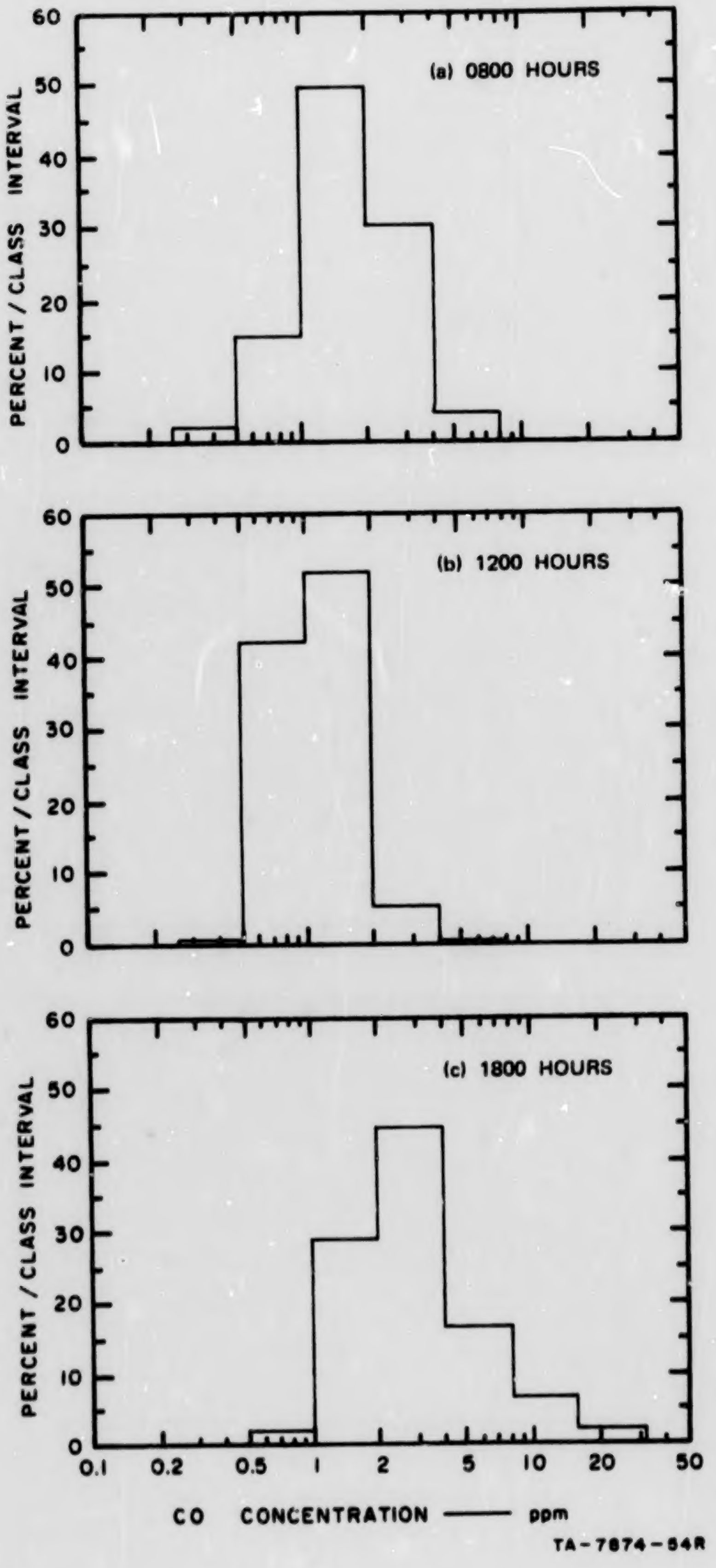

FIGURE 26 CALCULATED ST. LOUIS CAMP STATION CO CONCENTRATION FREQUENCY DISTRIBUTION FOR 1965 TRAFFIC CONDITIONS; 0800, 1200, AND 1800 HOURS

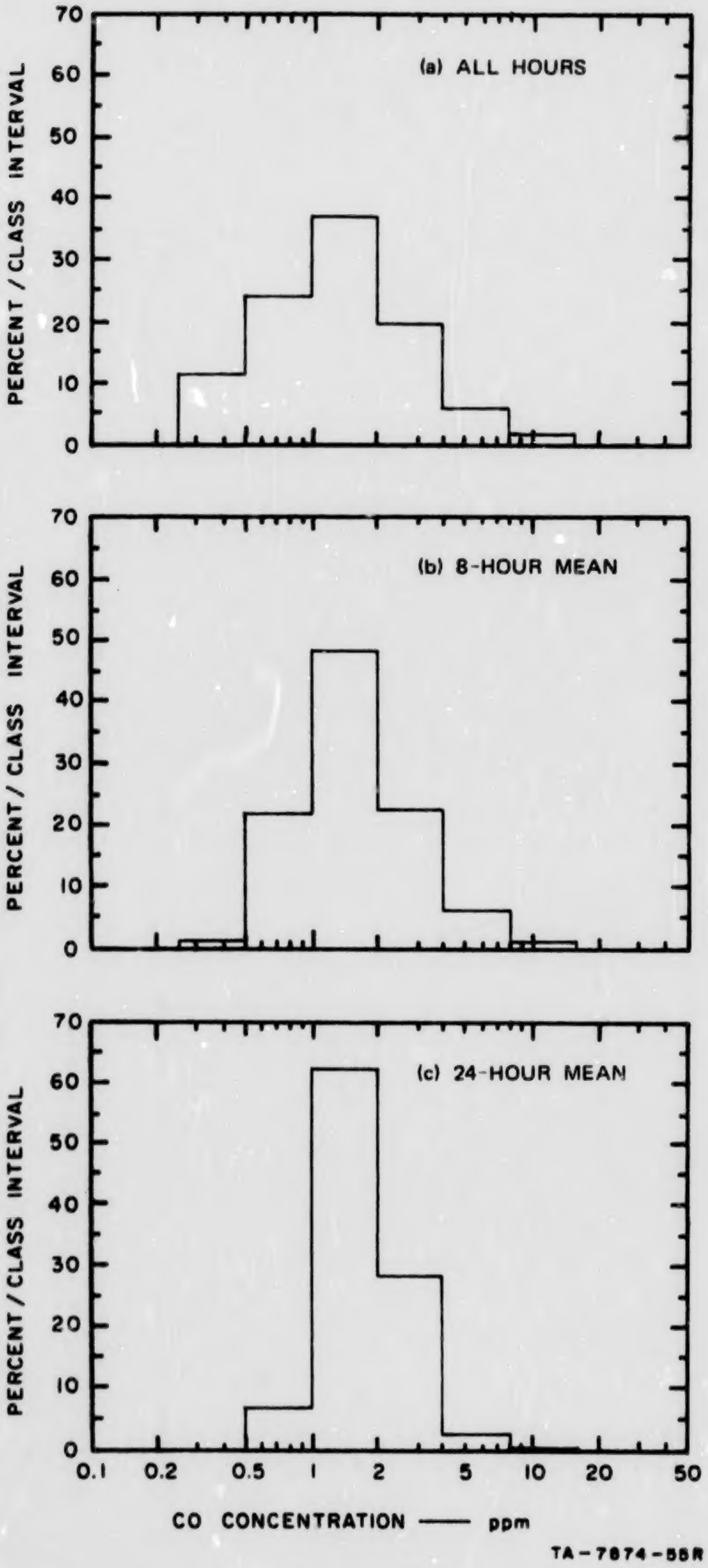

FIGURE 27 CALCULATED ST. LOUIS CAMP STATION CO CONCENTRATION FREQUENCY DISTRIBUTION FOR 1965 TRAFFIC CONDITIONS; 1-HOUR, 8-HOUR, AND 24-HOUR AVERAGES

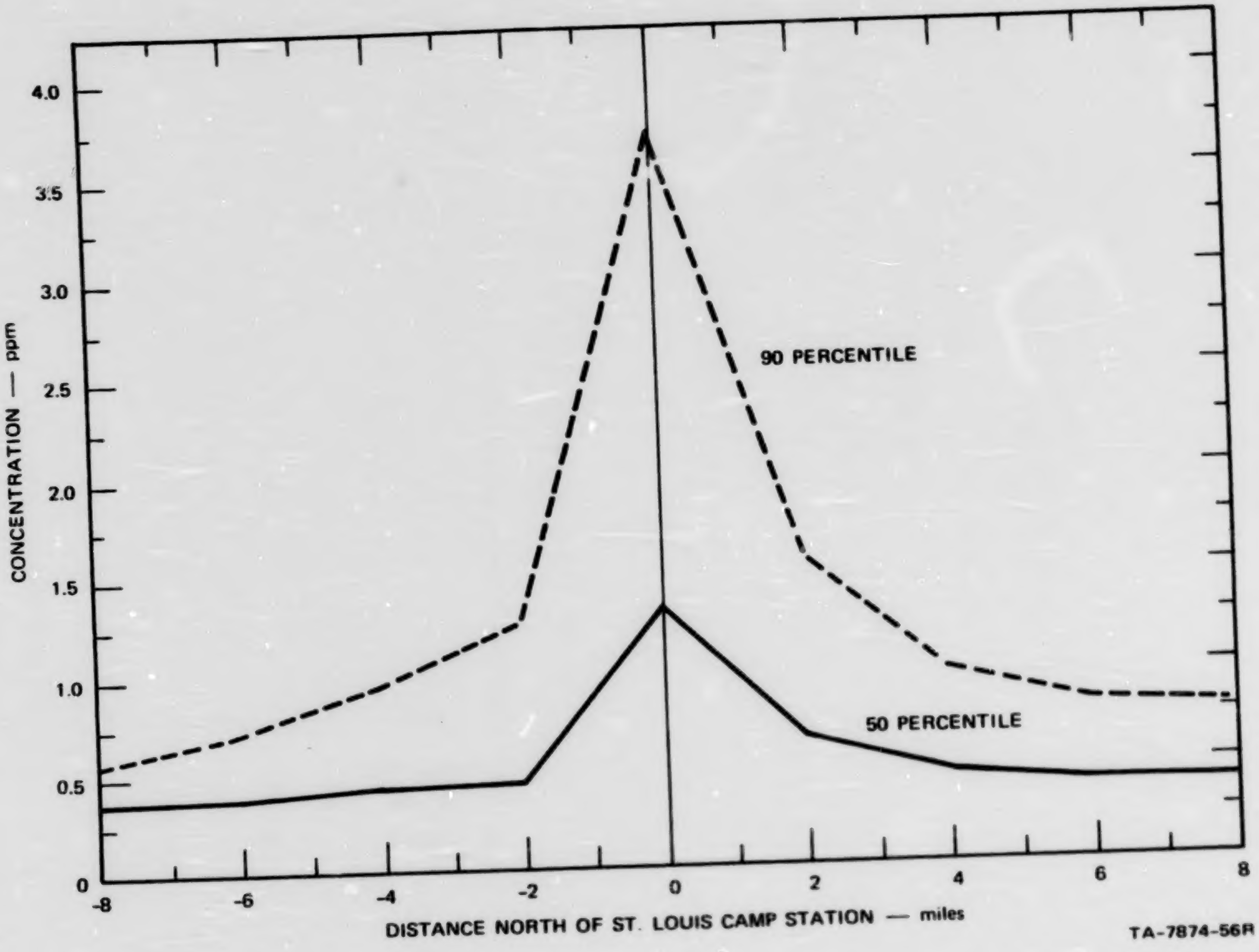

FIGURE 28 SPATIAL VARIATIONS OF CALCULATED ST LOUIS MEDIAN AND 90 PERCENTILE CONCENTRATIONS FOR 1965 TRAFFIC DATA

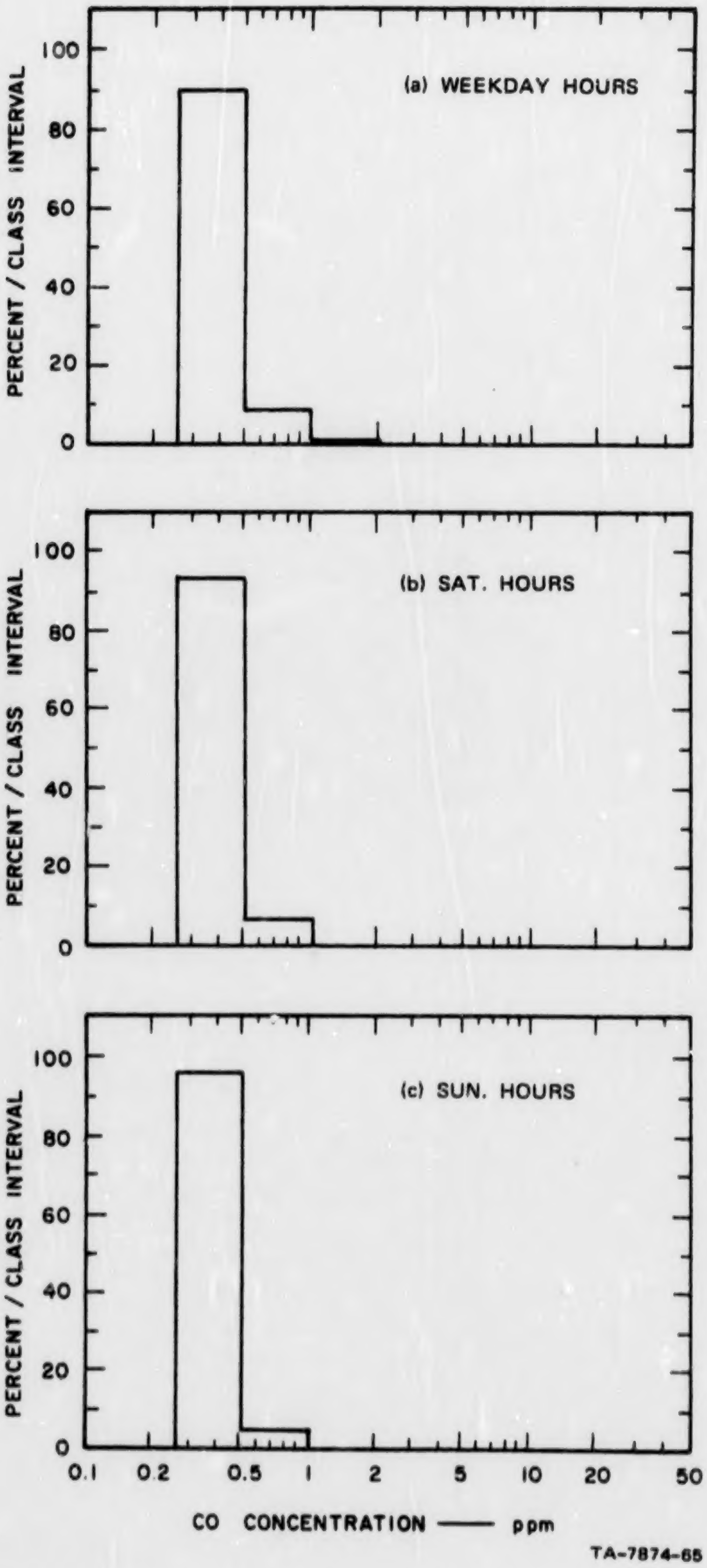

TA-7874-65

FIGURE 29 CALCULATED ST. LOUIS CAMP STATION CO CONCENTRATION FREQUENCY DISTRIBUTION FOR 1990 TRAFFIC CONDITIONS; WEEKDAY, SATURDAY, AND SUNDAY HOURS

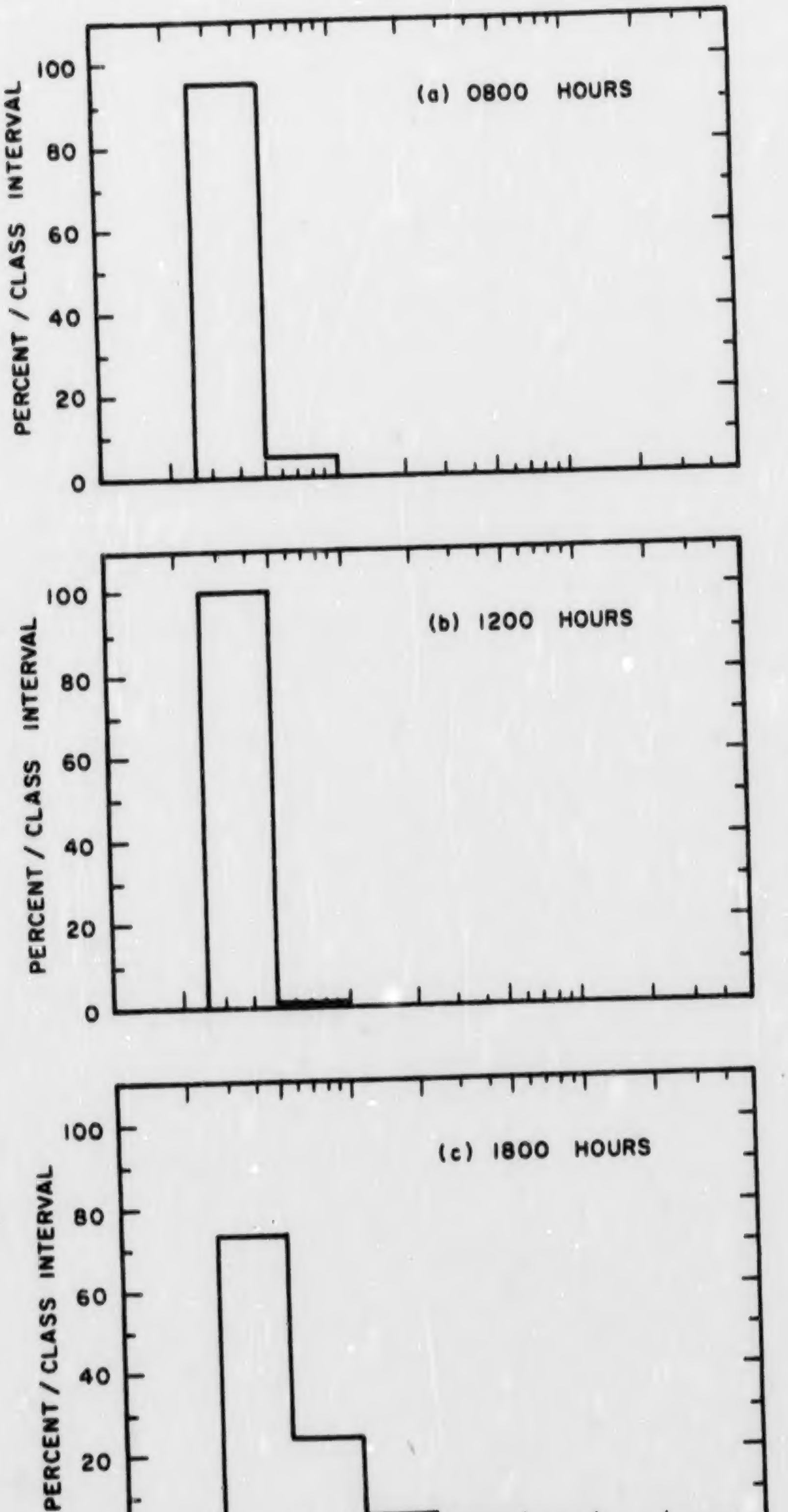

FIGURE 30 CALCULATED ST. LOUIS CAMP STATION CO CONCENTRATION FREQUENCY DISTRIBUTION FOR 1990 TRAFFIC CONDITIONS; 0800, 1200, AND 1800 HOURS

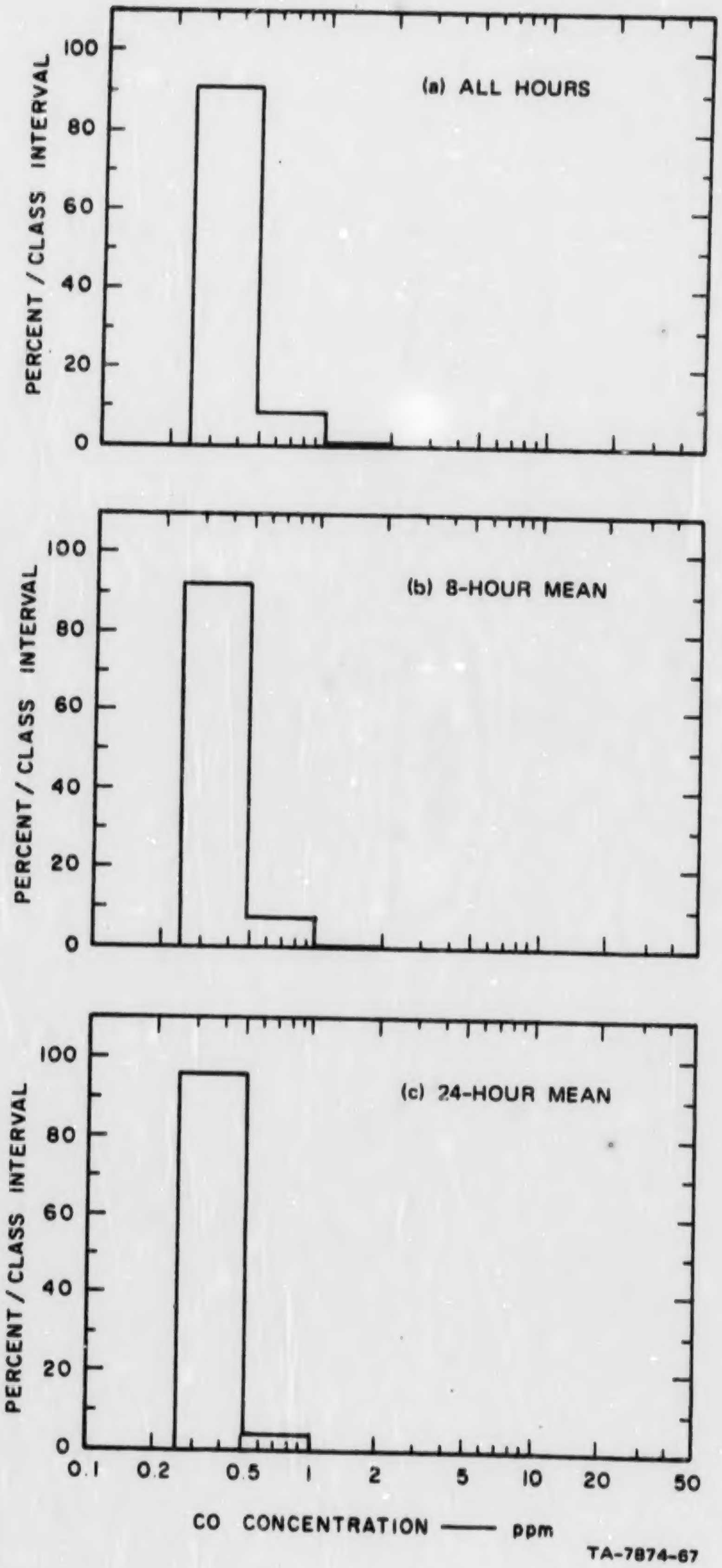

FIGURE 31 CALCULATED ST. LOUIS CAMP STATION CO CONCENTRATION FREQUENCY DISTRIBUTION FOR 1990 TRAFFIC CONDITIONS; 1-HOUR, 8-HOUR, AND 24-HOUR AVERAGES

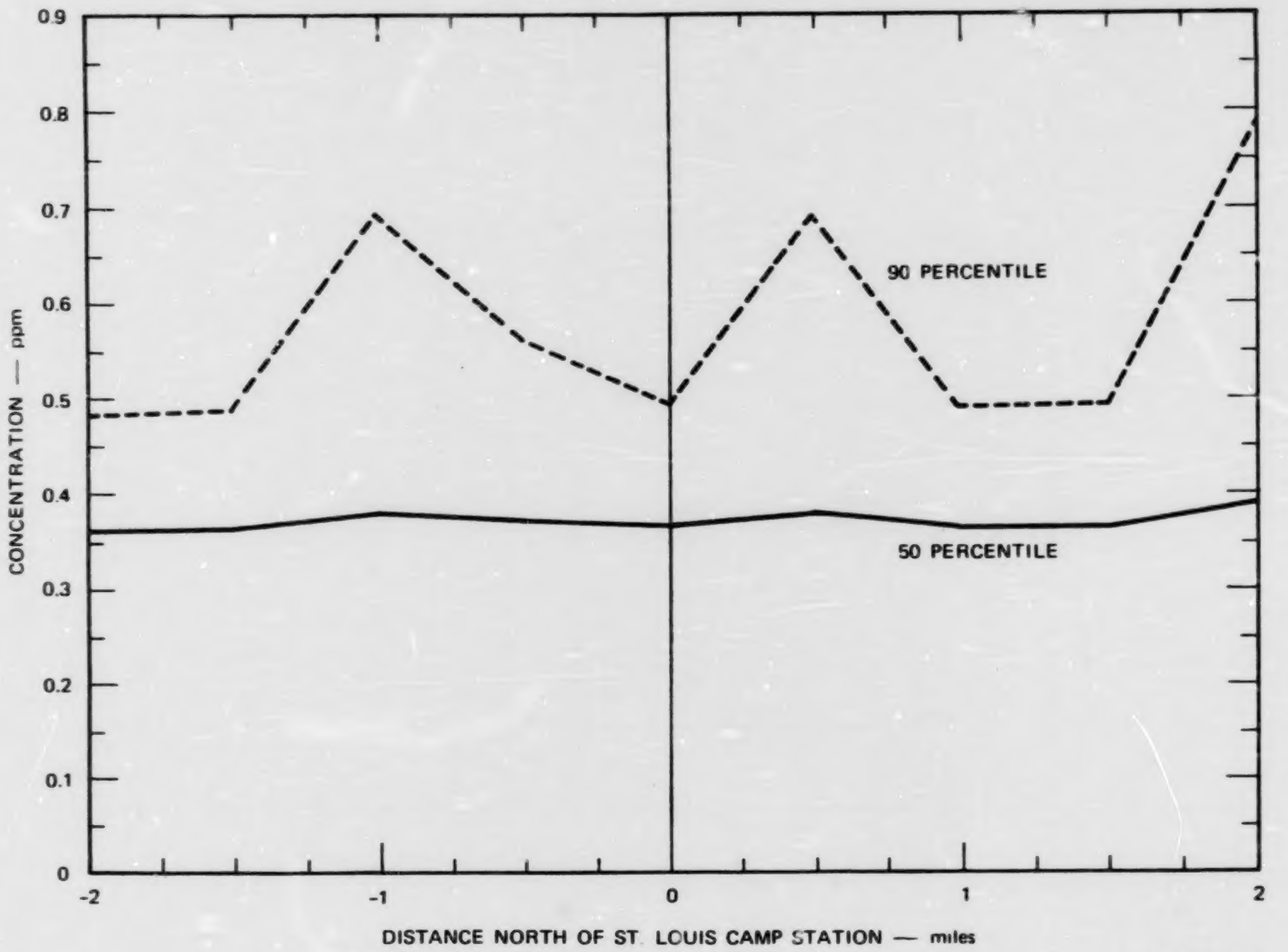

TA-7874-68

FIGURE 32 SPATIAL VARIATIONS OF CALCULATED ST. LOUIS MEDIAN AND 90 PERCENTILE CONCENTRATIONS FOR 1990 TRAFFIC CONDITIONS with emission controls

the 1990 frequency distributions at the CAMP site as were seen in those based on 1965 emissions. Figure 29 shows that the higher concentrations occur more frequently on weekdays than on weekends, and Figure 30 shows that higher concentrations are more likely at 1800 than at 1200 or 0800. These results are certainly as expected, considering that we have not changed the diurnal or weekend values of P_t used in Eq. (IV-6). If there were a foreseeable change in working hours, a change in these values might be justified.

Figure 31 for 1990 corresponds to Figure 27 for 1965. Again we see the reduction in the spread of the frequency distribution as the averaging period is increased. In this case the change is not so pronounced because there are so few high concentration cases in the distribution of the hourly values.

Figure 32 shows the change in the 1990 median and 90-percentile concentrations along a north-south line through the CAMP site. The scales on this figure are different than those on the corresponding figure for 1965, Figure 28. Some of the pronounced features of the 90-percentile curve may be artifacts caused by the log-linear interpolation used to determine the values. It suggests that smaller class intervals should be used when we know that the calculated concentrations will not reach high values. Regardless of the artifacts, the data show that the concentrations remain very nearly the same along this line for several miles through the downtown area.

BLANK PAGE

V TESTING AND IMPROVING THE MODEL

In the preceding sections, the design of the basic model was presented along with the techniques used to determine its inputs, and examples of the types of output that the model is capable of producing. In this section, we will discuss the way in which input accuracy affects the accuracy of the resultant outputs, i.e., the sensitivity of the model. We will also present the results of an attempt to "calibrate" the model by comparing its output to the observed concentrations.

A. Sensitivity Tests

It is important to know the effects in output values caused by changes in the inputs. If a very small change in a certain input results in a large change in the output, then the model is very sensitive to that input and we will be required to provide values of the input that are very accurate, if we are to avoid large errors in the output. On the other hand, if large changes in an input have little effect on the output, then little effort need be expended to achieve high input accuracy for that particular variable. Of course, sensitivity is not likely to remain constant over the whole range of values that a particular variable can assume. Thus it is possible that for certain combinations of parametric values, the model output will be totally independent of the changes in one or more inputs. This, as will be seen in this section, occurs with this model, and we have referred to it in earlier sections. This characteristic has allowed us to treat several different combinations of variables as though they were the same.

Preceding page blank

In the following we will discuss the inputs to the model and try to illustrate their interdependence and their effects on the output.

1. Source Strength

If source strength were to increase or decrease by some factor uniformly throughout the city, then the resultant change in the calculated concentration would be quite straightforward. The calculated concentration would increase or decrease by the same factor. Similarly, if our emission estimates were uniformly in error, then that error would show proportionally in our calculations.

A more realistic situation would be the case where the emissions are poorly estimated for individual upwind segments of the model. In this case the change in the output will depend not only on the relative magnitude of the error in emission, but also on the segment in which the error occurs and on mixing depth and stability. The relative effect also depends on the average emission rates in other segments.

To test the effects of errors in the different segments, calculations were made for a case where the true source strength was taken to decrease linearly away from the receptor and to reach zero at 32 km upwind. For a site at the center of the city, this is probably a reasonable approximation of the distribution of emissions. To test the sensitivity of the model to changes in source strength in the different segments, we doubled the emissions (relative to those specified by the assumption of a linearly decrease with distance) in one segment at a time. The results of these calculations are given in Table II. This table shows the percentage increases in the total calculated concentrations that result from the doubling of the source strength in the individual segments. Four stability types and two different mixing depths are represented in the table.

Table II

PERCENTAGE INCREASE IN CALCULATED CO CONCENTRATION RESULTING FROM THE DOUBLING OF EMISSION RATES IN DIFFERENT SEGMENTS

Stability Class*	Mixing Depth (m)	Segment with Doubled Emission								
		1	2	3	4	5	6	7	8	9
1	50	1.4	1.0	1.5	3.0	5.9	11.2	20.1	31.0	24.8
2	50	2.1	1.5	1.6	3.0	5.8	11.1	20.0	30.6	24.4
3	50	3.1	2.1	2.2	3.0	5.7	10.8	19.4	29.8	23.9
4	50	4.5	3.3	3.7	4.3	5.5	10.1	18.1	28.0	22.4
1	3000	26.9	17.8	15.2	9.1	3.5	3.6	6.4	9.8	7.8
2	3000	22.3	15.9	16.0	14.4	11.2	6.6	4.0	5.3	4.4
3	3000	14.6	10.2	10.4	11.1	11.7	12.3	12.5	11.4	5.7
4	3000	9.8	7.3	8.2	9.4	11.2	13.4	15.5	16.1	9.1

*1 = Extremely unstable
2 = Moderately unstable
3 = Slightly unstable
4 = Neutral.

For the low mixing depth case (50 m) there is a general increase in the contribution caused by changes in source strength as one progresses toward the segments farthest from the receptor. The box model is employed for most of the calculations when the mixing depth is low, and it specifies that the contribution from a segment is proportional to the upwind distance subtended by that segment. Since the outer segments are considerably larger than the nearby segments, their contribution is consequently greater. This effect is suppressed in the larger mixing depth cases where contributions from the nearer segments are mixed through a shallow layer compared to those from the further segments.

The table indicates that for some combinations of stability and mixing depth, appreciable uncertainties can be introduced into the calculations by uncertainties in the specification of source strength.

Other factors to be considered include the possibility that errors in specifying emissions may be compensating and therefore not so important.

Finally, errors in emission values due to improper location of highway links are much more apt to be large, relative to the total source emission in the smaller, close segments, than they are in the large outer segments. When the mixing depth is low, Table II shows that errors in nearby source strengths cause relatively small errors in the calculated concentration. It is only for the larger mixing depths that the errors in the nearby segments produce large relative errors in the calculated concentrations. However, for large mixing depths the concentrations tend to be lower and of much less importance to planners.

2. Wind Speed

Of all the inputs, the most straightforward effect on the model output comes from wind speed. Since both the Gaussian and box models yield concentrations that are inversely proportional to the wind speed, then the overall model will also have this characteristic regardless of where the transition occurs between the two submodels. As the model is presently constituted, observed wind speeds less than 1 m/s are not used, so for observed wind speeds less than this value the model output would not change. For higher wind speeds the calculated concentrations will vary inversely as the wind speed, providing the other parameters remain invariant.

3. Wind Direction

With regard to model sensitivity, wind direction and source strength are closely related parameters. Variations in wind direction only change the values used for the emissions in the segments upwind of the receptor, so the effects of changes of segment source strengths discussed earlier can, to some extent, be interpreted in terms of wind direction effect. However, this requires that we know something of the changes in source strength as a function of direction from the receptor. If the receptor is located at the edge of the city, then changes in wind direction can shift the emissions in the segments from large to small as the wind shifts from the city to the countryside. Such changes would be likely to occur in almost all the segments, for such a case.

For locations near the center of the city, the farther and larger segments are not likely to change much with direction because the large numbers of streets within the larger areas will tend to smooth out the fluctuations. However, for the nearby segments that may on the average contain only a few streets, the variations are likely to be large. Since the nearby segments contribute appreciably to the calculated concentrations, we may expect substantial variations.

To provide an example of the kinds of changes that might be expected to arise from changes in wind direction, some sample calculations have been made; they are illustrated in Figure 33. Two sets of meteorological conditions are shown; we can see that the relative changes are about the same in both cases. There is about a 3:1 difference between the largest and the smallest calculated concentrations. The calculations were made at 22.5° increments, and it can be seen that the largest difference between adjacent directions amounts to about 60 percent. Thus, it seems reasonable to estimate that an error in wind direction specification of 22.5° could result in errors as large as a factor of two.

4. Location of the Receptor

Another factor that is closely related to source strength is the accuracy with which we can specify the location of the receptor relative to the traffic links. The arguments are essentially the same as those given above for direction, i.e., moving the receptor relative to the links changes the location of the various upwind segments, and hence changes the source strengths used for the calculations.

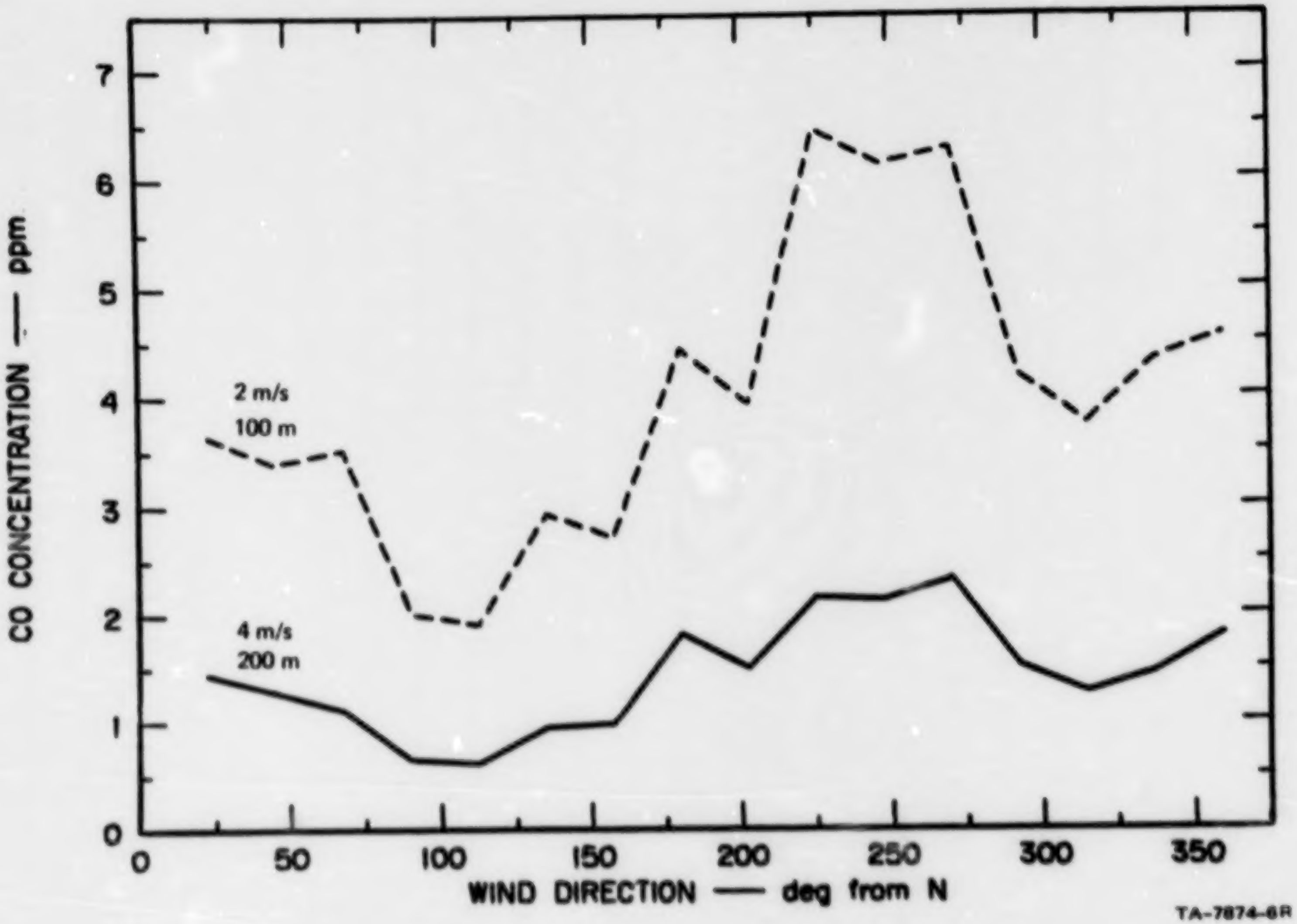

TA-7874-6R

FIGURE 33 EFFECT OF WIND DIRECTION ON CONCENTRATIONS COMPUTED FOR THE WASHINGTON, D.C., CAMP STATION. (0700-0800 LST, neutral stability, wind speeds and mixing depths as shown)

A study was made to determine the sensitivity of the model to errors in the location of the receptor. The study was conducted by moving the coordinates of the receptor point from its original location in increments of 0.1 mile and determining the effect of the displacement on the concentration. Increments of 0.1 (0.16 km) mile were chosen because this is the coding precision for most of the areas studied, although in crowded central areas, coordinates have been coded to the nearest 0.01 (0.016 km) mile. Figure 34 shows changes in the calculated CO concentration arising from displacements of the receptor in the downwind (x) and crosswind (y) directions. The initial location corresponds to the Washington, D.C., CAMP Station. In this area, with its dense network of major streets, concentrations are fairly sensitive to the location of the receptor relative to the streets. Outside the densely packed downtown area, the sensitivity to location is much less.

The figure shows that changes in calculated concentration of more than a factor of two do occur within 0.1 mile (0.16km). However, for a precision of location of about 0.01 mile (16 m), the changes would be limited to a few tens of percent or less, regardless of wind speed. The model would probably be more sensitive to these errors for the cases of low mixing depth and high stability.

5. Stability and Mixing Depth

Stability and mixing depth interact to determine which of the two submodels are used for the calculation of the contribution of emissions from a given segment. To determine the effects on the model output of variations in stability and mixing depth, calculations were made using two different configurations of carbon monoxide emission. In the first case, source strengths were assumed to be the same in all nine segments of the model. It was assumed that there were no emissions

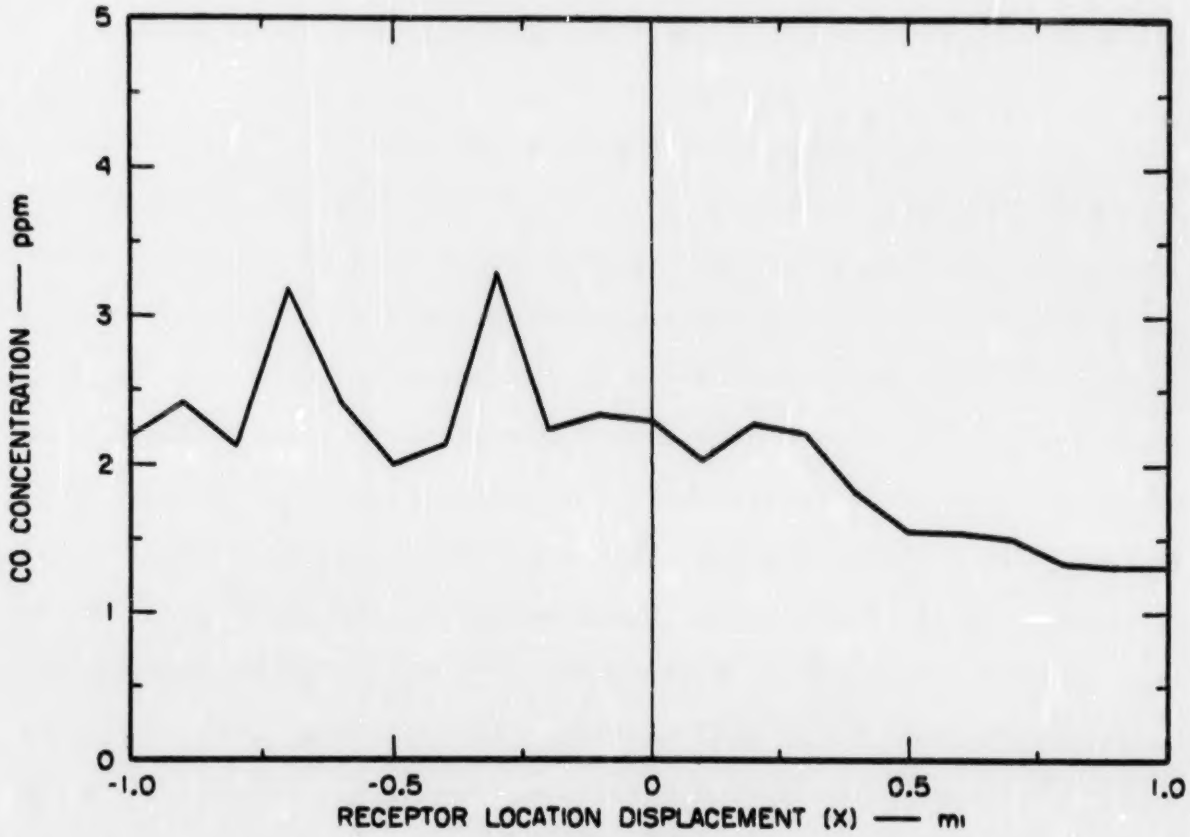

(a) ALONG-WIND

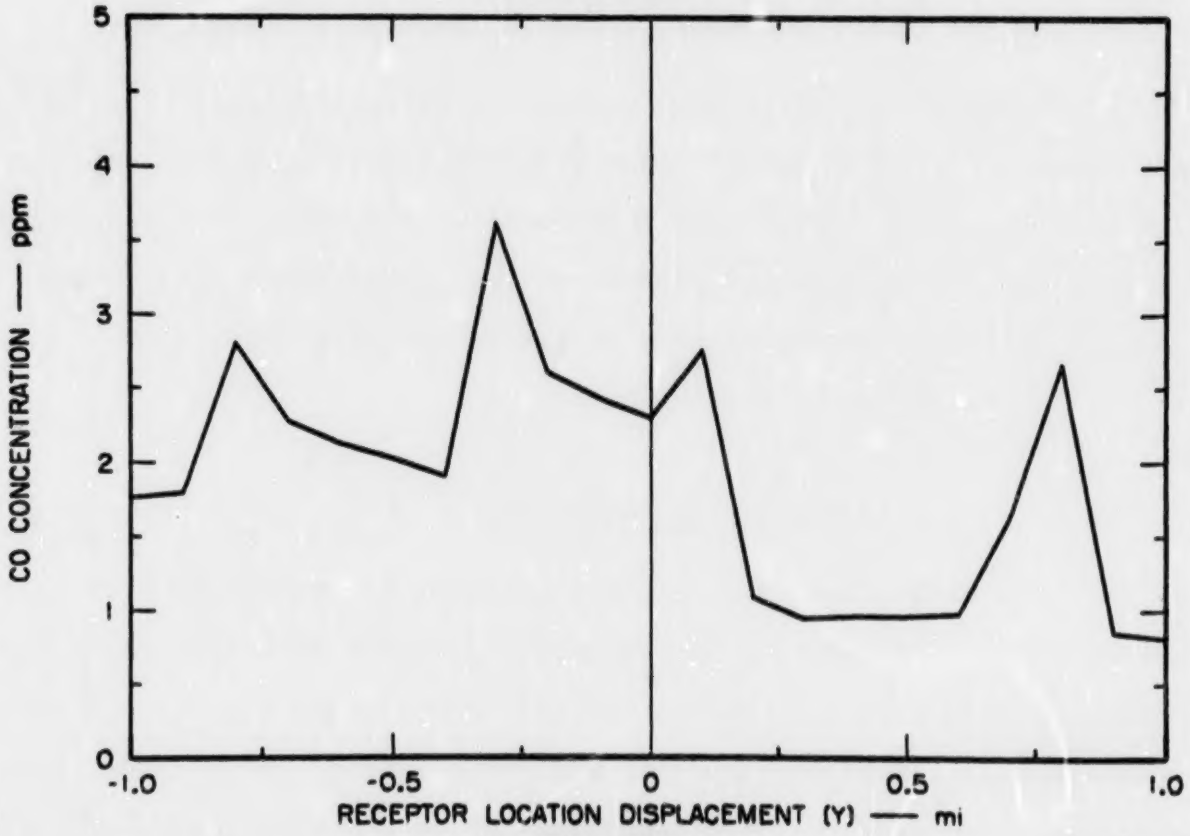

(b) CROSS-WIND

TA-7574-5R

FIGURE 34 EFFECT OF MOVING RECEPTOR POINT
(Washington, D.C., CAMP Station; 0700-0800 LST, wind 270°/4 ms^{-1}, neutral stability, mixing depth 200 m)

beyond the outer boundary of the last segment, 32 km from the receptor. The results of calculations for this source configuration and for various combinations of stability and mixing depth are shown in Figure 35(a). The results have been normalized to represent unit wind speed and unit source strength. In this figure we see that all the results are essentially the same for low values of mixing depth, regardless of stability. For very shallow mixing layers, the box model is used for almost the entire distance upwind of the receptor. Since the box model results are independent of stability, the fact that the results converge at small mixing depths is to be expected.

The neutral and slightly unstable cases shown in Figure 35(a) are unaffected by mixing depth for the larger values of the parameter. This too is quite reasonable because mixing of the emitted material proceeds rather slowly under the more nearly stable conditions and the mixing is uninhibited by the top of the mixing layer, if it is sufficiently high. In such cases, the Gaussian model is used for the concentration calculations throughout the entire 32-km upwind distance. The results of Gaussian model calculations are independent of mixing depth.

For the moderately unstable and extremely unstable cases the box model is used in the calculations, for at least some segments, for mixing depths to 3000 m. However, the number of segments for which the box model is applicable decreases with increasing mixing depth, so that calculated concentrations become less dependent on mixing depth as that parameter increases. This is reflected in the continual approach of the slope of the curves toward zero. It also suggests that the 4000 m upper limit that was placed on mixing depth, in some applications of the model, will have very little effect on the results.

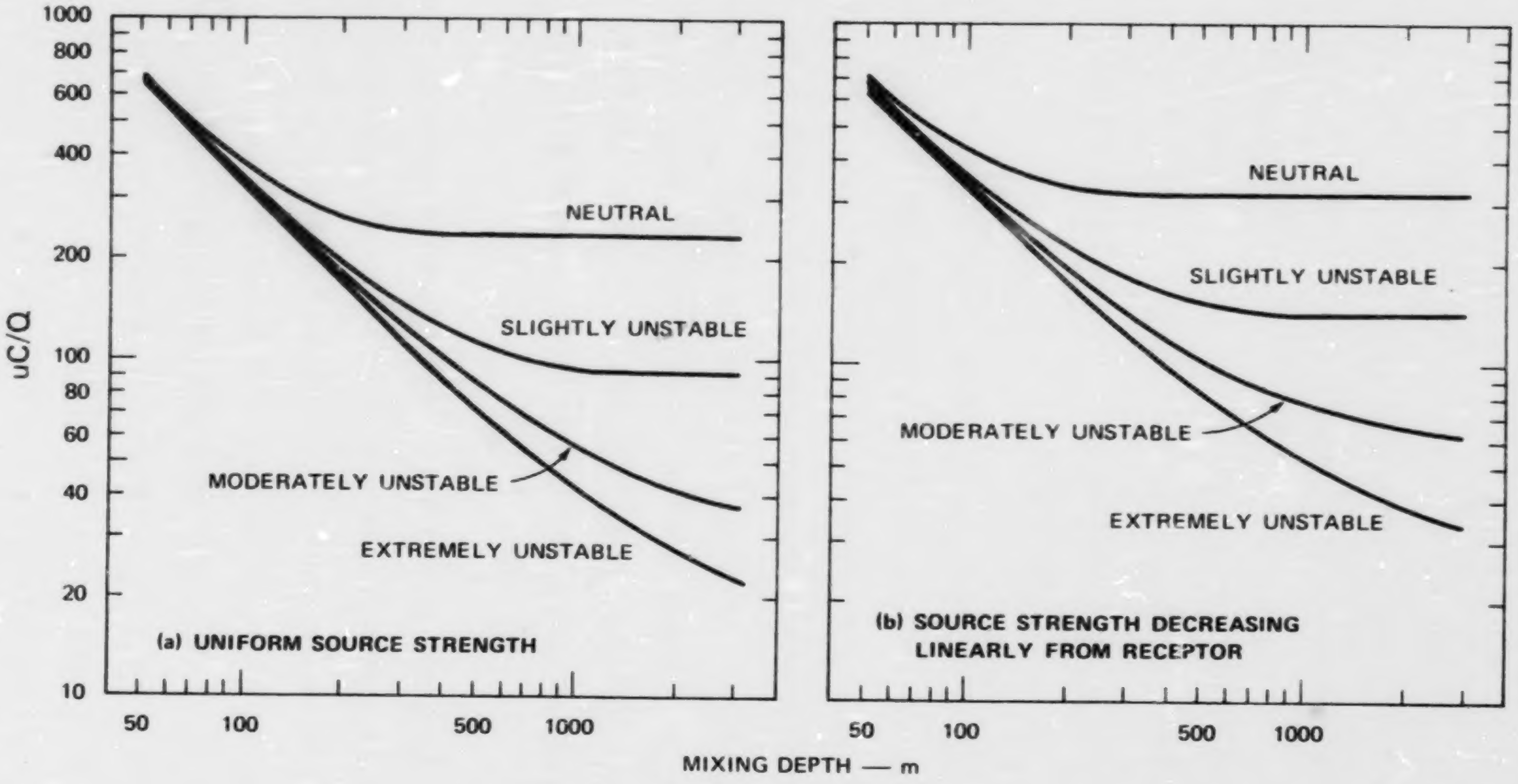

TA-7874-38

FIGURE 35 NORMALIZED CONCENTRATION AS A FUNCTION OF STABILITY AND MIXING DEPTH. Normalized for average source strength over 32-km upwind sector

As noted before, the assumption of a uniform source strength over the city is probably less realistic than an assumption of a source strength that decreases from the center of town to its edge. We recalculated the cases used for the curves in Figure 35(a), but used a source strength that linearly decreased from two units at the receptor to zero 32-km upwind. The results of these calculations are shown in Figure 35(b). Again, the results have been normalized to represent unit wind speed and unit average source strength. Qualitatively, the two source configurations produce similar results. However, the dependence on mixing depth is less for all cases. This is because the mixing depth dependence is the result of those parts of the calculation based on the box model. The Gaussian model is used for calculations of concentrations due to emissions from segments close to the receptor. The box model, if used at all, applies to the farther segments. In this source configuration the emission rates in the more distant segments are less than those in segments close to the receptor. Thus, the contributions that the box model makes to the results are smaller than those for the uniform area case. This decreases the effect of mixing depths upon the normalized concentrations.

The results displayed in Figure 35(a) suggest that for some values of mixing depth, the results obtained from the model are nearly independent of stability. For certain stability types, changes in the mixing depth produce no changes in the results, if the mixing depth is sufficiently large. We have made use of this latter fact in the development of the climatological model. It allows us to consider certain combinations of stability and mixing depth to be identical with certain others. As noted earlier, this simplifies calculations and reduces the amount of computer memory required.

B. Use of Observations to Improve the Model

1. Introduction

The formulation of the model given in earlier sections of this report was based entirely on empirical and theoretical considerations of traffic emissions, and meteorological diffusion and transport. No adjustable constants have been used. It is clear that the accuracy of this model could be improved if we were to make some use of observed carbon monoxide concentration data. In this section we will discuss a method whereby this information can be incorporated into the model. In developing a method, we have attempted to make statistical adjustments with as little damage to the physical basis of the model as possible. If the model is to be useful in a variety of cities, it should be developed from sound physical principles, rather than by purely statistical means. The physical phenemena underlying the model will remain the same from city to city, but we cannot assume the same to be true of the statistics. Of the inputs to the model, source strength, wind speed, and wind direction have been chosen as the most amenable to study through the use of statistical comparison with observed CO concentrations. Mixing depth and stability were discarded, partly because neither is amenable to statistical correction. Both are involved in the model in such nonlinear fashion that they cannot be isolated from the rest of the model for statistical treatment. Also, model results are not very sensitive to mixing depth under most conditions, as was shown in the preceding sensitivity analysis, so that if the mixing depth is specified incorrectly, it may be less serious than an incorrect wind speed or source strength, which are directly related to the output.

In considering source strength, we have assumed that it is directly related to the total daily traffic and to the average speeds, but there is uncertainty about how the emissions are distributed through the day. This uncertainty inseparably includes considerations of the proportionality of emission rates and traffic amounts. As will be seen in the following sections, uncertainties in source strength can be minimized by statistical techniques.

We know that wind speed has a very significant and direct effect on concentration. We also know that the transport wind that moves and dilutes pollutants in the city may be different than the airport wind that we have used for our calculations. The relationship between the two winds can be determined so as to minimize the differences between calculated and observed concentrations.

Finally, wind direction probably plays a part in determining the background concentrations entering the segment farthest from the receptor and in determining the aerodynamic effects of structures near the measuring point. The gross effects of wind direction at a given location can be checked through comparison of calculated and observed concentrations.

In the following section an approach to the "calibration" of the model is presented along with some results. This approach is by no means the only one possible, but we feel that it has a sound physical basis, and encouraging results have been achieved.

2. Attempted Improvements

As was shown in Section IV-C, the model can be most simply expressed in the following form

$$C = X_{j,m,d}\left(\frac{P_t}{u}\right) \quad , \qquad \text{(V-1)}$$

where

C = calculated concentration due to emissions within the city

$X_{j,m,d}$ = the sum of the products of average daily emissions in the upwind segments and the dilution ratios for the segments; depends on stability (j), mixing depth (m), and wind direction (d)

P_t = a factor used to give source strengths for the t^{th} hour, based on the daily distribution of traffic and changes in average speed during peak traffic hours

u = wind speed.

a. Background Concentration

The above equation can be related to the observed concentration C_o for a given time by the following

$$\begin{aligned} C_o &= C + \epsilon \\ &= X_{j,m,d}\left(\frac{P_t}{u}\right) + \epsilon_1 \quad , \end{aligned} \tag{V-2}$$

where ϵ_1 is the error in specifying the concentration. If we assume that part of the error arises from a background concentration β entering the farthest upwind segment of the model, then Eq. (V-2) can be written

$$\begin{aligned} C_o &= C + \beta + \epsilon_2 \\ &= X_{j,m,d}\left(\frac{P_t}{u}\right) + \beta + \epsilon_2 \quad . \end{aligned} \tag{V-3}$$

In this formulation β is a constant, although it can be made a function of wind direction; ϵ_2 is the error remaining after the background has been added to C.

b. Wind Speed

Let us assume that effective urban transport wind speed u is not correctly represented by the wind measured at the airport, u_a, and that the true value of its reciprocal can be approximated by a linear expression depending upon the reciprocal of the measured wind speed at the airport, i.e.,

$$\frac{1}{u} = a + \frac{b}{u_a} \quad , \tag{V-4}$$

where a and b are constants to be determined, and u_a is the measured airport wind, assumed to have a minimum value of 1 m s^{-1}. Assuming the dilution factor 1/u to be a linear function of the dilution due to the airport wind makes it much easier in practice to minimize errors than if we assumed a linear relation between the winds themselves.

Making the substitution in Eq. (V-3) gives

$$C_o = X_{j,m,d} \frac{\left(au_a + b\right) P_t}{u_a} + \beta + \epsilon \quad , \tag{V-5}$$

where ϵ is the residual after adjustments have been made.

The problem is then to use the observed data to determine the values of the constants. To do this we used the conventional approach and minimized the sum of the squares of the residuals. This procedure gives the following equations:

$$\beta N + a\Sigma X_{j,m,d}P_t + b\Sigma\left(\frac{X_{j,m,d}P_t}{u_a}\right) = \Sigma C_o \qquad (V\text{-}6)$$

$$\beta\Sigma X_{j,m,d}P_t + a\Sigma X^2_{j,m,d}P^2_t + b\Sigma\left(\frac{X^2_{j,m,d}P^2_t}{u_a}\right) = \Sigma C_o X_{j,m,d}P_t \qquad (V\text{-}7)$$

$$\beta\Sigma\left(\frac{X_{j,m,d}P_t}{u_a}\right) + a\Sigma\left(\frac{X^2_{j,m,d}P^2_t}{u_a}\right) + b\Sigma\left(\frac{X^2_{j,m,d}P^2_t}{u_a^2}\right) = \Sigma\left(\frac{C_o X_{j,m,d}P_t}{u_a}\right) , \qquad (V\text{-}8)$$

where N is the total number of cases over which the summations are performed. The above simultaneous linear equations were solved for β, a, and b using a standard matrix inversion computer program. This minimizes the root-mean-square error for the hypotheses represented in Eq. (V-5), and for the available data set.

c. Diurnal Distribution of Emissions

The values of P_t have been specified for the model on the basis of only a few measurements in a limited number of cities. After the wind speed corrections have been made, it is a simple matter to correct the values of each of the 24 values of P_t to minimize the total differences between observed and calculated values. After a new set of P_t values has been calculated, they can be used to recalculate the a, b, and β. This iterative procedure has been used on a set of St. Louis data (see the examples given in Section V-3); the correlation and root-mean-square error were found to stabilize after four repetitions.

d. Wind Direction

The wind direction effect could most easily be included in the background constant term. The data could be stratified according to wind direction and values of β calculated for each case. The average of these β values (weighted by the number of occurrences of each wind direction in the data set) would be the same as the value of β calculated from the procedure outlined in the preceding sections. We have not had sufficient data to stratify according to wind direction, so the example that follows has not considered that correction.

3. Example

The approach to calibration outlined on the preceding pages has been applied to data from St. Louis. The earliest CO concentration records that we have available from the CAMP Station in St. Louis were for the month of March 1964. The records were fairly complete for the rest of that year. This provided us with ten months of concentration data that were concurrent with values that had been calculated using the climatological model. We chose to determine the calibration constants on the basis of the available odd-numbered months and to use the even numbered months as independent data for checking the results.

To determine if there was an annual variability to the values of the constants a, b, and β, they were calculated separately for the weekdays in each of the odd numbered months. There appeared to be no regular changes in a and b, but β did seem to have a seasonal change. The seasonal change was incorporated into the corrections. For the independent months, values of β were interpolated between those found for the odd numbered months. The resulting calibrated equation is

$$C = \frac{0.07\, u_a + 1.4}{u_a} P_t X_{j,m,d} + \beta_m \quad , \qquad \text{(V-9)}$$

where

P_t = the adjusted traffic emission factors determined statistically

β_m = background concentration adjusted for monthly variations.

The adjusted values of P_t are shown in Figure 36. This figure also shows the values of P_t derived from trip data. The corrected curve shows greater midday emission and lower night emissions than had been

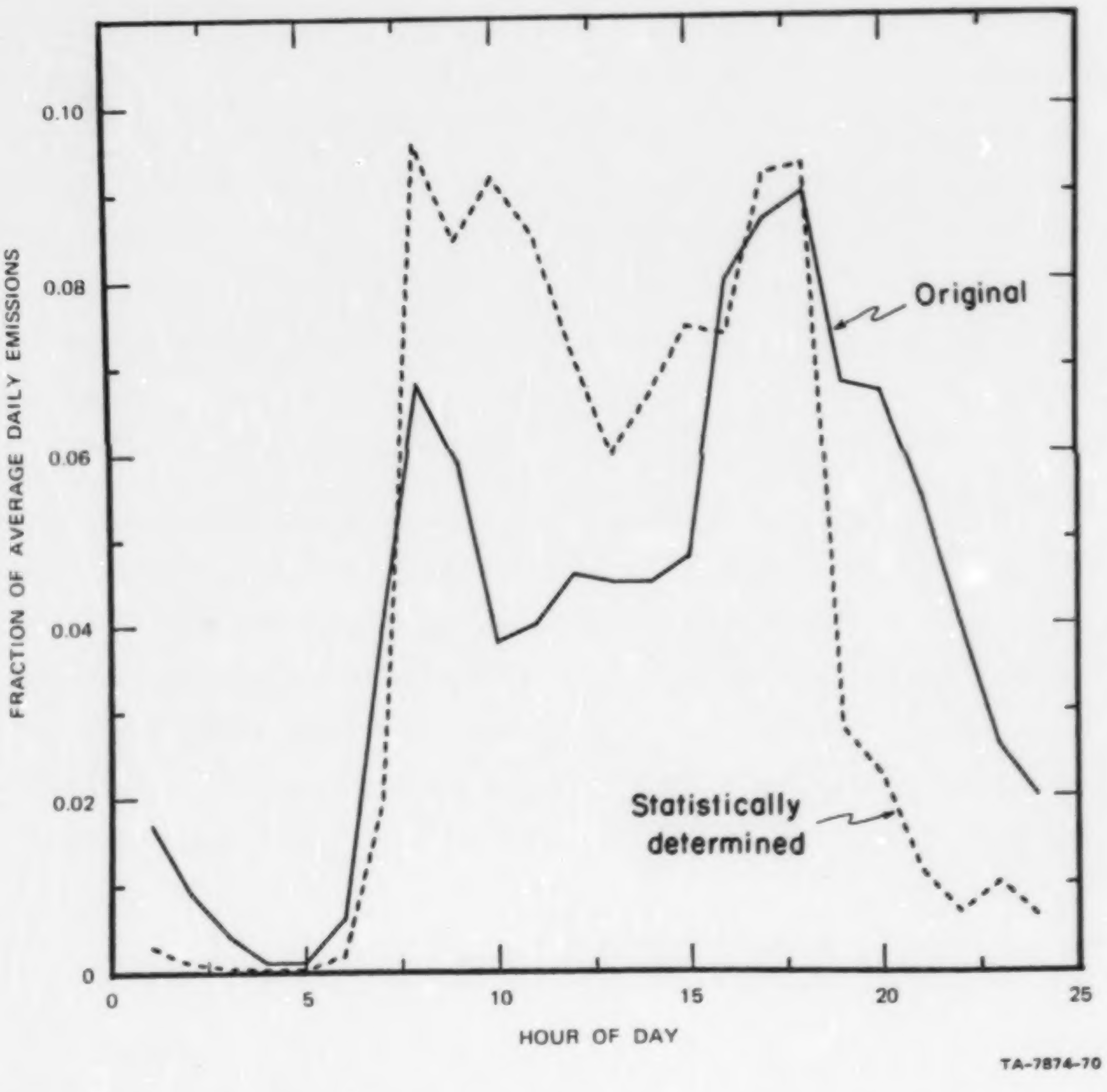

FIGURE 36 DIURNAL EMISSION PATTERNS FOR ST. LOUIS

originally postulated. This probably reflects the traffic conditions in the downtown area near the CAMP Station. Downtown areas attract considerable traffic during operating hours but very little at night. This is reflected in the very rapid increase in the value of P_t at the beginning of the business day and the corresponding rapid decrease at its end.

The performance of the model was considerably improved by the derived constants. Table III shows the correlation coefficient and root-mean-square errors of the calibrated and uncalibrated models for the ten months studied. The table also shows the values of β_m used for each month. With these calibration factors included, the model predicts the hour-by-hour concentrations for the independent months with a root-mean-square error[*] of 3.1 ppm.

The correlation and root-mean-square error resulting from the use of "persistence" values have been calculated for the weekdays of the five independent months. For these calculations, the observed CO concentration at the CAMP Station was compared with the concentration observed during the same hour of the preceding weekday. The correlation was 0.64, with a root-mean-square error of 3.0 ppm, so the calibrated model performed very nearly as well as persistence. Of course, the persistence method cannot be used with forecast traffic data to estimate conditions in future years.

---

[*] Root-mean-square error = $\sqrt{[\Sigma(C_o - C_c)^2]/N}$

where

N = number of cases

C_o = observed concentration

C_c = calculated concentration.

Table III

RESULTS OF MODEL CALIBRATION

Month (1964)	β_m (ppm)	Uncalibrated		Calibrated	
		Correlation Coefficient	Root-Mean-Square Error (ppm)	Correlation Coefficient	Root-Mean-Square Error (ppm)
Calibration Months					
March	4.2	0.45	5.5	0.59	2.0
May	5.6	0.29	6.2	0.61	2.2
July	7.0	0.26	8.8	0.63	2.3
September	5.6	0.27	5.7	0.58	3.8
November	4.2	0.45	5.9	0.61	3.4
Independent Months					
April	4.9	0.28	6.9	0.58	2.3
June	6.3	0.32	8.1	0.50	3.7
August	6.3	0.16	5.0	0.63	3.2
October	4.9	0.26	4.7	0.53	3.3
December	3.5	0.39	5.4	0.61	2.9

A second comparison is also available for judging the model's performance. We can compare it to climatology. The root-mean-square difference between the observed concentrations and the mean concentration is the standard deviation of the observed values. For the independent data this is 3.5, somewhat greater than the model's root-mean-square error of 3.1. As with persistence, the concentration climatology is not a useful tool for estimating future conditions.

One final check can be made of the performance of the calibrated model. We can see how well it reproduces the frequency distribution of observed concentrations. This has been done for the independent weekday hours used in the above calculations; the results are shown in Figure 37. In this figure, cumulative frequencies are plotted on a log-probability graph. On such a graph, log-normal distributions appear as straight lines. It can be seen that both the calculated and observed distributions differ somewhat from the ideal log-normal. For the high percentile values, the two frequency distributions agree quite well. Between the 50 percentile and the 99.9 percentile, the agreement between the observed and calculated concentrations is generally within 25 percent. It is the high percentile concentrations that are of greatest importance to planners, and for these the calibrated model appears to perform very well.

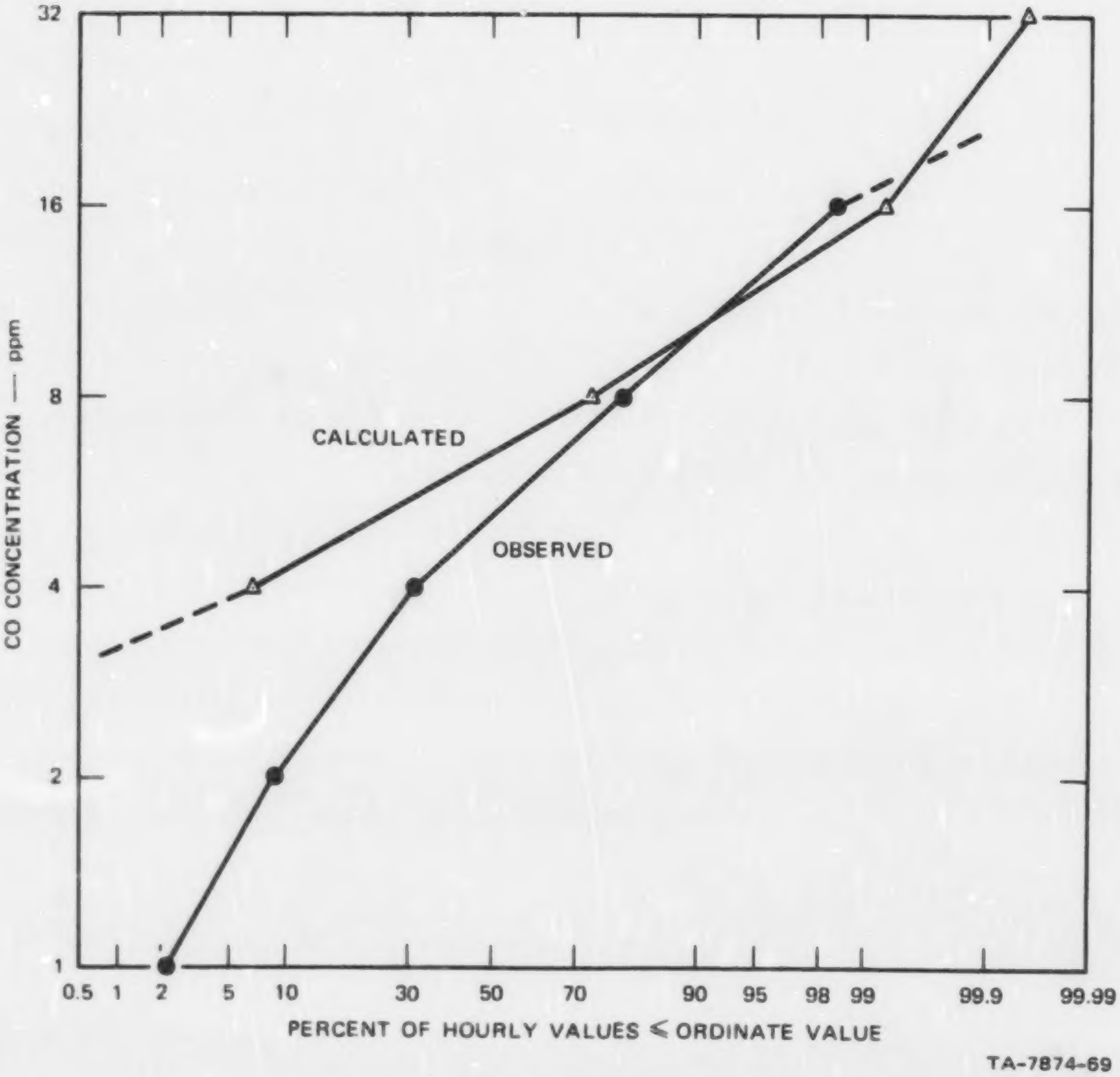

FIGURE 37 OBSERVED AND CALCULATED FREQUENCY DISTRIBUTIONS FOR FIVE MONTHS OF INDEPENDENT DATA

VI DISCUSSION AND FUTURE PLANS

This report has presented an approach to modeling urban CO concentrations that meets most of the established objectives. The model can calculate hourly concentrations at one or many points in a city. It can determine frequency distributions and other statistical information about CO concentrations. Source strengths can be determined from estimates of traffic, either historical or forecast, but assumptions have to be made about the CO emissions to be expected from the automobiles of the future. The meteorological inputs for the model can be determined from readily available weather data.

The model is quite versatile, in that a wide variety of parameters can be calculated without the need for esoteric input data. In these respects the model is satisfactory, but its performance has been disappointing in one most important respect. For those few places from which data are available, the hourly concentrations calculated with the model and those observed are generally in poor agreement.

The discrepancies between observed and calculated concentrations may be due to many different causes. In general, these causes can be divided into three categories: (1) inadequate or inaccurate input data for the model, (2) invalid assumptions used in the formulation of the model, and (3) unrepresentativeness or inaccuracy of the CAMP observations. Specific examples that fall into these categories are discussed in the following paragraphs.

The first category of observation/calculation discrepancy is errors in input data. Errors in source strength specification immediately come to mind as an example in this category. Source strength errors can arise from erroneous or unrepresentative historical traffic data, or from inaccurate relationships between average speeds and emission rates. Such errors can come from anomalous traffic situations such as accidents or large sporting events, or from assuming an incorrect distribution of the total daily traffic among the individual hours of the day. The results given in Figure 36 suggest that there may be significant differences between the assumed and the actual distributions in central St. Louis. The calculated concentrations are directly proportional to the emissions from traffic, so inaccuracies in its specification can contribute substantially to the differences between observed and model results.

Meteorological observations from a single station, usually at the airport outside the city, are used for the inputs to the model. Except for wind, these observations are not used directly, but are transformed to give the basic inputs to the model, i.e., stability type and mixing depth. Thus the sources of potential input error are twofold. First the meteorological observations themselves may not represent conditions in the city, and secondly the methods used to transform the observations into values of mixing depth and stability may not be totally appropriate. The sensitivity analyses in the report have shown some of the effects of such errors on the calculated concentrations. Wind speed and calculated concentration are inversely proportional. The relationship among mixing depth, stability, and concentration is more complicated. For unstable conditions and small mixing depths, the calculated concentration is almost inversely proportional to mixing depth, other things being equal. For large mixing depths, calculated concentration increases quite rapidly with increasing atmospheric stability. In any event, the results achieved with the model can be quite sensitive to the inputs, so inaccuracies in their specification represent potentially important sources of the discrepancies between model results and observations.

The second category for possible causes of the discrepancies between calculations and observations includes those that might arise from any invalid assumptions used in the formulation of the model. The first assumption made is that the Gaussian model provides a reasonably accurate description of the diffusion of pollutants from sources near the receptor, and the next is that the rates for this Gaussian diffusion can be defined by the Pasquill-Gifford empirical functions based on data from nonurban areas. While it would be difficult to change the model to remove the Gaussian assumption, it would be quite easy to use other functions to describe the diffusion rates. Because of increased mechanical and thermal turbulence in cities we might expect the diffusion to proceed more rapidly than given by the Pasquill-Gifford functions, which would mean that the presently calculated concentrations are biased to the high side by this effect. However, the presence of large buildings in downtown areas restricts the volume into which the pollutants can mix, and such an effect might counteract those caused by increased turbulence.

Another assumption that is included in the model in its current form is that of uniform meteorology throughout the urban area. It is certain that winds in cities are not uniform, and the same is true of mixing depth (e.g., Clarke, 1969). The stability index also changes between the edges of a city and its center. It may be that these factors are not so serious as it first appears because the results that have been achieved with the model seem to indicate that sources close to the receptor are the most important in determining concentrations. If this is indeed true, then wind, stability, and mixing depth close to the receptor are very important, but their values at greater distances are much less so. This would mean that different values of the inputs could be used for different receptor locations, but the basic form of the model would not have to be changed to accommodate changes of the parameters with distance upwind of each individual receptor point.

One of the most serious remaining weaknesses of the fundamental model is the assumption that it can be applied to calm conditions (if such conditions ever actually exist) by assuming that some slight organized air movement is present. After we identify and correct other possible sources of discrepancy between observations and calculations, it may be feasible to develop a better method for treating this important special case. Studies of air motions within cities during calm and near calm conditions would probably be of some help.

The third possible source of error is unrepresentative observations of CO concentrations. Before discussing examples, the term should be defined. For our purposes, a representative observation is one that has very nearly the same value as most of those that would have been obtained if the measurements had been made simultaneously at many other points in the same "general area." For studies with this model, the "general area" to be considered should have dimensions comparable to the resolution of the model, or about 100 to 200 m. Thus, we would consider observations to be unrepresentative of an area if significantly different results were likely to be obtained by moving the instrument to some randomly chosen points within about 200 m of its original location. This definition of representativeness implies that a monitoring station should be located at a point where its surroundings are reasonably uniform for about 200 meters in all directions. Such locations are virtually impossible to find in most cities. The CAMP Stations that served as data sources for the examples given in this report are probably located about as well as is possible (see Appendix I), but their locations cannot be considered "representative" in the above defined sense. The readings from these stations are likely to be biased or otherwise made unrepresentative by the presence of parking lots, traffic signals, and the aerodynamic effects of large nearby buildings.

The accuracy of the available observations of CO concentration is somewhat limited by the precision to which observations are reported. Values are given to the nearest part-per-million, resulting in an uncertainty of about 0.5 ppm.

Interferences from other atmospheric constituents are also possible with the instruments. The most likely interferent is water vapor, so the usual measurement procedures either remove the water vapor itself from the air to be analyzed, or else neutralize its infrared absorption interference with optical filters. Nevertheless some questions of possible interference remain. For instance, at the Washington CAMP Station it has been found that the removal of CO from ambient air by Hopcalite does not produce the anticipated readings of zero ppm when the CO-free air is analyzed; instead, the instrument indicates CO levels of 2 to 3 ppm.* If the instruments consistently indicate CO concentrations higher than those actually present, then the actual discrepancies between observed and calculated concentrations would be somewhat smaller than presently indicated. However, only a small portion of the disagreement can be explained by CO measurement errors.

A continuation of the work described in this report is currently underway. It is directed toward determining the source of the discrepancies discussed above. The major portion of the program will be devoted to field measurements of carbon monoxide concentrations and meteorological parameters within urban areas. Results from the earlier experimental studies of diffusion through cities (e.g., Stanford

---

*Letter to W. B. Johnson, dated 10 October 1969, from C. E. Couchman, Chief, Air Pollution Division, District of Columbia Department of Public Health.

University Aerosol Laboratory, 1953 a, b, c, d; Perkins, 1962; Pooler, 1966; Hilst and Bowne, 1966) will continue to be used for the further development and refinement of the CO model, along with the new data to be obtained. Although these previous studies are generally limited to point and line-source releases of tracers and their determinations of diffusion in the vertical are limited, they should be useful in refining the Gaussian model for urban applications.

To test the representativeness of CAMP Station measurements, we plan to measure CO concentrations at various locations around the St. Louis CAMP Station using a mobile instrument. Mobile measurements will also be made in other areas of St. Louis and San Jose in order to study the small-scale spatial variability of concentration.

Other studies of spatial variability are also planned. These will involve CO, wind, and temperature measurements around downtown intersections in St. Louis and San Jose at several levels from rooftop to about ten feet above street level. These studies should help to relate rooftop concentrations, which we believe are better represented by the model, with concentrations at lower levels, where measurements are usually made and where most people are exposed to the pollutants. The observations should also help to determine the nature and importance of aerodynamic effects caused by airflow around buildings and through the street canyons. These measurements will test the validity of using airport meteorological data to represent conditions throughout a city. Additional observations of temperature profiles and mixing depth variations across the urban area will check the methods we have used for estimating mixing depths.

Another input that will be tested during the program is the relation of observed traffic to the rate at which CO is generated. It is planned to use the detailed traffic data available from a relatively dense, computer-monitored network of sensors in downtown San Jose. By knowing the details of the traffic flow near the CO measuring stations, it should be possible to test the validity of the relationships between traffic and CO generation that have been used with the model.

Appendix A

PRINCIPAL SOURCES OF CO IN URBAN AREAS

Preceding page blank

Appendix A

PRINCIPAL SOURCES OF CO IN URBAN AREAS

The model considers only the mobile sources of carbon monoxide. The literature was surveyed to determine the importance of other sources of CO. Table A-I shows the fraction of total CO emissions arising from various sources for nine individual American cities and a 28-city average. The table shows that transportation CO emissions range from about 77 to 99 percent of the total for the different cities. According to Mason's (1969) data, about 98 percent of the CO emissions due to transportation are from motor vehicles.

San Francisco is the only city shown in the table that has nontransportation emissions greater than ten percent of the total. The major nontransportation source in the San Francisco Bay Area was incineration. As of 1 January 1970, incineration has been banned in the Bay Area. If we assume that the other CO sources remained the same, but all CO generated by incineration was eliminated, then the San Francisco Bay Area CO emissions from transportation would be about 92 percent of the total. This is very nearly the same as the other cities shown.

Inasmuch as more than 90 percent of the CO in urban areas is generated by traffic, we ignore fixed sources in our model. In the future we may treat some of the diffuse sources (such as space heating) in the same way that we now treat residential area streets. Very strong individual point sources, if they exist, may have to be treated separately at a later time. For now, we feel that inclusion of the more than 90 percent of the total CO emissions arising from traffic will give results

Preceding page blank

Table A-1

PERCENT CO CONTRIBUTION BY SOURCE CATEGORY

City	Category				
	Transportation	Industry	Incineration	Power Plants, Space Heating, and Other Sources	References
Washington, D.C. Area, 1965-1966	98.7	--	0.8	0.5	NAPCA (1968a)
Los Angeles Metropolitan Area, 1967	98.2	--	1.8	--	NAPCA (1968b)
Boston, Massachusetts Area, 1967	91.3	--	8.4	1.2	NAPCA (1968c)
San Francisco Bay Area, 1967	77.2	6.5	16.3	--	NAPCA (1968d)
Pittsburgh Metropolitan Area, 1967	92.1	--	1.0	6.9	NAPCA (1969a)
Cleveland Metropolitan Area, 1967	94.3	2.0	2.1	1.5	NAPCA (1969b)
Kansas City Metropolitan Area, 1966	95.2	--	4.3	0.5	NAPCA (1969c)
Metropolitan Baltimore	95.7	1.2	1.8	1.3	NAPCA (1969d)
Hartford-Springfield Area, 1967	94.2	1.1	3.8	0.9	NAPCA (1969e)
Average of 28 Major Metropolitan Areas	91.5	2.6	1.9	4.0	Mason et al. (1969)

that are quite consistent with the accuracies of the other input parameters.

Other potentially important nontraffic sources of carbon monoxide are the airports. Carbon monoxide emissions at airports are comparable with those of surrounding communities (Bastress, 1969). Increased air traffic may increase these levels. One of the problems to be considered in the modeling of airports as CO sources is that they do not constitute a ground level source. Much of the emission occurs in a volume above the area occupied by the airport. For this reason, the box model would seem appropriate to the treatment of emissions from an airport regardless of its distance from the receptor.

The distribution of airport emissions through the mixing layer appears to minimize their contribution to ground level concentrations. However, this should be checked and if airports contribute significantly to ground level concentrations, they should be added to future versions of the model.

Appendix B

THE URBAN TRANSPORTATION PLANNING PROCESS

Preceding page blank

Appendix B

THR URBAN TRANSPORTATION PLANNING PROCESS

The purpose of this appendix is to describe the urban transportation planning process so that its capabilities and limitations may be assessed, and to show how data generated in the planning process can be used as inputs to the urban diffusion model.

1. Background

The first major urban transportation planning effort was undertaken for the Detroit area by the Detroit Metropolitan Area Transportation Study (DMATS) in the early 1950's. Dr. Douglas Carroll and his staff developed many of the concepts and the methodology that are still used. The Carroll study team staffed subsequent studies in Chicago, Pittsburgh, and New York. The methods and techniques have been developed and refined in the succeeding years, strongly aided by increasingly efficient data processing equipment. It is a requirement of the Federal Aid Highway Act of 1962 that every community with a population over 50,000 have a transportation plan to participate in federal highway programs.

2. Structure of a Transportation Study

A transportation study produces a plan for future transportation facilities. A five-step process is generally followed: (1) inventory, (2) model development, (3) forecast, (4) system design, and (5) system evaluation. There is considerable iteration and feedback among these steps, as described below.

Preceding page blank

3. Inventory

Three kinds of data are collected:

(1) Complete descriptions of present transportation facilities

(2) Numbers of trips presently taken, their purposes, and demographic data that may serve as trip-predicting variables

(3) Descriptions of land uses in the study area.

The study area is divided into small "traffic zones," and the trip-taking and land use data are collected for the traffic zones. Traffic zones are usually related to census tracts, with one or more tracts in each traffic zone. Census tracts are used because they provide the most readily available historical and forecast data on population, income, and other demographic variables.

The transportation system inventory is a description of the local highway network of major arterial streets and freeways. A map of the highway network is prepared. The network is described by the intersections, or nodes, and the characteristics of the links that connect the nodes. For example, traffic capacity, observed speed, observed volume, and type of facility are recorded for each link in the network. Public transportation facilities are described by their frequency of service, kind of equipment, capacity, and current patronage.

The trips taken at the present time are determined from a household survey in each traffic zone. Households are asked to report the number of trips taken by household members on a specified day, the purpose of the trips, and the destinations. Household income, number of persons in the household, ages of household members, and number of automobiles are also determined.

Land use and employment in each traffic zone are determined from planning agencies, surveys, and in some cases from field observations.

4. Model Development

To develop the model, the data collected in the inventory are related in such a way that trips between zones can be predicted from demographic and land-use data. Three submodels are used: the trip production model, the trip attractions model, and the trip distribution model.

The trip production model relates the number of trips originating in a zone to characteristics of the zone, e.g., population, average household income, etc. The trips are characterized by their purpose, e.g., to work, to social or recreational activity, to health or medical treatment, etc. The trip production model is a statistical regression, concerned only with the number of trips that originate in the zone, not their destinations.

The trip attraction model relates the number of trip destinations in a zone, by purpose, to zone characteristics, e.g., land use, total employment, etc. The trip attraction model is concerned statistically only with the number of trips that end in a zone, not their points of origin.

The trip distribution model describes the relation between trip productions and attractions: i.e., the number of trips between each zone pair. The distribution model describes the number of trips between each zone pair by a formula of the form:

$$t_{ij} = p_i a_j / d_{ij}^k \quad ,$$

where

t_{ij} = the number of trips from zone i to zone j

p_i = the number of productions in zone i

a_j = the number of trip attractions in zone j

d_{ij} = the impedance between zones i and j, usually expressed as the travel time between the zones, but occasionally as distance or cost

k = an exponent that depends upon the travel characteristics of the area's residents.

Because of its form, the trip distribution model is commonly called the "gravity" model. The exponent k is determined from the frequency distribution of trips between zone pairs as revealed by the household interview data.

5. Forecast

In the forecast step, the land use, employment, population, and income are forecast for some future year. The travel in that future year is forecast from these variables, using the models developed in the previous step. The demographic variables must be forecast for each zone. Frequently, this is done by allocating overall population and income projections among the zones, using models that have been developed for that purpose.

Future land use may be a function of the transportation system adopted, so there is feedback between the transportation system design and the land use forecast. Further, zone-to-zone travel time will be influenced by the transportation system, so there must be iteration between the forecast and the design. The division of trips between private automobiles and public transit is estimated by using a model based on relative time and cost.

6. System Design

In the system design step, alternative changes to the existing transportation system are postulated. These must meet the forecast travel demand. They may include addition of freeway links, increase in capacity of arterials or freeways by widening, or the addition of new public transportation facilities. A network description is prepared for each of the alternatives.

7. System Evaluation

In the system evaluation step, the costs of the alternative systems are determined and compared. Costs include the costs of construction, costs of rights-of-way, costs of equipment, annual maintenance and operating costs, and user and community costs. User costs include those of operating, parking, and owning an automobile; the costs of accidents; transit fares; and the value of all travelers' time. Community costs include disruption, noise and emission pollution, and the cost of limited access to employment and other opportunities. Because these costs occur at different times, and the expenditure patterns may be different for different alternatives, future costs are discounted according to compound interest formulas to obtain comparable values for all outlays. Costs that cannot be expressed in dollar terms are described qualitatively.

The heart of the evaluation process is the series of computer programs that make up the traffic assignment model. This model is capable of determining the minimum time path between zone pairs for a given transportation network and can assign zone-to-zone trips to the links along that minimum path. Thus, the total traffic volume on each link is predicted. This defines the needed capacity, the traffic speed, and finally the total travel time and vehicle operating cost. The diffusion model uses link volume and link speed outputs. These are obtained directly from the magnetic tape outputs of the traffic assignment programs. The network descriptions are also on magnetic tape. Thus, it is possible to forecast future pollution concentrations from the forecast traffic. The pollution forecasts will provide additional information for the transportation planners to evaluate alternatives.

Appendix C

METHODS FOR DETERMINING STABILITY CATEGORY

BLANK PAGE

Appendix C

METHODS FOR DETERMINING STABILITY CATEGORY

This appendix discusses two methods for determining stability category for use with the model described in this report. One of the methods has not been presented elsewhere in the literature.

1. Turner's Method

Turner (1964) developed criteria for determining stability from routinely available meteorological data. His procedure estimates the stability class on the basis of cloud cover, ceiling height, wind speed, and solar elevation. In his paper, Turner presents a series of computational steps that effectively constitute the flow chart for a computer program. His model requires the following inputs: cloud cover, ceiling height, wind speed, and, if daytime, solar elevation. The parameters, other than solar elevation, that are required for the application of Turner's stability determination method are all available from routine hourly meteorological measurements. For application of Turner's approach with the synoptic model, an approximate formula was used to determine solar elevation. The approximation assumes that the earth has a circular orbit and that the station lies at the center of its time zone. With these simplications the following useful relation is obtained:

$$\alpha = \arcsin\left[\sin \delta \sin \Phi + \cos\left(\frac{12 - H}{2\pi}\right)\cos \delta \cos \Phi\right] \qquad \text{(C-1)}$$

and

$$\delta = \arctan\left[-\tan 23.5^\circ \cos\left(\frac{2\pi(N + 10)}{365}\right)\right] \qquad \text{(C-2)}$$

Preceding page blank

where

α = the solar elevation

δ = the solar declination

Φ = station latitude

H = the hour of the day (24 is midnight)

N = the number of days since 1 January.

2. Method Based More Directly on Pasquill's Classifications

In the work that Pasquill (1961) did to determine the spread of a plume with distance traveled, atmospheric conditions were classified according to prevailing insolation strength and wind speed, for daytime conditions, and according to cloud cover and wind speed for night conditions. His classification scheme, which Turner also used in developing his method, is summarized in Table C-I. The table, as presented here

Table C-I

STABILITY CATEGORIES[*]

Surface Winds (knots)	Daytime Insolation			Night Clouds	
	Strong	Moderate	Slight	≥5/10	≤4/10
≤3	1	2	2	5	5
3-6	1	2	3	4	5
6-10	2	3	3	4	4
10-12	3	3	4	4	4
≥13	3	4	4	4	4

[*] 1 = extremely unstable, 2 = moderately unstable, 3 = slightly unstable, 4 = neutral, 5 = slightly stable.

has been changed slightly from the form presented by Slade (1968). First, that table contains some cases where the stability falls between the accepted classes; these have been assigned to a single category. Second, the moderately unstable case in the original table has been redefined as slightly unstable and the two slightly unstable cases have been redefined as neutral. We feel this is more appropriate to urban conditions, where very stable conditions are uncommon. In the original scheme, no categories were defined for the near-calm wind cases at night. We have assumed such cases to be slightly stable over an urban area.

The next problem was to define an objective method for determining the strength of insolation. The strength of the insolation depends on the solar elevation, the cloud cover, and the atmospheric turbidity. The latter factor is not routinely measured and was ignored because its attenuating influence should be small compared to cloud cover. The following equation approximately describes the flux density of solar energy on a horizontal surface:

$$\text{Insolation strength} = k(1 - AN)\sin\alpha \qquad \text{(C-3)}$$

where

k = a proportionality factor, depending on the solar constant, and atmospheric transmission

A = the average albedo or reflectance of the clouds

N = the fraction of the sky obscured by cloud

α = the elevation angle of the sun.

Of course, this equation applies only to an average insolation over an area sufficiently large that the effects of the irregular distribution of clouds are minimized.

A reasonable value of A would be 0.5, so that Eq. (C-3) becomes

$$\text{Insolation} = k(1 - 0.5\ N)\sin\alpha \quad . \qquad \text{(C-4)}$$

Of necessity, we assume that k is constant, i.e., the insolation is proportional to $(1 - 0.5\ N)\sin\alpha$. This term can assume values from 0 to 1. If we divide that interval in three equal parts, corresponding to Pasquill's three insolation categories, we then have the following relationships:

Slight Insolation: $0 < (1 - 0.5\ N)\sin\alpha \leq 0.33$

Moderate Insolation: $0.33 < (1 - 0.5\ N)\sin\alpha \leq 0.67$

Strong Insolation: $(1 - 0.5\ N)\sin\alpha > 0.67$.

These simple expressions are used to determine the insolation type. When combined with the wind speed information, they give the stability classification more directly than does the scheme devised by Turner (1964). This method also seems somewhat more consistent with Pasquill's original specification of the stability types.

In using Table C-I and the insolation expressions given above, it is still necessary to determine the solar elevation for the time of day; cloud cover and wind speed are measured parameters. To economize on calculation time, the subroutine using this scheme to preprocess the data (see Appendix G) does not calculate α, but uses a table of values of $\sin\alpha$ obtained by means of Eq. (C-1). Values are given for each month of the year and each hour of the day. The five cities studied in this report are all within ±3° of 40° north latitude, so a single table for that latitude has served for all calculations.

The procedure for determining stability has been improved by using "opaque" cloud cover. This is a regularly recorded parameter. In determining the opaque cloud cover, the very thin semitransparent clouds are ignored. Thus, the assumption of an average cloud albedo of 0.5 is probably more accurate when applied to these types of cloud than when applied to the total cloud cover.

Appendix D

METHODS FOR DETERMINING MIXING DEPTH

Preceding page blank

Appendix D

METHODS FOR DETERMINING MIXING DEPTH

One of the model's required inputs is mixing depth. The most commonly used method for determining the top of the mixing layer for afternoon conditions is to assume that it is at the height where the potential temperature on the morning sounding is equal to the afternoon surface maximum potential temperature (e.g., Miller and Holzworth, 1967). This is the method used with the synoptic model. Potential temperature, θ, is defined as

$$\theta = T(1000/p)^{R/c_p} \qquad \text{(D-1)}$$

where

T = temperature (°K)

p = pressure (mb)

R/c_p = the ratio of the gas constant for air to its specific heat at constant pressure (0.287).

To determine afternoon mixing depth, the morning sounding* from the nearest radiosonde station and the afternoon maximum temperature were used. Potential temperature is calculated for the surface maximum temperature first, and then for each of the successively higher reported radiosonde levels until the potential temperature at some level exceeds the surface maximum value. The pressure where the surface maximum and upper level potential temperatures are equal is determined by linear interpolation between values for the reported levels. If we assume a constant average temperature $\overline{T}$, through the mixing layer, then we can use the thickness equation (e.g., Panofsky, 1957) to convert the pressure at the top of the layer, p_h, to height

---

*For this model we used the pressures and temperatures at the significant levels, Deck 505, available from the National Weather Records Center, Asheville, North Carolina.

$$h = \ln\left(p_o/p_h\right)(R\overline{T}/g) = 29.3\ \overline{T}\ \ln\left(p_o/p_h\right) \quad . \qquad \text{(D-2)}$$

In this equation, g is the acceleration of gravity, p_o is the surface pressure, and $\overline{T}$ is taken to be the average of the temperatures at the surface and the top of the mixing layer.

The estimation of nighttime mixing depth over the city for use with the synoptic model is based on Summers' (1966) model of the urban heat island and Ludwig's (1968, 1970) empirical relationship between rural lapse rates and the intensity of urban heat islands. If we assume T to be a linear function of the logarithm of pressure (very nearly the same as Summers' assumption of T as a linear function of height), then the temperature T_h at some height h outside the city is given by:

$$T_h = T_o + \frac{dT}{d\ln p}\Delta \ln p \approx T_o + \overline{p}\,\frac{dT}{dp}\,\ln\left(\frac{p_h}{p_o}\right) \qquad \text{(D-3)}$$

where T_o and p_o are the rural surface temperature and pressure, respectively, p_h is the pressure at h, and $\overline{p}$ is the average of p_o and p_h.

If air moving into a city is heated from below to the extent that complete mixing takes place through a depth h, then the temperature at height h will remain T_h, and the lapse rate below h will become adiabatic. The dry adiabatic lapse rate γ_d (in pressure coordinates) is given by

$$\gamma_d = \frac{TR}{pc_p} = 0.287\ \frac{T}{p} \approx 0.287\ \frac{\overline{T}}{\overline{p}} \quad , \qquad \text{(D-4)}$$

where T and p are absolute temperature and pressure, and $\overline{T}$ and $\overline{p}$ are their average values within the layer from the surface to height h. For the urban situation, Eq. (D-3) becomes

$$T_h = T_u + \overline{p}\ \gamma_d\ \ln\left(\frac{p_h}{p_o}\right) \quad , \qquad \text{(D-5)}$$

where T_u is the surface air temperature in the center of the urban area. Subtracting Eq. (D-5) from Eq. (D-3) gives:

$$T_u - T_o = \overline{p}\left[\ln\left(\frac{p_h}{p_o}\right)\right]\left(\frac{dT}{dp} - \gamma_d\right) \quad . \qquad \text{(D-6)}$$

Substituting Eq. (D-4) into Eq. (D-6) gives:

$$T_u - T_o = \left[\ln\left(\frac{p_h}{p_o}\right)\right]\left(\overline{p}\ \frac{dT}{dp} - 0.287\ \overline{T}\right) \quad . \qquad \text{(D-7)}$$

Ludwig (1970) has shown that the urban-rural temperature difference $(T_u - T_o)$ can be approximated within about ±2° C by the following equation:

$$T_u - T_o = \Phi^{1/4}\left(0.0633 - 0.298\ \frac{dT}{dp}\right) \quad , \qquad \text{(D-8)}$$

where Φ is the population of the urban area and dT/dp is expressed in °C/mb. The equation is based on 85 sets of data from 18 different cities. Substituting Eq. (D-8) into Eq. (D-7) gives:

$$\ln\left(p_h/p_o\right) = \Phi^{1/4}\ \frac{\left(0.0633 - 0.298\ \frac{dT}{dp}\right)}{\left(\overline{p}\ \frac{dT}{dp} - 0.287\ \overline{T}\right)} \quad . \qquad \text{(D-9)}$$

The value of dT/dp is determined from the lowest portion of the morning sounding (using the differences in temperature and pressure at the surface and the first significant level above the surface; $\overline{p}$ and $\overline{T}$ are the averages of the pressures and temperatures at these points.

To convert $\ln(p_h/p_o)$ to mixing depth, we use Eq. (D-2). Making that substitution gives

$$h = \frac{29.3\,\overline{T}\,\Phi^{1/4}\left(0.298\,\frac{dT}{dp} - 0.0633\right)}{\overline{p}\,\frac{dT}{dp} - 0.287\,\overline{T}} \quad . \qquad \text{(D-10)}$$

This is the equation that was used to determine the predawn values of urban mixing depth from 1200 GMT soundings.

The above equation has an idiosyncracy that should be noted. For increasing positive values of dT/dp, h becomes larger, as it should, but at some point where dT/dp is approximately adiabatic, h becomes infinitely large. If dT/dp increased further still, h becomes negative. This behavior arises because of the assumption that the observed rural lapse rate is less than the adiabatic rate. Large positive lapse rates are quite rare in the early morning hours, so the assumptions are not seriously misleading. However, it is necessary to provide for the eventuality in the computer program. This has been done by assigning a large positive value to h whenever the above equation yields a negative value. The value chosen was 4000 m. This same value was also assigned to h whenever the equation gave a positive value larger than 4000 m.

This assignment of a maximum mixing depth will not affect the calculations, except for moderately or extremely unstable conditions, and according to the stability classification system used (see Appendix C), such stabilities cannot be assigned at night.

We have also used the 4000-m maximum mixing depth for afternoon calculations in order to limit the amount of radiosonde data necessary to apply the program. As is shown in Section V of this report, this has very little effect on the results.

Inspection of the mixing depth equation given above indicates that there is a minimum positive value that h can assume, given a fixed city size and fixed values of $\overline{p}$ and $\overline{T}$. This minimum occurs when dp/dT is infinitely negative. For a city of 9×10^5 population, an average pressure of 925 mb, and an average temperature of 280° K, the minimum nighttime urban mixing depth should be about 79 meters.

This number appears reasonable considering that the heat generated by the city, and the mechanical mixing produced by the airflow over its rough surface probably set a lower bound on urban mixing depths. From this it follows that daytime mixing depths are also likely to have some minimum value in the city. We have arbitrarily chosen 50 meters as that minimum, although there is no minimum intrinsic in the procedure used to determine afternoon mixing depths. This choice seems to be physically reasonable. However, its main function is to prevent h from assuming a value of zero, which could give an infinite calculated concentration.

The use of radiosonde soundings for mixing depth computations is time-consuming and expensive on the computer. This is particularly true for climatological applications where large amounts of data are required. The sounding data are not universally available on magnetic tape from the National Weather Records Center, and several years of punched-card data are very cumbersome to process. Fortunately, Holzworth (1967) has calculated forenoon and afternoon mixing depths for a large number of U.S. cities, using the morning (1200 GMT) temperature soundings. Mr. Holzworth has been very cooperative and has allowed us to use his tabulations of mixing depth for several stations. His tabulations generally cover the period 1960-1965, and most U.S. radiosonde stations are represented. These data are considerably more convenient as a source for mixing-depth computations than the original radiosonde data. This body of data does adrequire some modification for use with the diffusion model. These adjustments are described below.

The afternoon mixing depths given in Holzworth's tabulations were determined by the conventional method described at the beginning of this appendix, so we have taken his tabulated values and used them without change.

Holzworth determines his forenoon mixing depth from the intersection, on a thermodynamic diagram, of the morning sounding and an adiabat passing through a surface temperature 5° C greater than the observed early morning minimum temperature. Thus, his forenoon mixing depth, h_f (meters), can be related to the morning vertical temperature gradient dT/dZ by the following approximation, which is exact if dT/dZ is constant to the height h_f, and if the surface radiosonde temperature is the minimum temperature:

$$T_{sfc} + h_f\left(\frac{dT}{dZ}\right) \approx T_{sfc} + 5^\circ + h_f\left(\frac{dT}{dZ}\right)_a \quad , \tag{D-11}$$

where $(dT/dZ)_a$ is the adiabatic temperature gradient, -9.8×10^{-3} °C m^{-1}. Substituting and simplifying, Eq. (D-11) becomes:

$$\frac{dT}{dZ} = \frac{\left[5^\circ\ C - \left(9.8 \times 10^{-3}\ ^\circ C/m\right) h_f\right]}{h_f} \quad . \tag{D-12}$$

The gas law and the hydrostatic equation can be combined to give:

$$\frac{dZ}{dp} = -\frac{RT}{pg} \quad . \tag{D-13}$$

Using Eq. (D-13) we can reduce Eq. (D-12) to the following

$$\frac{dT}{dp} = \frac{RT\left[9.8 \times 10^{-3}\ (^{\circ}C/m)h_f - 5^{\circ}\ C\right]}{pgh_f} \quad . \qquad (D\text{-}14)$$

Virtually all cities in the U.S. are located at altitudes such that the atmospheric pressures in the lowest layers are between about 850 mb and 1000 mb. Thus, we introduce an error of less than 10 percent, assuming p to be constant and equal to 925 mb.

Similarly, temperature can be assumed constant and equal to 280° K without introducing errors greater than about 10 percent. Substituting these, and the values for the constants gives:

$$\frac{dT}{dp} \approx \left(8.7 \times 10^{-2} - 44/h_f\right) \frac{^{\circ}C}{mb} \quad . \qquad (D\text{-}15)$$

We have already shown that the early morning mixing depth, h, over the city can be related to this low level lapse rate. Recalling Eq. (D-10)

$$h = \frac{29.3\ \bar{T}\ \Phi^{1/4}\left(0.298\ \frac{dT}{dp} - 0.0633\right)}{\bar{p}\ \frac{dT}{dp} - 0.287\ \bar{T}} \quad ,$$

where Φ is the population of the urban area. Using the same values of T and p as used in the development of Eq. (D-15) and substituting from that gives:

$$h = \Phi^{1/4}\ \frac{1.1 \times 10^{5} + 307\ h_f}{4.1 \times 10^{4} + 0.02\ h_f}\ \text{meters} \quad . \qquad (D\text{-}16)$$

For those cases of importance, where h_f would be less than about 10^4 m, the term $0.02\ h_f$ in the denominator will be very small compared to the constant 4.1×10^4 and can be ignored. Then Eq. (D-16) becomes:

$$h \approx \Phi^{1/4}\left(2.6 + 7.5 \times 10^{-3}\ h_f\right)\ \text{meters} \quad . \qquad \text{(D-17)}$$

This equation was used to convert Holzworth's tabulated forenoon mixing depths to values appropriate to the early-morning hours for use with the climatological model.

Equation (D-17) has the same characteristic as Eq. (D-10), in that there is a minimum value that h can have. It is, as expected, the same as found with Eq. (D-10), if the conditions are the same.

As with the methods based on radiosonde data, we have assigned the same minimum and maximum values of mixing depth, when appropriate, to those obtained from Holzworth's tabulated values.

The two methods described above provide values of mixing depth for only two hours of the day, one in the early morning, predawn hours and one for the time of the afternoon temperature maximum. To obtain values for other hours of the day, interpolation must be used. Two schemes have been employed with the model. The first approach combines time and surface temperature interpolations. The second uses time only as the basis of the interpolation. The time-temperature interpolation has been used with radiosonde data to obtain mixing depths for the examples that illustrate the use of the synoptic model in this report. The time-only interpolation was used with Holzworth's mixing depths in the examples that illustrate the climatological model.

When the temperature interpolation scheme was used, the following equation gave mixing depths from the first hour after sunrise through the first hour after sunset:

$$h = \left(\frac{T - T_{min}}{T_{max} - T_{min}}\right)\left(h_d - h_n\right) + h_n \qquad \text{(D-18)}$$

where

h = mixing depth

h_d and h_n = mixing depth at time of maximum temperature and at time of the morning sounding

T, T_{max}, T_{min} = current, maximum, and minimum temperature.

Temperature interpolation during the day is reasonable because the top of the mixing layer is usually marked, on a thermodynamic diagram, by the intersection of the morning sounding and the adiabat passing through the current surface air temperature. If the slope of the morning sounding is constant up to this height, the change of mixing depth will be very nearly proportional to the change of surface air temperature.

From the second hour past sunset through midnight, the mixing depth is interpolated by time. At the first hour past sunset it has the value given by the above equation. At midnight it has the value of h_n determined from the next morning's soundings. Observations presented by Ludwig and Kealoha (1968) for Dallas and Ft. Worth, Texas, show that the urban heat island develops rather quickly in the evening and then tends to stabilize about midnight. If the urban heat island and the urban mixing layer are related, as suggested by Summers' (1966) model, then the mixing depth should also reach its early morning value by the middle of the night as does the heat-island intensity. For this reason the early morning value of mixing depth is assumed to apply from midnight until the first hour past sunrise on the next day.

Figure D-1 gives a schematic representation of the results of applying the temperature-time interpolation to a typical day's data.

The second interpolation scheme, based on time alone, has many of the same features as the hybrid approach described above. For instance,

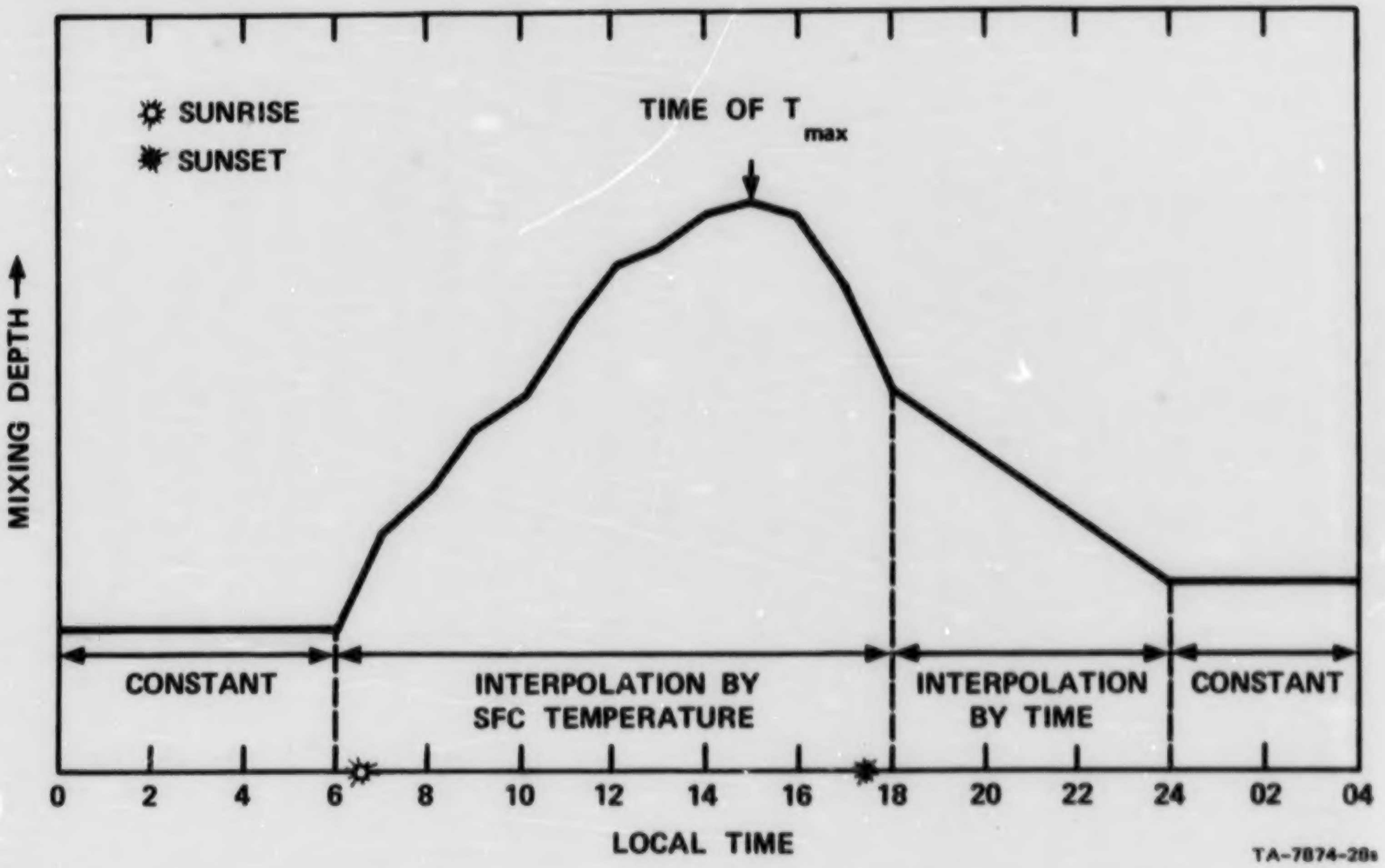

FIGURE D-1 SCHEMATIC REPRESENTATION OF THE DIURNAL TEMPERATURE/TIME INTERPOLATION OF MIXING DEPTH the early morning mixing depth, h_n, is used throughout the hours from midnight until sunrise. We have assumed that the afternoon mixing depth, h_d, occurs at 1400 local standard time. The hourly mixing depths, h, are interpolated for the hours between sunrise and 1400 using the following equation

$$h = h_n + \frac{H - H_{sr}}{14 - H_{sr}} \left(h_d - h_n\right) \qquad \text{(D-19)}$$

where

H = current hour of the day

H_{sr} = the first integral hour after sunrise, determined from tables of solar elevation angle, e.g., 0600, 0700, etc.

From 1400 local standard time until midnight, a similar interpolation is used between h_d and the mixing depth for the following morning.

The advantage to using a time-based interpolation is that an hourly sequence of mixing depths can be determined from either soundings or from the Holzworth tabulated data without concurrently handling the hourly surface temperature data.

Appendix E

INCREASING THE SPATIAL RESOLUTION FOR EMISSIONS IN THE FIRST SEGMENT

Preceding page blank

Appendix E

INCREASING THE SPATIAL RESOLUTION FOR EMISSIONS IN THE FIRST SEGMENT

For the first segment, which covers the upwind area from the receptor to a distance of 125 m, the Gaussian model is used. As noted in the text, the standard deviation, σ_z, in this segment is presumed to remain constant, so the exponent, $b_{i,j}$ is zero in the exponential representation of σ_z, and the Gaussian equation becomes:

$$C_{1j} = \frac{0.8 \cdot 125}{u\ a_{1j}} Q_1 = \frac{100}{u\ a_{1j}} \frac{E_1}{A_1} \qquad \text{(E-1)}$$

where

C_{1j} = the concentration due to remissions from the first segment, for j type stability (gm m^{-3})

Q_1 = the average source strength in the first segment (gm m^{-2} s^{-1})

a_{1j} = a constant for the first segment, for j type stability (m)

E_1 = the emission rate in the first segment (gm s^{-1})

A_1 = the area of the first segment (m^{-2}).

If we divide the first segment in two, part A extending to 62.5 m and part B from 62.5 to 125 m, then

$$a_{1j} = a_{Aj} = a_{Bj} \qquad \text{(E-2)}$$

Preceding page blank

$$A_1 = A_A + A_B \tag{E-3}$$

$$A_A = A_1/4 \tag{E-4}$$

$$A_B = 3A_1/4 \tag{E-5}$$

$$E_1 = E_A + E_B \quad . \tag{E-6}$$

It follows that

$$\begin{aligned} C_{Aj} + C_{Bj} &= \frac{0.8}{u\ a_{1j}} \left(62.5\ \frac{E_A}{A_A} + 62.5\ \frac{E_B}{A_B}\right) \\ &= \frac{100}{u\ a_{1j}\ A_1} \left(2E_A + \frac{2}{3}\ E_B\right) \quad . \end{aligned} \tag{E-7}$$

If we let

$$Q_{AB} = \left(2E_A + \frac{2}{3}\ E_B\right)/A_1 \quad , \tag{E-8}$$

then we can use Q_{AB} as an "effective" source strength for the first segment, replacing Q_1 in Eq. (E-1), and we obtain the same results that we would had we divided the nearest segment into two parts. By using the effective source strength, Q_{AB}, we do not have to add to the numbers of segments treated in many stages of the calculations.

Appendix F

TREATMENT OF EXTRAURBAN SOURCES AND STREET EFFECTS

BLANK PAGE

Appendix F

TREATMENT OF EXTRAURBAN SOURCES AND STREET EFFECTS

1. Introduction

In an earlier report (Johnson, et al., 1969) we discussed submodels to account for the amounts of carbon monoxide arriving from outside the city and for the aerodynamic effects associated with airflow around buildings and through street canyons. For completeness, the submodel used to account for CO concentrations resulting from extraurban sources is described below. This model was used in the calculations that illustrated the use of the synoptic model in the text of this report. A constant background was used for many of the calculations with the climatological model. In the text it was shown that a background could also be accounted for on the basis of statistical modeling, using observed CO concentrations. At this time the statistical model appears to give the better results, if adequate data is available. If not, the model described in this section would be preferred.

Because of a number of problems encountered in applying the empirical street effects submodel on a general basis, it was judged inadequate for our purposes and has not been incorporated into the diffusion model. No attempt was made to include street and building effects directly in the calculations used as examples in this report.

2. Extraurban Model

The development of the following model accepts, a priori, the assumption that the treatment of extraurban transport and diffusion should be considerably more gross than the treatment of nearby sources.

Preceding page blank

The first problem to be faced in the development of an extraurban diffusion model is that there is no convenient way of knowing the upwind trajectory of the air arriving at a city. We can either determine the trajectory from past and present meteorological data or we can assume that the air has come from somewhere within a very large upwind segment. This latter approach is much more practical.

We apply the box model to a quadrant centered on the upwind direction and extending from 32 to 1000 km upwind of the receptor. The source strength is assumed to be constant in time and space throughout the sector, and is estimated from yearly fuel consumption for those states (Federal Highway Administration, 1966) and Canadian provinces (Dominion Bureau of Statistics, 1968) whose centers fall within the sector. To determine the total emission rate within the area, we use the total amount of motor vehicle fuel consumed and the conversion factor: 1 gallon of fuel yields 1.32×10^{3} grams of carbon monoxide. If the yearly (3.15×10^{7} s) consumption of fuel within the quadrant extending to 1000 km is given by F, then the average CO emission rate Q in the area (7.86×10^{11} m^{2}) is given by:

$$Q = 5.32 \times 10^{-17} F \left(g\ m^{-2}\ s^{-1}\right) \quad . \qquad \text{(F-1)}$$

The extraurban model input for a given city includes a table of 16 values of F, one for each wind direction used. A different table is used for each city. An average wind direction is used based on the direction observed with the highest hourly wind speeds.

According to the box model, the concentration C from some upwind segment is

$$C = \frac{Q\left(r_2 - r_1\right)}{uh} \quad , \qquad \text{(F-2)}$$

where r_2 and r_1 are the distances to the outer and inner segment boundaries (in this case 10^6 and 32×10^3 m), u is the wind speed, and h is the depth of the layer through which the material is mixed. Substituting Q from Eq. (F-1) and the values of r_1 and r_2 gives the following equation for concentration from extraurban sources, C_e:

$$C_e = \frac{5.15 \times 10^{-11} F}{uh} \quad . \qquad \text{(F-3)}$$

The afternoon mixing depth is used in Eq. (F-3) because the pollutants are likely to have traveled for long enough periods that they will have had time to be mixed through the depth of the afternoon layer. We are aware that the local mixing depth will not necessarily be appropriate to the region upwind of the city, but more detailed treatment of this problem does not seem to be warranted. To approximate the normal increase in wind speed with height in the lower atmosphere, we have taken the average transport wind velocity through the depth of the mixing layer to be 1.5 times the maximum airport winds for the day.

In addition to the material generated within the segment extending to 1000 km, the general "worldwide" background is included. Robinson and Robbins (1967) have estimated this to be about 0.2 ppm (about 2.4×10^{-4} g m^{-3}) at sea level in the midlatitudes of the northern hemisphere. This value is added to that calculated from Eq. (F-3) to give the total extraurban concentration, which generally amounts to a few tenths ppm. In applying the synoptic model, the extraurban contribution was calculated once for each 24-hour period. The same value was used from one midnight to the next.

3. Street Effects Model

Because of the finite spacing of sources within a city, area-source simulation such as is used in the intraurban model is best applied at scales above a certain lower limit. This minimum spatial scale can be considered to be on the order of a city block, hence the choice of 62 m as the finest resolution in the intraurban model. For shorter source-receptor distances, an alternative technique is needed.

Additional complications arise because, contrary to the usual situation in nonurban diffusion studies, the scale of the largest urban roughness elements (buildings, etc.) is very large compared to the local scales of emission and reception. This means that the aerodynamic effects of structures become important.

Models that do not include the effects of microscale diffusion will normally undercalculate concentrations in comparison with those measured at CAMP Stations, which are often located near streets. For example, the model used by Ott, et al. (1967) gave average concentrations that amounted to 36 percent of the CAMP average.

The street effects have great importance for two reasons. First, they must be considered if we are to use existing data to verify the performance of our model. Most available observations are taken near streets in downtown areas where local effects are likely to be significant. The second reason for the importance of the street effects is that they contribute substantially to those concentrations to which large parts of the population are exposed.

Current knowledge about street effects on CO concentrations is based largely upon the extensive measurements of Georgii, et al. (1967) in Frankfurt/Main, Germany; McCormick and Xintaras (1962), Schnelle, et al. (1969), and Rouse (1951) have also made experimental contributions in this area.

Georgii's experiment involved extensive measurements of CO concentrations and wind speeds at different levels above three different streets in built-up areas, along with occasional traffic counts. A major finding was that the CO concentrations on the leeward sides of buildings were considerably higher than those on the windward sides, implying a helical cross-street circulation component in the opposite direction from the roof-level wind. In addition, the averaged data showed that (1) the vertical concentration profiles on either side of the street assume an exponential form, (2) the mode of air circulation above the street apparently changes when the roof-top wind speed exceeds about 2 m/s, and (3) the concentrations are exponentially related to traffic density. Examination of the measurements reported by Schnelle, et al. (1969) also indicates general agreement with (1) and (2) above; their data are insufficient for verifying (3).

Georgii's observations show that the roof-level concentrations differ only slightly from windward to leeward sides of the street-side buildings. It is reasonable to assume that the urban background concentrations calculated by the intraurban model are approximately equivalent to roof-level concentrations. The effect of the street is to increase incoming roof-level concentrations by a factor that depends upon the receptor location relative to the wind direction, the height above the street, the wind speed at average roof level, and the traffic density.

A street effects submodel, empirically derived from Georgii's observations, was discussed in an earlier report (Johnson, et al., 1969). Because of a number of problems encountered in applying the empirical model on a general basis, it has not been incorporated into the diffusion model.

The statistically derived adjustments to the model discussed in the text would probably account for much of the aerodynamic effects associated with buildings and streets, but those parts of the results that were directly attributable to street effects would not be easily separated from those due to other causes. Also, statistically derived results could not be transferred with any confidence to other locations.

Because of the importance of the street effects, a program of field measurements is planned. The results of this program should provide the data necessary for the development of an adequate model of CO diffusion on the microscale in a city.

Appendix G

PROGRAM FOR PREPROCESSING OF THE DATA FOR THE CLIMATOLOGICAL MODEL

Appendix G

PROGRAM FOR PREPROCESSING OF THE DATA FOR THE CLIMATOLOGICAL MODEL

The preprocessing of the meteorological data for use in the climatological model is done in two steps. First, the Holzworth tabulated values of mixing depth for afternoon and forenoon are processed to give a series of hourly values. The equations used have been enumerated in Appendix D to this report. Figure G-1 shows a simplified flow chart of the program used for converting Holzworth's mixing depth tabulations into a sequence of hourly values.

After the magnetic tape records of hourly mixing depth are produced, they are merged with conventional hourly meteorological records obtained from the National Weather Records Center. The methods used to convert solar elevation, opaque cloud cover, and wind speed to stability index have already been discussed in Appendix C to this report and need not be repeated here. The organization of the preprocessing is summarized in the simplified flow chart in Figure G-2. The magnetic tape record of the condensed historical meteorological data that results from this program is then used as the climatological basis for calculating extended sequences of CO concentrations.

Preceding page blank

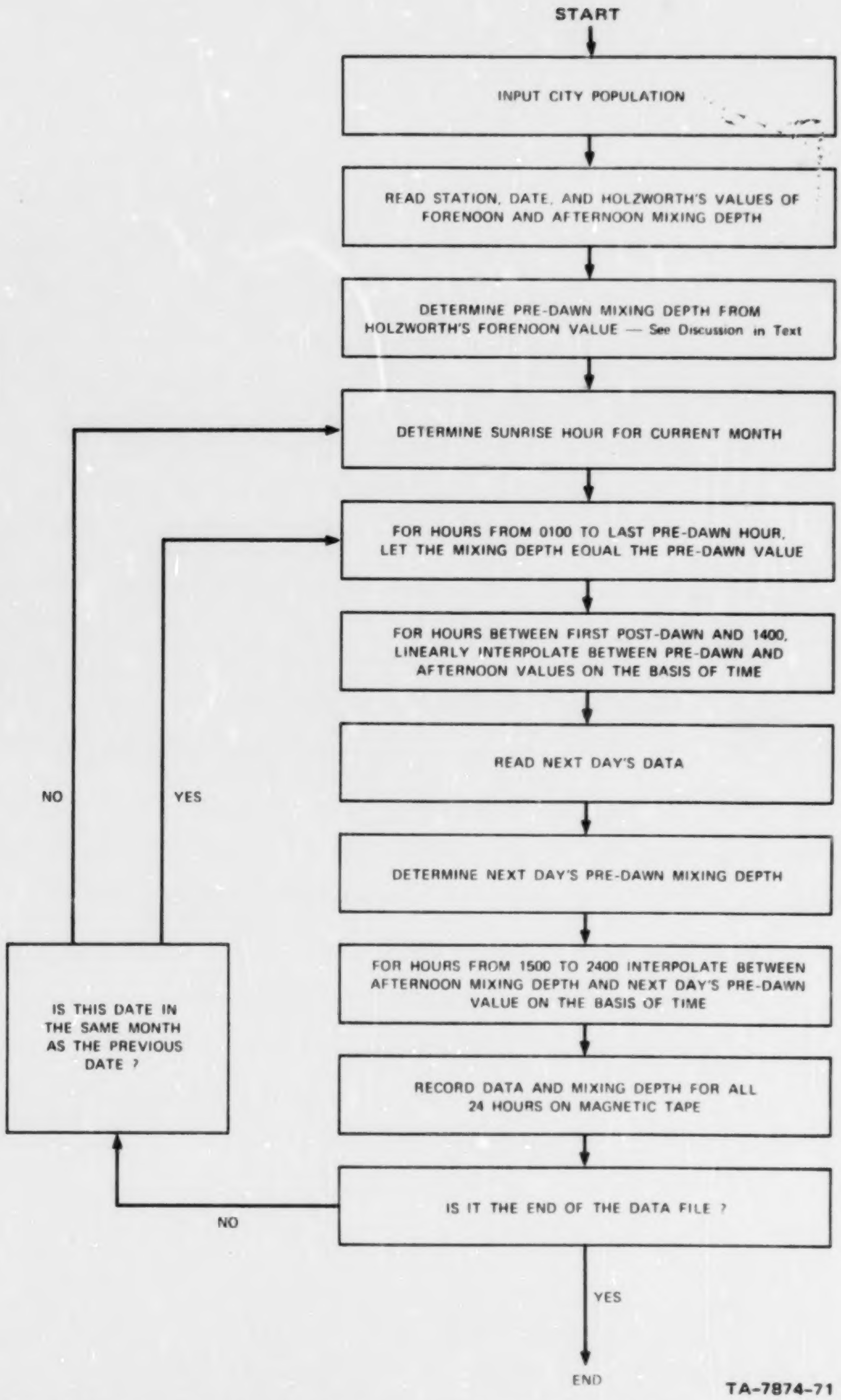
START
INPUT CITY POPULATION
READ STATION, DATE, AND HOLZWORTH'S VALUES OF FORENOON AND AFTERNOON MIXING DEPTH
DETERMINE PRE-DAWN MIXING DEPTH FROM HOLZWORTH'S FORENOON VALUE — See Discussion in Text
DETERMINE SUNRISE HOUR FOR CURRENT MONTH
FOR HOURS FROM 0100 TO LAST PRE-DAWN HOUR, LET THE MIXING DEPTH EQUAL THE PRE-DAWN VALUE
FOR HOURS BETWEEN FIRST POST-DAWN AND 1400, LINEARLY INTERPOLATE BETWEEN PRE-DAWN AND AFTERNOON VALUES ON THE BASIS OF TIME
READ NEXT DAY'S DATA
DETERMINE NEXT DAY'S PRE-DAWN MIXING DEPTH
FOR HOURS FROM 1500 TO 2400 INTERPOLATE BETWEEN AFTERNOON MIXING DEPTH AND NEXT DAY'S PRE-DAWN VALUE ON THE BASIS OF TIME
RECORD DATA AND MIXING DEPTH FOR ALL 24 HOURS ON MAGNETIC TAPE
IS IT THE END OF THE DATA FILE ?
NO
YES
IS THIS DATE IN THE SAME MONTH AS THE PREVIOUS DATE ?
NO
YES
END
TA-7874-71

FIGURE G-1 SIMPLIFIED FLOW CHART OF PROGRAM FOR CONVERTING HOLZWORTH'S MIXING DEPTHS TO HOURLY VALUES

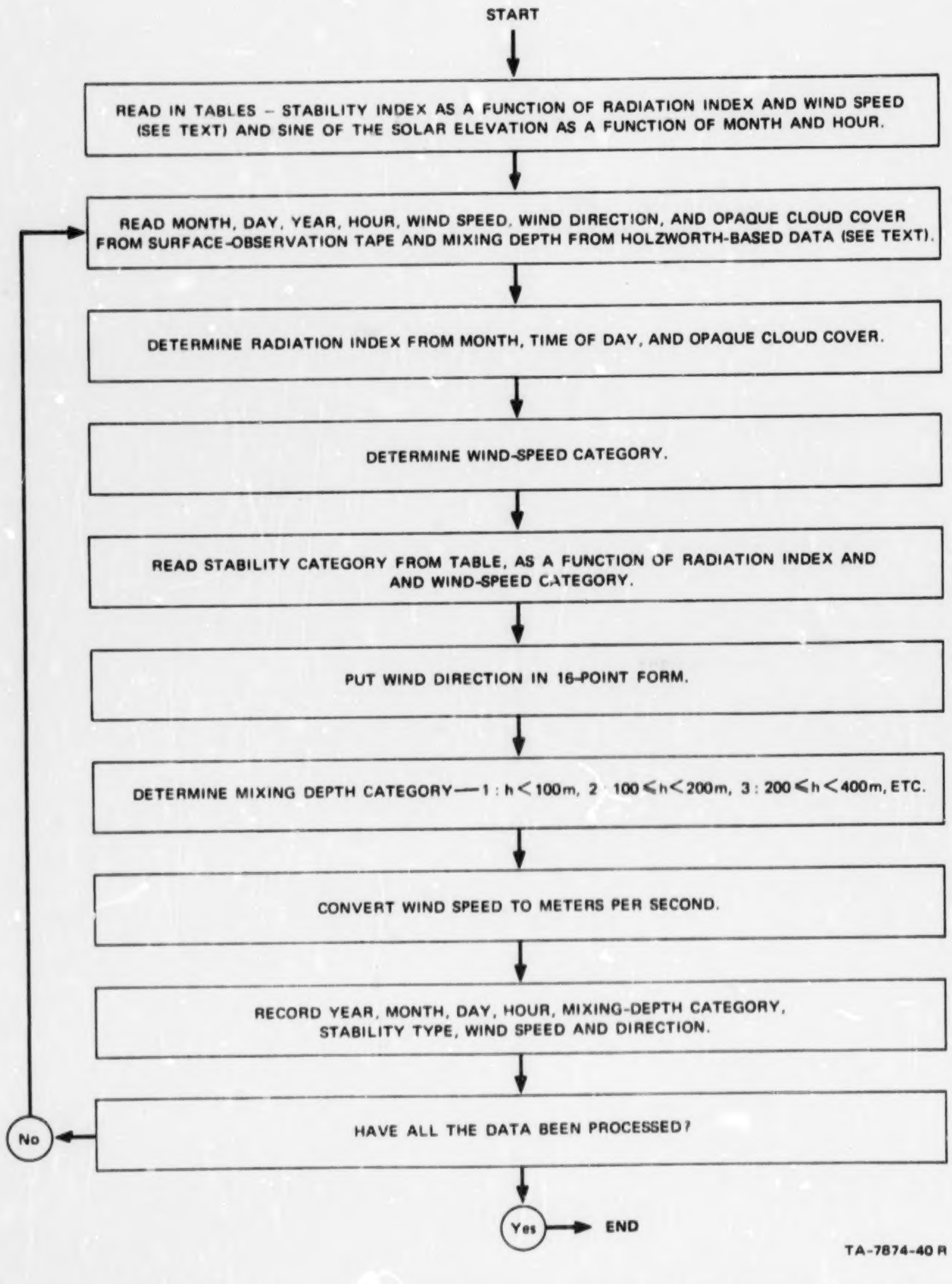
START
READ IN TABLES – STABILITY INDEX AS A FUNCTION OF RADIATION INDEX AND WIND SPEED (SEE TEXT) AND SINE OF THE SOLAR ELEVATION AS A FUNCTION OF MONTH AND HOUR.
READ MONTH, DAY, YEAR, HOUR, WIND SPEED, WIND DIRECTION, AND OPAQUE CLOUD COVER FROM SURFACE-OBSERVATION TAPE AND MIXING DEPTH FROM HOLZWORTH-BASED DATA (SEE TEXT).
DETERMINE RADIATION INDEX FROM MONTH, TIME OF DAY, AND OPAQUE CLOUD COVER.
DETERMINE WIND-SPEED CATEGORY.
READ STABILITY CATEGORY FROM TABLE, AS A FUNCTION OF RADIATION INDEX AND AND WIND-SPEED CATEGORY.
PUT WIND DIRECTION IN 16-POINT FORM.
DETERMINE MIXING DEPTH CATEGORY—1 : h < 100m, 2 : 100 ≤ h < 200m, 3 : 200 ≤ h < 400m, ETC.
CONVERT WIND SPEED TO METERS PER SECOND.
RECORD YEAR, MONTH, DAY, HOUR, MIXING-DEPTH CATEGORY, STABILITY TYPE, WIND SPEED AND DIRECTION.
HAVE ALL THE DATA BEEN PROCESSED?
No
Yes
END
TA-7874-40 R

FIGURE G-2 SIMPLIFIED FLOW CHART OF THE DATA PROCESSING PROGRAM USED WITH THE CLIMATOLOGICAL MODEL

Appendix H

THE EQUIVALENCE OF CERTAIN COMBINATIONS OF STABILITY AND MIXING DEPTH

Preceding page blank

Appendix H

THE EQUIVALENCE OF CERTAIN COMBINATIONS OF STABILITY AND MIXING DEPTH

As was noted in the discussion of the climatological model in the text of this report, it can be simplified to the following form:

$$C = \frac{P_t}{u} \sum_{i=1}^{9} \left(\frac{\chi}{Q}\right)_{i,j,m} \bar{Q}_{i,d} \qquad \text{(H-1)}$$

where

C = CO concentration at the receptor (gm m^{-3}).

P_t = A factor that gives the source strength for the t^{th} hour, based on daily distribution of traffic, and changes in average speed during peak traffic hours.

u = Wind speed (m s^{-1}).

$(\chi/Q)_{i,j,m}$ = Ratio of the CO concentration received from the i^{th} segment to the emissions in that segment (for unit wind speed). The values of these ratios depend on stability class, j, and mixing-depth class, m.

$\bar{Q}_{i,d}$ = Average daily source strength in the i^{th} segment, and the d^{th} direction upwind of the receptor, based on the total daily traffic and the average speeds on the different types of roads within the segment (gm m^{-2} s^{-1}).

Preceding page blank

It is the term $(\chi/Q)_{i,j,m}$ that is of interest here. It will be shown that, for some combinations of j and m, the values are independent of stability and mixing depth.

First, the mixing depth class will be defined. Table H-I shows the mixing depth intervals for each class and geometric mean, h_m, for each of the classes.

Table H-I

MIXING DEPTH CLASSES

m, Mixing Depth Class	Mixing Depth Interval (meters)	h_m, Geometric Mean of Depth
1	<100	70.7*
2	100-200	141
3	200-400	283
4	400-800	566
5	800-1600	1131
6	1600-3200	2262
7	>3200	4525*

*For classes 1 and 7, the geometric mean was calculated as though the classes were bounded.

We can calculate the values of $(\chi/Q)_{i,j,m}$ for all the combinations of j and m. These values are based on the Gaussian model for those segments totally inside that distance where the Gaussian and box models give the same ground level concentration. For those segments wholly beyond that distance, the box model values are used. For the segment in which the transition occurs, $(\chi/Q)_{i,j,m}$ is based on a combination of the two models, as discussed in Section II of this report. Values of $(\chi/Q)_{i,j,m}$ were calculated using the values of h_m shown in Table H-I and the exponential approximations of the Pasquill-Gifford curves of the vertical standard deviation as discussed in the text. These values of $(\chi/Q)_{i,j,m}$ are presented in Table H-II.

The values in Table H-II are those that are used in the climatological model. Inspection of the table shows that there are rows that are identical. For instance, the rows of $(\chi/Q)_{i,j,m}$ values are identical when the stability class, j, is 5 and the mixing depth class, m, has any value from 3 through 7. The same is true for stability class 4, except that for $i = 9$ and $m = 3$ the value differs slightly from the values found for $m > 3$. In applying the climatological model, this slight difference was ignored.

The last column of Table H-II gives a type number that was assigned to each row. Rows with the same type number have been taken to be identical for purposes of applying the model. Inspection of the last column shows that the number of rows that need to be considered separately has been reduced from 35 to 25. When this fact is employed in the application of the model, it results in a reduction of required memory space of about 28 percent. This allows for much more efficient use of the computer.

Table H-II

VALUES OF $(\chi/Q)_{i,j,m}$. FOR UNIT WIND SPEED

Stability Class, j	Mixing Depth Class, m	Segment, i									Type
		1	2	3	4	5	6	7	8	9	
1	1	4.60	3.04	3.60	7.07	14.14	28.3	56.6	113.2	226.	1
2	1	6.89	4.92	4.99	7.07	14.14	28.3	56.6	113.2	226.	2
3	1	10.38	7.22	7.49	8.24	14.14	28.3	56.6	113.2	226.	3
4	1	16.11	11.91	13.48	15.74	19.17	28.5	56.6	113.2	226.	4
5	1	23.0	16.67	18.96	22.50	27.6	34.9	56.6	113.2	226.	5
1	2	4.60	3.04	2.62	3.54	7.07	14.14	28.3	56.6	113.2	6
2	2	6.89	4.92	4.99	4.60	7.07	14.14	28.3	56.6	113.2	7
3	2	10.38	7.22	7.49	8.08	8.79	14.14	28.3	56.6	113.2	8
4	2	16.11	11.91	13.48	15.74	19.17	24.2	31.5	56.6	113.2	9
5	2	23.0	16.67	18.96	22.5	27.6	34.9	47.1	67.4	113.2	10
1	3	4.60	3.04	2.61	1.96	3.54	7.07	14.14	28.3	56.6	11
2	3	6.89	4.92	4.99	4.55	4.03	7.07	14.14	28.3	56.6	12
3	3	10.38	7.22	7.49	8.08	8.75	9.65	14.16	28.3	56.6	13
4	3	16.11	11.91	13.48	15.74	19.17	24.2	31.1	42.0	60.5	14
5	3	23.0	16.67	18.96	22.5	27.6	34.9	47.1	67.4	100.3	15
1	4	4.60	3.04	2.61	1.58	1.77	3.54	7.07	14.14	28.3	16
2	4	6.89	4.92	4.99	4.55	3.60	3.54	7.07	14.14	28.3	17
3	4	10.38	7.22	7.49	8.08	8.75	9.65	10.89	14.50	28.3	18
4	4	16.11	11.91	13.48	15.74	19.17	24.2	31.1	42.0	59.3	14
5	4	23.0	16.67	18.96	22.5	27.6	34.9	47.1	67.4	100.3	15
1	5	4.60	3.04	2.61	1.58	0.955	1.77	3.54	7.07	14.14	19
2	5	6.89	4.92	4.99	4.55	3.60	2.38	3.54	7.07	14.14	20
3	5	10.38	7.22	7.49	8.08	8.75	9.65	10.9	12.97	16.37	21
4	5	16.11	11.91	13.48	15.74	19.17	24.2	31.1	42.0	59.3	14
5	5	23.0	16.67	18.96	22.5	27.6	34.9	47.1	67.4	100.3	15
1	6	4.60	3.04	2.61	1.58	0.67	0.884	1.77	3.54	7.07	22
2	6	6.89	4.92	4.99	4.55	3.60	2.88	1.83	3.54	7.07	23
3	6	10.38	7.22	7.49	8.08	8.75	9.65	10.89	12.97	16.3	21
4	6	16.11	11.91	13.48	15.74	19.17	24.2	31.1	42.0	59.3	14
5	6	23.0	16.67	18.96	22.5	27.6	34.9	47.1	67.4	100.3	15
1	7	4.60	3.04	2.61	1.58	0.604	0.442	0.884	1.77	3.54	24
2	7	6.89	4.92	4.99	4.55	3.60	2.28	1.28	1.77	3.54	25
3	7	10.38	7.22	7.49	8.08	8.75	9.65	10.89	12.97	16.3	21
4	7	16.11	11.91	13.48	15.74	19.17	24.2	31.1	42.0	59.3	14
5	7	23.0	16.67	18.96	22.5	27.6	34.9	47.1	67.4	100.3	15

Appendix I

CONTINUOUS AIR MONITORING PROGRAM STATIONS

Appendix I

CONTINUOUS AIR MONITORING PROGRAM STATIONS

The only generally available carbon monoxide measurements that can be used to verify the performance of the diffusion model are those taken at the stations of the Continuous Air Monitoring Projects (CAMP). This appendix has been included to provide some information about the sites at which the measurements were taken. In this program we have used data from the stations in St. Louis, Cincinnati, Chicago, Washington, and Denver. These stations are pictured in Figures I-1 through I-5. All are located in or near the downtown sections of their respective cities.

The individual sites have certain characteristics that make their measurements not entirely comparable to the computations made with the model. As can be seen from Figure I-1, the St. Louis site is adjacent to a parking lot that has considerable in and out traffic during business hours. This traffic, which is not included in the model calculations, undoubtedly influences the measured CO concentrations.

The location of the Cincinnati CAMP Station, also in a parking lot (Figure I-2), is similar to that of the St. Louis station, but there is probably less in-and-out traffic during the day at the Cincinnati site. The Cincinnati parking lot is near a theater, so that anomolously high measurements may occur at times when there are public events at that theater.

The Chicago site represents a different type of problem. Figure I-3 shows that the station is situated just at the foot of a tall building. The airflow around that building is likely to be considerably different than the airport wind used for the computations. For example, airflow around the building may cause the measurements to reflect the high emission rates on the adjacent street, although the airport wind may indicate that those emissions would be swept away from the site. These aerodynamic effects are to be investigated during the coming year.

The Washington and Denver CAMP Stations (Figures I-4 and I-5) are probably better located than the others, being somewhat farther away from tall buildings and parking lots. However, their measurements may not be entirely free of such interferences.

NOT REPRODUCIBLE

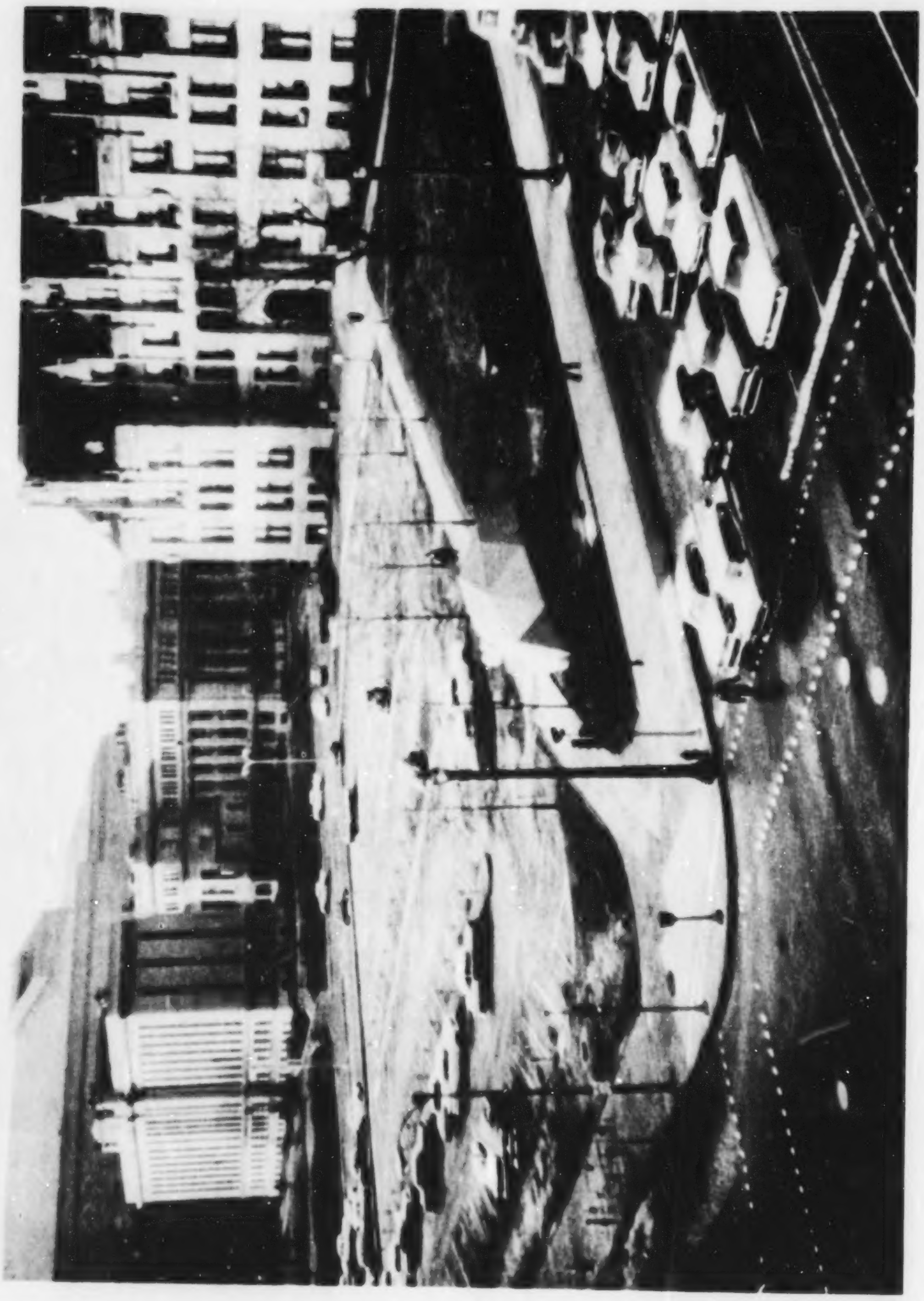

TA-7874-72

FIGURE I-1 ST. LOUIS CAMP STATION

NOT REPRODUCIBLE

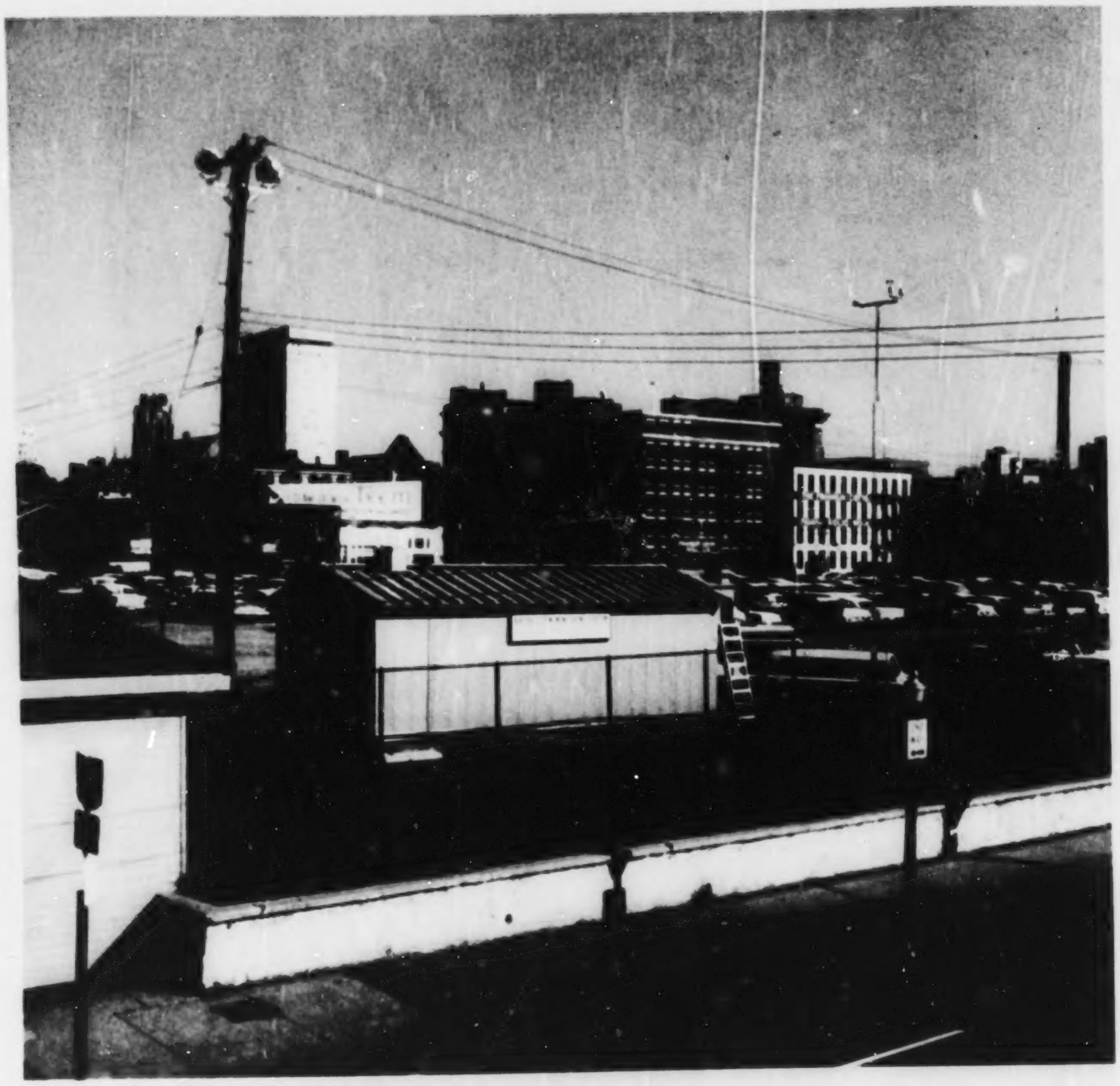

TA-7874-73

FIGURE I-2 CINCINNATI CAMP STATION

NOT REPRODUCIBLE

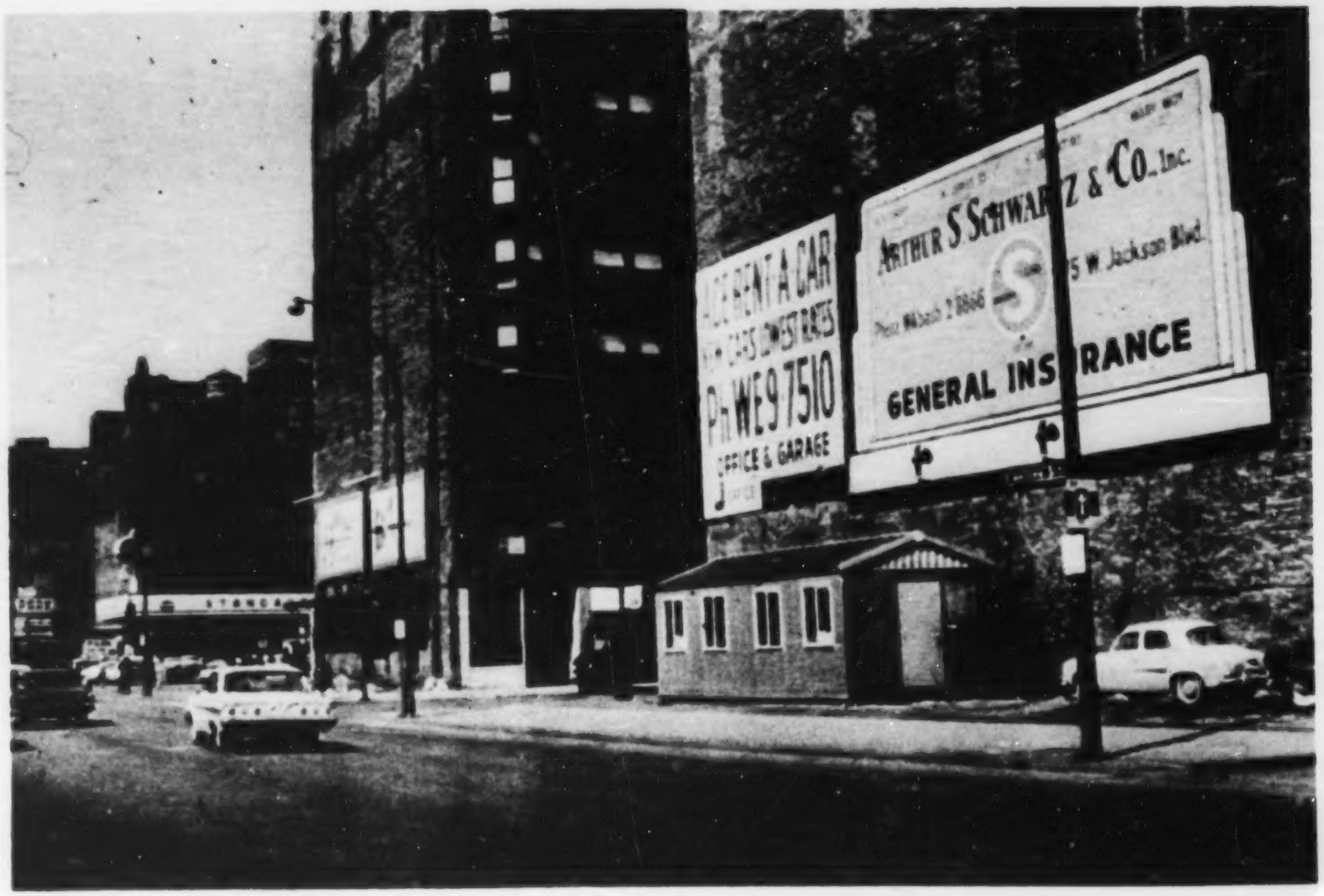

TA-7874-74

FIGURE I-3 CHICAGO CAMP STATION

NOT REPRODUCIBLE

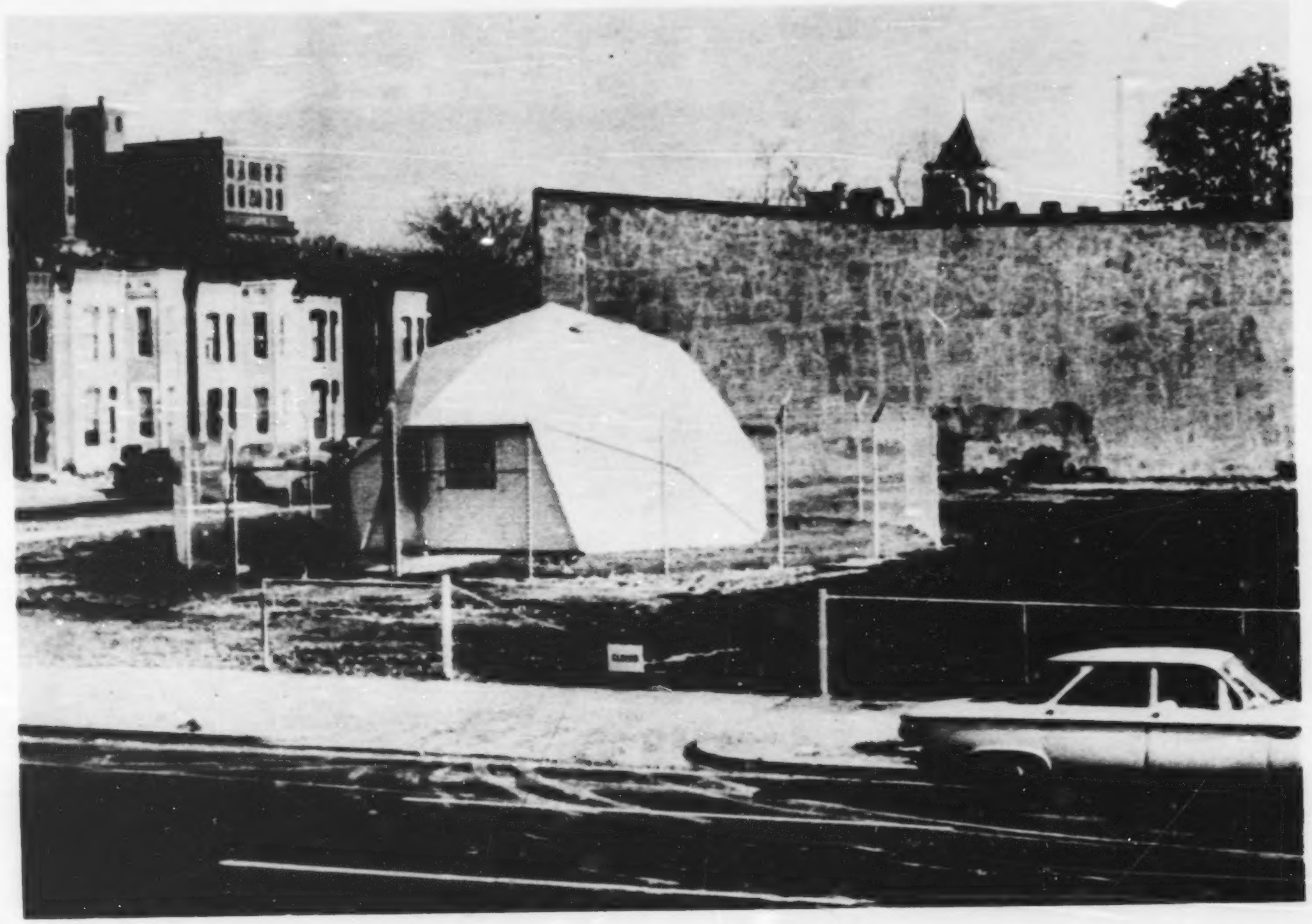

FIGURE I-4 WASHINGTON, D.C., CAMP STATION

TA-7874-75

NOT REPRODUCIBLE

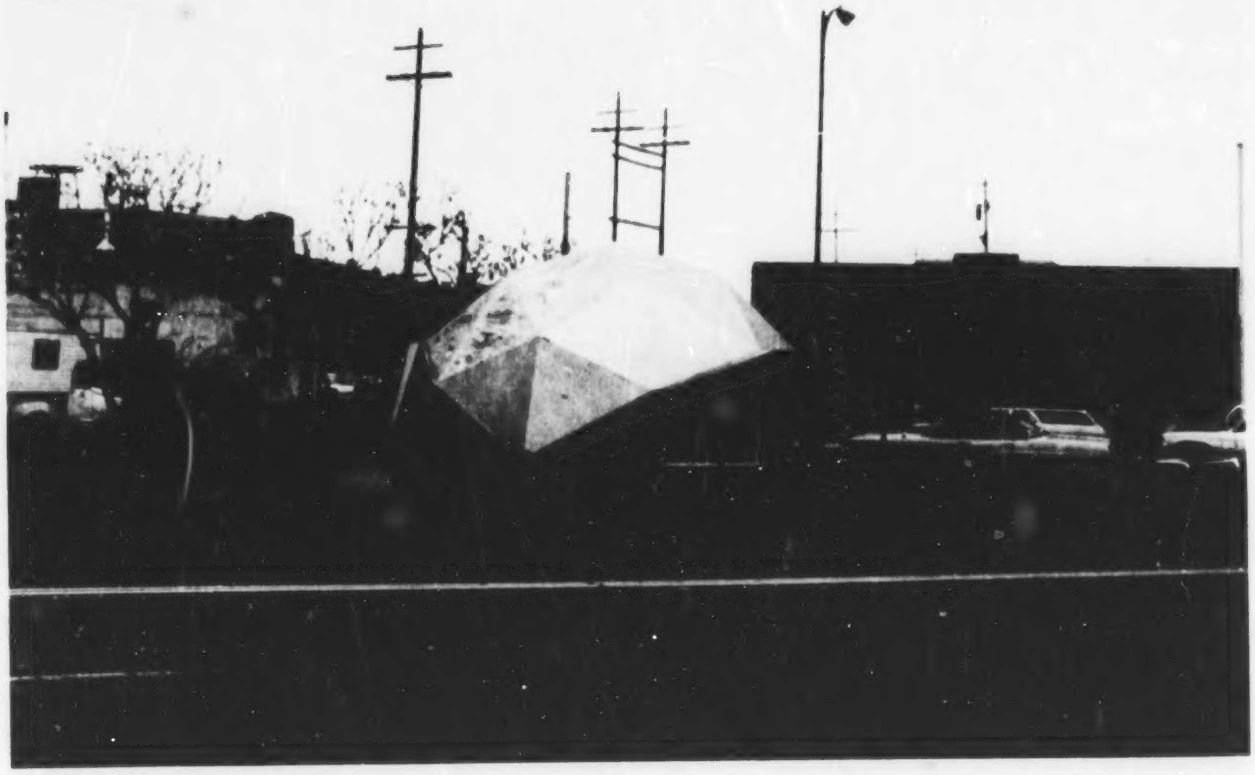

FIGURE I-5 DENVER CAMP STATION

TA-7874-76

ACKNOWLEDGMENTS

We are grateful for the able assistance of the following individuals at Stanford Research Institute: the late Mrs. Shirley Reid, who secured and supervised the reduction of the traffic data; Mr. Hisao Shigeishi, who programmed much of the model and carried out computer trials; Miss Joyce Kealoha, who assembled and cataloged our library of urban pollution model studies, and who helped with numerous other aspects of the work; Mr. Elmer Robinson, who aided in planning the model development; and Mrs. E. Cox, Miss S. Hanson, Miss M. Ray, and Mrs. D. Orr, who have typed the reports required on this project.

We also thank the members of the CRC-APRAC Urban Diffusion Project Group for their guidance and suggestions, and for supplying useful technical information.

The assistance of Messrs. Charles Hosler and George Holzworth of NAPCA and of Messrs. V. Hagarty and D. Calloway of the National Weather Records Center are gratefully acknowledged for their cooperation in supplying us with special and conventional meteorological data.

Finally, we thank all the state and local traffic agencies that were so cooperative in supplying historical or forecast traffic data. The following personnel and agencies provided such information for St. Louis: Messrs. J. R. Turner and R. Weldinger, Missouri State Highway Department; Mr. C. Sweet, St. Louis Land Use and Transportation Study; and Mr. R. L. Grady, St. Louis Department of Streets. For the Washington, D.C., metropolitan area, traffic data were supplied by: Mr. L. E. Brett, Jr., Virginia Department of Highways; Mr. W. C. Scruggs, Arlington County Traffic Engineering Division; Mr. D. E. Tyler, District of

Preceding page blank

Columbia Bureau of Administrative Services; and Mr. G. W. Cassell, Maryland State Road Commission. For Chicago traffic data, we acknowledge the assistance of Messrs. E. W. Campbell and J. Miller, Chicago Area Transportation study; and Mr. H. R. Handley, Illinois Division of Highways. Mr. C. Ball, Denver Regional Council of Governments, and the Colorado Department of Highways provided Denver traffic information. Messrs. C. Ball and A. H. Hessling, Ohio-Kentucky-Indiana Regional Transportation and Development Plan, provided traffic data for the Cincinnati area.

REFERENCES

Bastress, E. K., 1969, Nature & Control of Aircraft Engine Exhaust Emissions, APCA No. 69-190.

Beckman, E. W., W. S. Fagley, and Jorma O. Sarto, 1967: "Exhaust Emission Control by Chrysler--The Cleaner Air Package," Air Pollution--1967 (Automotive Air Pollution), Hearings before the Subcommittee on Air and Water Pollution of the Committee on Public Works, United States Senate, Ninetieth Congress, First Session, Part 1, pp. 411-424.

Bornstein, R. D., 1969: Observations of the urban heat island effect in New York City, J. Appl. Meteorol., 7, 575-582.

Clarke, J. F., 1964: A simple diffusion model for calculating point concentrations from multiple sources, J. Air Poll. Cont. Assoc., 14, 347-352.

Clarke, J. F., 1969: Nocturnal Boundary Layer over Cincinnati, Ohio, Mon. Wea. Rev., 97, 582-589.

Dominion Bureau of Statistics, 1968: Canada Year Book, 1968, Ottawa, Canada, 815 pp.

Federal Highway Administration, 1966: Highway Statistics for 1966, U.S. Government Printing Office, 186 pp.

Georgii, H. W., E. Busch, and E. Weber, 1967: Investigation of the Temporal and Spatial Distribution of the Immission Concentration of Carbon Monoxide in Frankfurt/Main, Report No. 11 of the Institute for Meteorology and Geophysics of the University of Frankfurt/Main (Translation No. 0477, NAPCA).

Gifford, F. A., Jr., 1961: Use of routine meteorological observations for estimating atmospheric dispersion, Nuclear Safety, 2, 48.

Gilman and Co., 1959: St. Louis Metropolitan Area Traffic Study, Prepared for City and County of St. Louis by W. C. Gilman & Co., 55 Liberty Street, New York, New York.

Graham, I. R., 1968: An analysis of turbulence statistics at Fort Wayne, Indiana, J. Appl. Meteor., 7, 90-93.

Highway Research Board, 1968: Comparative Analysis of Traffic Assignment Techniques with Actual Highway Use, Report No. 58, National Cooperative Highway Research Program.

Hilsmeier, W. F. and F. A. Gifford, Jr., 1962, Graphs for estimating atmospheric dispersion, USAEC Rpt ORO-545, Weather Bureau, Oak Ridge, Tennessee.

Hilst, G. R. and N. E. Bowne, 1966: A Study of the Diffusion of Aerosols Released from Aerial Line Sources Upwind of an Urban Complex, Final Report, Vols. I and II, prepared for U.S. Army Dugway Proving Ground, by the Travelers Research Center, Inc., Hartford, Connecticut.

Holzworth, G. C., 1967: Mixing depths, wind speeds and air pollution potential for selected locations in the United States, J. Appl. Meteor., 6, 1039-1044.

Institute of Traffic Engineers, 1965: Traffic Engineers Handbook, Washington, D.C.

Johnson, W. B., Jr., F. L. Ludwig, and A. E. Moon, 1969, "Development of a Practical, Multipurpose Urban Diffusion Model for Carbon Monoxide," Paper presented at Symposium on Multiple-Source Urban Diffusion Models, Chapel Hill, North Carolina, 28-30 October 1969.

Larsen, R. I., 1969: A new mathematical model of air pollutant concentration, averaging time and frequency, J. Air Poll Cont. Assoc., 19, 24-30.

Leahey, D. M., 1969: A model for predicting the variation of pollution within the urban heat island, APCA paper No. 69-107.

Ludwig, F. L., 1968: Urban temperature fields, paper presented at WMO Symposium on Urban Climates and Building Climatology, Brussels, 15-25 October 1968.

Ludwig, F. L., 1970: Urban air temperatures and their relation to extraurban meteorological measurements, paper presented at January 1970 Meeting of Amer. Soc. Heat., Refrig. and Vent. Eng., San Francisco.

Ludwig, F. L. and J. H. S. Kealoha, 1968: Urban Climatological Studies, Final Report, Contract CD-DAHC-20-67-C-0136 (Work Unit 1235A), Stanford Research Institute, Menlo Park, California.

Mason, D. V., G. Ozolins, and C. B. Morita, 1969: Sources and Air Pollutant Emission Patterns in Major Metropolitan Areas, APCA 69-110.

McCormick, R. A. and C. Xintaras, 1962: Variation of carbon monoxide concentrations as related to sampling interval, traffic, and meteorological factors, J. Appl. Meteor., 1, 237-243.

McElroy, J. L., 1969: A comparative study of urban and rural dispersion, J. Appl. Meteor., 8, 19-31.

McGuire, T. and K. Noll: Relationships Between Concentrations of Atmospheric Pollutants and Averaging Time, paper presented at 11th Conf. on Methods in Air Pollution and Industrial Hygiene, U. of California, Berkeley, 30 March-1 April 1970, 13 pp.

Meade, P. J., 1960: Meteorological Aspects of the Safety and Location of Reactor Plants, World Meteorological Organization, Tech. Note No. 33.

Miller, M. E. and G. C. Holzworth, 1967: An atmospheric diffusion model for metropolitan areas, J. Air Poll. Contr. Assoc., 17, 46-50.

Moses, H., 1969: Mathematical Urban Air Pollution Models, Report No. ANL/ES-RPY-001, Argonne National Laboratory, Argonne, Illinois.

National Air Pollution Control Administration, 1968a: Report for Consultation on the Washington, D.C., National Capital Interstate Air Quality Control Region, U.S. Dept. of HEW.

National Air Pollution Control Administration, 1968b: Report for Consultation on the Metropolitan Los Angeles Air Quality Control Region, U.S. Dept. of HEW.

National Air Pollution Control Administration, 1968c: Report for Consultation on the Metropolitan Boston Intrastate Air Quality Control Region, U.S. Dept. of HEW.

National Air Pollution Control Administration, 1968d: Report for Consultation on the San Francisco Bay Area Quality Control Region, U.S. Dept. of HEW.

National Air Pollution Control Administration, 1969a: Report for Consultation on the Metropolitan Pittsburgh City Intrastate Air Quality Control Region, U.S. Dept. of HEW.

National Air Pollution Control Administration, 1969b: Report for Consultation on the Greater Metropolitan Cleveland Intrastate Air Quality Control Region, U.S. Dept. of HEW.

National Air Pollution Control Administration, 1969c: Report for Consultation on the Metropolitan Kansas City Intrastate Air Quality Control Region, U.S. Dept. of HEW.

National Air Pollution Control Administration, 1969d: Report for Consultation on the Metropolitan Baltimore Intrastate Air Quality Control Region, U.S. Dept. of HEW.

National Air Pollution Control Administration, 1969e: Report for Consultation on the Hartford-Springfield Interstate Air Quality Control Region (Connecticut-Massachusetts), U.S. Dept. of HEW.

Neiburger, M., 1968: Diffusion Models of Urban Air Pollution, WMO Symposium on Urban Climates and Building Climatology, Brussels, 15-20 October 1968.

Ott, W., J. F. Clarke, and G. Ozolins, 1967: Calculating future carbon monoxide emissions and concentrations from urban traffic data, PHS Publ. No. 999-AP-41, National Center for Air Pollution Control, Cincinnati, Ohio.

Panofsky, H., 1957: Introduction to Dynamic Meteorology, Pennsylvania St. U., University Park, Pennsylvania, 243 pp.

Pasquill, F., 1961: The estimation of the dispersion of windborne material, Meteorol. Mag. (London) 90, 33-49.

Perkins, W. A., 1962: Some effects of city structure on the transport of airborne material in urban area, paper presented at Air over Cities Symposium, R. A. Taft Sanitary Engineering Center, Cincinnati, Technical Report A62-5, pp. 197-205.

Pooler, F., 1963: Airflow over a city in terraine of moderate relief, J. Appl. Meteorol., 2, 446-456.

Pooler, F., 1961: A prediction model of mean urban pollution for use with standard wind roses, Intern. J. Air and Water Poll., 4, 199-211.

Pooler, F., 1966: A tracer study of dispersion over a city, *J. Air Poll. Contr. Assoc.*, *11*, 677-681.

Robinson, E. and R. C. Robbins, 1967: Sources, Abundance, and Fate of Gaseous Pollutants, Prep. for Amer. Petroleum Inst. Final Report, Proj. PR-6755, Stanford Research Institute, Menlo Park, California.

Rose, A. H. and W. D. Krostek, 1969: *Emission Factors*, U.S. Dept. of Health, Education and Welfare, National Air Pollution Control Administration, p. 5.

Rose, A. H., R. Smith, W. F. McMichael, and R. E. Kruse, 1964: Comparison of Auto Exhaust Emissions from Two Major Cities, U.S. Public Health Service, Cincinnati, Ohio.

Rouse, H., 1951: Air tunnel studies of diffusion in urban areas, *Meteor. Mono.*, *1*, 39-41.

Schnelle, K. B., F. G. Ziegler, and P. A. Krenkel, 1969: A study of the vertical distribution of carbon monoxide and temperature above an urban intersection, APCA Paper No. 69-152.

Slade, D. H. (Ed.), 1968, Meteorology and Atomic Energy U.S. Atomic Energy Commission, Div. Tech. Info., Oak Ridge, Tennessee.

Smith, M. (Ed.), 1968, Recommended guide for the prediction of the dispersion of airborne effluents, *Amer. Soc. Mech. Eng.*, New York.

Smith, M. E. and I. A. Singer, 1966: An improved method of estimating concentrations and related phenomena from a point source emission, *J. Appl. Meteor.*, *5*, 631-639.

Smith, Wilbur and Associates, 1958: Transportation Survey--National Capital Region, prepared for National Capital Planning Commission by W. Smith and Assoc., 495 Orange Street, New Haven, Connecticut.

Stanford University Aerosol Laboratory and The Ralph M. Parsons Co., 1953a: Behavior of aerosol clouds within cities, Joint Quarterly Report No. 3, January-March 1952, Contracts DA-18-064-CML-1856 and DA-18-064-CML-2282, DDC No. AD31711, January.

Stanford University Aerosol Laboratory and The Ralph M. Parsons Co., 1953b: ibid., Joint Quarterly Report No. 4, April-June 1953, DDC No. AD31508.

Stanford University Aerosol Laboratory and The Ralph M. Parsons Co., 1953c: ibid., Joint Quarterly Report No. 6, Vol. I, October-December 1953, DDC No. AD31510.

Stanford University Aerosol Laboratory and The Ralph M. Parsons Co., 1953d: ibid., Joint Quarterly Report No. 6, Vol. II, October-December 1953, DDC No. AD31711.

Stern, A. C., 1969: The Systems Approach to Air Pollution Control, Pub. No. 216, Dept. of Environ. Science and Engineering, Univ. of North Carolina, Chapel Hill, Presented at Clean Air Conference, Sydney, Australia, 21 May 1969.

Summers, P. W., 1966: The seasonal, weekly, and daily cycles of atmospheric smoke content in central Montreal, J. Air Poll. Contr. Assoc., 16, 432-438.

Swinnerton, J. W., V. J. Linnenbom, and C. H. Cheek, 1969: Distribution of methane and carbon monoxide between the atmosphere and natural waters, Environ. Sci. and Tech., 3, 836-838.

Turner, D. B., 1964: A diffusion model for an urban area, J. Appl. Meteor., 3, 83-91.

Wanta, R. C., 1968: Meteorology and air pollution, Chap. 7 of Air Pollution, Vol. 1, 2nd Edition, A. C. Stern, Ed., Academic Press, New York, 187-227.

Went, F. W., 1966: On the nature of Aitken condensation nucleii, Tellus, 18, 549-556.